

Recent Developments in Multianalyte Immunoassay

Zhifeng Fu^{1,2}, Hong Liu¹, Zhanjun Yang¹, Huangxian Ju^{1*}

¹ Key Laboratory of Analytical Chemistry for Life Science (Ministry of Education of China), Department of Chemistry, Nanjing University, Nanjing 210093, P.R. China

² College of Pharmaceutical Sciences, Southwest University, 400716, P.R. China

* For correspondence - hxju@nju.edu.cn

Abstract

Multianalyte immunoassay has gained increasing attention due to its high sample throughput, short assay time, low sample consumption and reduced overall cost per assay. Most of the current developed approaches for multianalyte immunoassay are based on spatial-resolved, multilabel or separation mode. This paper reviews the progress of multianalyte immunoassay and its applications in different fields with 90 references. The outlook of this promising technique has been discussed.

Keywords

Immunoassay; Immunosensor; Multianalyte immunoassay; Array; Review

Introduction

As a promising approach for selective and sensitive analysis, immunoassay has recently gained increasing attention in different fields including environmental monitoring, clinical diagnosis, food safety, pharmaceutical analysis and bacteria identification. It is often necessary to monitor or quantitate several components in a complex system. For example, due to the limited specificity and sensitivity of biomarkers for clinical diagnosis, the measurement of a single biomarker is usually insufficient for diagnostic purpose. Some studies have showed that the measurement of biomarkers panel can avoid false

positive or false negative results to improve their diagnostic value (1). Traditionally, immunoassay of analytes panel is performed as discrete tests, i.e., one analyte per assay run, and several runs are needed to detect all components in a complex system. Great consumptions of time, reagent and labor limit the application. To dissolve these limitations, multianalyte immunoassay (MAIA) that can measure two or more analytes in a single run has become a long-cherished goal of immunochemist since simultaneous radioimmunoassay of human insulin and growth hormone in serum sample using I-131 and I-125 as labels was reported in 1966 (2). Compared with parallel single-analyte immunoassay methods, MAIA offers some remarkable advantages, such as high sample throughput, improved assay efficiency, low sample consumption and reduced overall cost per assay (3). This review focuses on the progress and applications of MAIA, including spatial-resolved, multilabel and separation modes.

1. Spatial-Resolved Mode

The spatial resolution of different immunoreaction areas using a universal label for fluorescent, chemiluminescent (CL), spectrophotometric, electrochemical, and piezoelectric detections with array detectors including charge-coupled device (CCD) camera and multichannel electrochemical workstation is the most popular MAIA method.

1.1 Optical detection

Antigen and antibody arrays dotted on planar supports, such as multi-well plate, nylon membrane and glass slide, combined with fluorescent probes (4-10) and enzymes (9, 11-13) as labels are traditionally adopted to perform spatial-resolved MAIA using CCD and laser scanner detector.

Weller's group (14) proposed a parallel affinity sensor array for the rapid analysis of 10 antibiotics in milk. Microscope glass slide modified with (3-glycidyloxypropyl) trimethoxysilane was used for the preparation of hapten microarray and inserted into a flow cell to act as an automated flow-through CL multianalyte immunosensor. After incubation process, the horseradish peroxidase labeled immunocomplexes of the 10 antibiotics generated enhanced CL signals, which were recorded with a CCD camera. The fully automated liquid handling and sample processing enabled one analysis cycle to be completed in less than 5 min. With the similar device and protocol, multiple herbicides (15, 16) and allergen-specific IgE in human serum (17) have been assayed in array mode.

Jiang et al. (18) reported a miniaturized, microfluidic version of serial-dilution fluorescent immunoassay for antibodies in HIV+ human serum. In this assay, serially diluted solutions of serum flowed in channels across orthogonal, parallel strips of HIV ENV proteins (gp41 and pg 120) adsorbed on a polycarbonate membrane. The bound antibodies could be measured using a second, fluorescent labeled antibody. This assay used a microdilutor network to achieve serial dilution and allowed simultaneous, quantitative analysis of multiple analytes with high concentrations on a single chip.

Some immunosensors arrays composed of recognition component, fluidics component for

movement of various solutions and detector for collection of signals produced from positive samples have been developed at the Naval Research Laboratory, USA. Sandwich fluoroimmunoassays are performed on the surface of microscope slides previously patterned with stripes of capture antibodies. After both sample and fluorescent tracer antibodies are introduced in a direction perpendicular patterned with stripes of capture antibodies, the immunocomplexes formed can be observed as a checkerboard pattern of fluorescent spots excited by evanescent wave on the surface. These array immunosensors have been successfully applied in MAIA of proteins, bacteria and biohazards (19-27).

Barzen et al. (28-30) proposed several optical multianalyte immunosensors for environment pollutants based on flow-injection immunoassay coupled with total internal reflection fluorescent detection. They immobilized haptens on the different areas of transducer surface of the flow cell and determined simultaneously multiple pollutants in a spatial-resolved and competitive mode. Rodriguez-Mozaz et al. (31) simultaneously detected atrazine, isoproturon and estrogen estrone in river water using an immunosensor fabricated with a similar protocol (Figure 1). The performance of the developed immunosensor was evaluated against a well-accepted traditional method based on solid-phase extraction followed by liquid chromatography-mass spectrometry, and the results obtained from the two methods indicated good agreement.

A one-step lateral flow immunoassay on a strip format for the rapid and simultaneous detection of free and total prostate specific antigens (f-PSA and t-PSA) and estimation of f-PSA to t-PSA ratio (f/t-PSA) in serum has been reported (32). Herein, f-PSA or t-PSA is sandwiched between anti-f-PSA or anti-t-PSA monoclonal antibodies parallel immobilized on the strip and a colloidal gold labeled anti-PSA tracer antibody. The

presence of f-PSA and t-PSA results in the appearance of two parallel pink colour lines. Two membrane-based competitive immunoassays using gold particles and horseradish peroxidase (HRP) as tracers in lateral flow format have also been developed for MAIAs of carbaryl and endosulfan (33). The visual detection limits for carbaryl and endosulfan are 100 and 10 $\mu\text{g/L}$ with gold and 10 and 1 $\mu\text{g/L}$ with HRP as labels, respectively.

Yacoub-George et al. (34) designed a portable multichannel immunosensor for biological warfare agents, which was based on a capillary ELISA technique in combination with a miniaturized fluidics system and used CL as the detection principle (Figure 2). The fluidic system allowed three CL immunoassays to be performed simultaneously within three fused silica capillaries with three photodiodes as detectors. Koch et al. (35) also presented a portable optical multichannel immunosensor for the simultaneous operation of three flow-through capillary enzyme immunoassays. The parallel operation was achieved by stop-flow incubation. When one capillary was in the process of signal collection, the other two were in incubation procedure. This work represented a versatile tool for immunoassay of several biological warfare agents in parallel with only one non-array detector.

The application of a surface plasmon resonance-based biosensor with four flow channels in combination with a mixture of four specific antibodies resulted in a competitive inhibition MAIA for the simultaneous detection of five aminoglycosides in reconstituted skimmed milk (36). Chung et al. (37) developed a sequential method for the analysis of HRP and bovine serum albumin using a surface plasmon resonance biosensor. Non-array fluorescent detector has also been used for spatial-resolved detection of multiple pesticides (38), hormones (39) and proteins (40) by moving the antigens or

antibodies immobilized affinity microcolumn and capillary immunosensor with a motorized translational stage. Owing to the relatively complicated detection device, this strategy needs to be further improved.

1.2 Electrochemical detection

Amperometric immunosensor array fabricated with multiple working electrodes sharing one common counter electrode and reference electrode has been successfully used for MAIA of pepsinogens (41), tumor markers (42-45) and hormones (46). CombiMatrix Corporation (47) developed a microarray of individually addressable electrodes using conventional CMOS integrated circuitry. This microarray system provided a host for MAIA due to the large number of electrodes available, which integrated over 1000 electrodes per square centimeter. The results for human α 1 acid glycoprotein, ricin, M13 phage, *Bacillus globigii* spore, and fluorescein indicated that this method was one of the most sensitive available, with limits of detection in the attomole range. Electrochemical sensor array often suffers from cross-talk due to the diffusion of electroactive product generated at one electrode to a neighboring electrode (43,45). Thus, an enough spatial distance between adjacent electrodes is necessary to counter the diffusion procedure. Use of double siloxane layer (45) and iridium oxide (42-44) matrix can retard the diffusion of enzyme-generated product to lower cross-talk.

Ju et al. (48,49) proposed two disposable immunosensor arrays for simultaneous electrochemical determination of multiple tumor markers. The low-cost immunosensor arrays were fabricated simply using cellulose acetate membrane to co-immobilize thionine as a mediator and antigens on different working electrodes of a screen-printed chip, on which the immobilized thionine shuttled electrons between HRP labeled to antibodies and the electrodes for

enzymatic reduction of H_2O_2 to produce detectable signals. This chip could avoid the electrochemical and electronic cross-talks between the electrodes, which enabled the arrays to be miniaturized without considering the distance between immunosensors.

Kong et al. (50,51) proposed two arrays of eight electrodes for label-free capacitive and conductive immunoassay of liver fibrosis markers using ultrathin α 1 alumina sol-gel films and electrochemically deposited polypyrrole to immobilize antibodies, respectively.

1.3. Mass-sensitive detection

Luo et al. (52) constructed a 2x5 model piezoelectric immunosensor array fabricated with disposable quartz crystals for quantification of microalbumin, 1-microglobulin, α 2 microglobulin, and IgG in urine. With the piezoelectric immunosensor array, 4 urinary proteins could be quantified within 15 min. This method had an analytical interval of 0.01-60 mg/L. Similarly, a novel simultaneous immunoassay technique has been developed for the determination of complement factors (C_4, C_5, C_{1q} and B factor) by constructing a piezoelectric quartz crystal array system (53). These mass-sensitive piezoelectric immunosensor arrays can provide a convenient label-free approach to MAIA.

1.4. Optical encoding and addressing

Spatial-resolved arrays are typically manufactured by labor-intensive methods requiring high precision such as ink-jet printing, micromachining, photolithography, and photodeposition. Randomly ordered addressable sensor array developed in Walt's laboratory (54) provided an alternative approach to array fabrication. In this approach, micrometer-sized sensors were produced by immobilizing different recognition molecules on the surface of microparticles encoded using two fluorescent

dyes. The addressing procedure was performed by taking the fluorescence intensity at each emission wavelength and then dividing the two values to get the signature of that particular ratio. With this principle, multiple drugs (55), proteins (56-58), biological warfare agents (59) and cytokines (60) were simultaneously detected with CL or fluorescent method and randomly ordered antibodies immobilized copolymer microspheres or metallic particles as microsensors.

Theoretically, thousands of antigens or antibodies can be spotted onto one single planar support to screen thousands of analytes. Although this mode can screen large numbers of analytes, accurate quantitative data in these arrays are usually limited or difficult to be obtained (44). Requiring of complicated and expensive spotting technique with high precision also greatly limits its application. Although optical encoding and addressing allows randomly ordered sensor arrays to be identified for MAIA, the encoding process complicates the manipulation. Furthermore, spatial-resolved MAIA is typically performed with expensive array detector such as CCD camera for optical detection or multi-channel workstation for electrochemical measurement (61).

2. Multilabel Mode

The second dominant mode for MAIA is performed using different labels to tag antibodies or antigens (one per analyte), including radioisotopes, enzymes, fluorescent and metal compounds. Different analytes can be easily distinguished using these labels by such parameters as potential, wavelength, decay time and so on.

2.1 Wavelength resolution

ELISA for MAIA involves labeling the analytes with various enzymes, whose catalyzed reactions can easily be distinguished from each other by

absorption spectra (62, 63). Selection of the enzyme labels is a key step in the development of an ELISA based MAIA. Blake et al. (62) mentioned that the ideal enzyme labels for MAIA should meet the following requirements: (i) the enzymes should be readily available, inexpensive, and have high turnover numbers; (ii) each enzyme must be stable under the selected simultaneous assay conditions and not easily to be interfered by other enzyme or its substrate; (iii) all enzymes must have similar optimal assay conditions; (iv) the assay method for each enzyme should be simple, sensitive, rapid, and cheap; (v) all enzymes should not occur in the practical sample to be assayed, and interfering factors should be absent; (vi) each enzyme should contain potentially reactive groups that allow linking to antigen or antibody while retaining the enzyme activity; (vii) the spectra of the products of the enzyme-catalyzed reactions should not overlap with each other.

Ihara et al. (64) immobilized a mixture of antigenic peptides of FAK and c-Myc to nanospheres with red emission, and a mixture of c-Myc and α catenin to green nanospheres, respectively. As seen in Figure 4 (64), anti-FAK and anti α catenin antibodies could form aggregates with red and green emissions, respectively. The anti-c-Myc antibody could form aggregate emitting yellow light as a result of color overlapping. This strategy enabled specific antibodies to be detected in one-step procedure with color-encoded nanospheres. Swartzman et al. (65) proposed a bead-based two-color MAIA for cytokines IL-6 and IL-8 using Cy5.5 and Cy 5 as fluorescent labels, respectively. The linear dynamic ranges of them were 125-4000 pg/mL and 15.6-2000 pg/mL, respectively. This work utilized fluorometric microvolume assay technology to image and measure bead-bound fluorescence while the background fluorescence was ignored. Consequently, no wash steps were required to remove unbound antibody, ligand, and

fluorophore. Goldman et al. (66) used antibody-conjugated quantum dots with emission maximums at 510, 555, 590, and 610 nm to demonstrate multiplex assays for four protein toxins present in the same sample. However, a deconvolution of composite spectra was needed to distinguish the overlapping signals.

2.2. Time resolution

The fluorescence of lanthanide chelates has the advantages of high quantum yield, long decay time, exceptionally large Stoke's shift, and narrow emission peak. Specific chelate fluorescence can be easily distinguished from the sample matrix fluorescence and the scattered light, and the fluorescence from different lanthanides can also be easily discriminated due to their difference in decay time and emission wavelength, which makes the lanthanide chelates preferable to any other probes for developing multilabel-based time-resolved MAIA. Of the 15 lanthanide ions, Eu^{3+} , Sm^{3+} , and Tb^{3+} are the most commonly employed probes, and have been widely used for time-resolved fluorescent MAIA of multiple tumor markers (67), hormones (68), recombinant proteins (69) and antibodies (70).

Ito et al. (71) developed a simple and rapid time-resolved fluoroimmunoassay for simultaneous determination of alpha-fetoprotein (AFP), human chorionic gonadotropin (hCG) and estriol (E3) using Eu^{3+} and Sm^{3+} chelates. In this proposed method, a 96-well microtiter plate for AFP and hCG assay and a transferable solid phase plate for E3 assay were combined to perform MAIA of the three analytes with only two probes. The measurable ranges for AFP, hCG and E3 were 3.91-1000 ng/mL, 877-250 000 IU/L and 0.39-100 ng/mL, respectively.

2.3. Potential resolution

The dual-analyte homogeneous immunoassay of phenobarbital and phenytoin was carried out simultaneously at physiological pH by square-

wave voltammetry on Nafion-loaded carbon paste electrode. Phenobarbital and phenytoin were labeled by cobaltocenium salt and ferroceneammonium salt with standard redox potentials of -1.05V and 0.26 V, respectively. Detection limits of 0.25 and 0.2 μ g were achieved for the two antiepileptic drugs, respectively (72). As seen in Figure 5 (73), an electrochemical stripping immunoassay protocol using different inorganic nanocrystal as tracers and magnetic beads as support has been developed for the simultaneous measurements of proteins. Each biorecognition event yields a distinct voltammetric peak, whose position and size reflect the identity and concentration of the corresponding analyte, respectively. This protocol has been used for a simultaneous immunoassay of β 2 microglobulin, IgG, bovine serum albumin, and C-reactive protein using ZnS, CdS, PbS, and CuS colloidal crystals as labels, respectively (73). Hayes et al. (74) proposed a MAIA method for human serum albumin and IgG. Bismuth and indium ions were coupled to the two proteins through the bifunctional chelating agent diethylenetriamine-pentaacetic acid. Following the competitive reactions between unlabeled and labeled proteins for limited amount of specific antibodies immobilized on polystyrene, the bound metal ion labels were released by acidification and detected by differential pulse anodic stripping voltammetry with detection limits of 1.8 and 0.6 μ g/mL for human serum albumin and IgG, respectively.

2.4. *M/e resolution*

Zhang et al. (75) developed a dual-label immunoassay method for the simultaneous determination of AFP and free hCG β in human serum. Monoclonal antibodies immobilized on microtiter plates captured AFP and hCG β , which were detected by Eu^{3+} -labeled AFP and Sm^{3+} -labeled hCG β tracer antibodies with inductively coupled plasma mass spectrometry

(ICPMS) after Eu^{3+} and Sm^{3+} were dissociated from the plates with HNO_3 solution. However, this technique could not be used for microarray detection since it was necessary to dissolve the elemental tags before introducing them into the plasma source. They (76) also reported the detection of multiple proteins on each spot of the immuno-microarray by laser ablation ICPMS. AFP, carcinoembryonic antigen (CEA) and human IgG were detected as model proteins in sandwich format on a microarray with Sm^{3+} -labeled AFP antibody, Eu^{3+} -labeled CEA antibody, and Au nanoparticle-labeled IgG antibody as tracer antibodies. The detection limits were 0.20, 0.14, and 0.012 μ g/mL for AFP, CEA, and human IgG, respectively. This detection method allowed detection of multiple analytes from each spot of microarray with a spatial resolution at micrometer range, which could alleviate the stress to fabricate high-density arrays.

2.5. *Scintillation energy resolution*

In 1966, as the founder of MAIA, Morgan (2) proposed an original simultaneous radioimmunoassay of human insulin and growth hormone in serum sample using I-131 and I-125 as labels and exploiting the difference in scintillation energy produced from the two radioisotopes to discriminate the two analyte. Similarly, the simultaneous radioassay of vitamins (77) and hormones (78) could be carried out using Co-57 and I-125 as probes. Recently, few attention is paid to the radioimmunoassay based MAIA due to the damage of radioisotopes to environment and operator.

2.6. *Substrate zone resolution*

It has been noted that the different labels used in multilabel mode often need markedly different optimal assay conditions, and traditionally simple combination of multiple labels often leads to loss of assay performance (2). Furthermore,

this mode sometimes suffers from signal overlapping of different labels (66).

Ju et al. (61) designed a substrate zone-resolved multianalyte immunosensing system, with which HRP labeled carcinoma antigen 125 (CA 125) immunocomplex and alkaline phosphatase labeled CEA immunocomplex were sequentially detected in their corresponding CL substrate zones. This designed technique solved two key problems in multilabel mode: one was to obtain distinguishable CL signals without consideration of wavelength, and the other was to enable each CL reaction to be catalyzed by the label in its optimal assay condition without loss of assay performance. Unfortunately, as other MAIA methods based on multilabel mode, this technique encountered a difficulty to find more available enzyme labels, which limited the number of analytes. In order to overcome this limitation, this group further proposed a two-dimensional resolution system of channels and substrate zones (79). Using CA 125, CA 153, CA 199 and CEA as two couples of model analytes, two couples of capture antibodies were immobilized in two channels, respectively. With a sandwich format the CL substrates for alkaline phosphatase and horseradish peroxidase were delivered into the channels sequentially to perform multiplex immunoassay after the sample and trace antibodies were introduced into the channels for on-line incubation. When three or four channels were used in the flow-through device, the detectable analytes in a single run could be 6 or 8, respectively, with a 10 s longer analytical time for each added channel.

3. Separation Mode

Another method coupled with separation techniques such as capillary electrophoresis (CE) and high-performance liquid chromatography (HPLC) can be used for MAIA. Competitive immunoassay combined with fluorescent detection is generally adopted to perform CE

based MAIA, the analytes includes abused drugs (79, 81) and peptides (82). Obviously this strategy often suffers from the adsorption of immunoreagents on inner wall of the capillary, which can be prevented by optimization of separation buffer type and pH that allows application of high electric field (82). An on-line coupling of a label-free reflectometric interference spectroscopic biosensor to a HPLC system has been described for MAIA of four pesticides (83). In this system a highly cross-reactive antibody against the four pesticides is used to bind the pesticides. The eluate of the HPLC is mixed continuously with the antibodies, and the presence of antigens is detected by a reduction of the antibody binding to the transducer.

Roda et al. (84) proposed a field-flow fractionation (FFF)-CL based solid-phase competitive immunoassay, in which micrometer-sized beads coated with the capture antibody were used as solid phase, and analyte-HRP conjugate was used as tracer. Once the competitive immunoreaction took place within the injection loop of the system, the antibody-bound tracer was separated from tracer in solution in a few minutes by means of FFF. FFF-based MAIA could be developed by use of beads with different sizes (1-50 μ m), each coated with the specific antibody for one analyte. The beads could be fractionated by FFF before CL signals collection to realize detection of multiple analytes in a single run.

The thermosensitive poly (N-isopropylacrylamide) (PNIP) and magnetic beads have been widely utilized as the separation carriers for immunoassays. A fast homogeneous immunoreaction as well as a simple heterogeneous separation process is carried out for MAIA in the light of some certain characteristics of water-soluble PNIP and magnetic beads, and thus, lower nonspecific affinity and higher sensitivity are accomplished

(85). The results of CL detection of IgG and IgA indicate the detection limits as low as 2.0 and 1.5 ng/mL, respectively.

4. Cross-Reactivity

Cross-reactivity is a crucial analytical parameter regarding specificity and reliability of MAIA, which is frequently encountered in MAIA of small molecule analytes. In many cases, the antibodies recognize a variety of analogs and metabolites of the target analyte, for example, some *s*-triazines and their metabolites with similar structures shown in Figure 6 (86). Even monoclonal antibodies are often unable to discriminate absolutely molecular analogs with small structural differences. Efforts to derive monoclonal antibodies to small analytes generally produce panels of antibodies that differ in their cross-reactivity for the primary target analyte and its analogs and metabolites. Antibodies arrays combined with some chemometric means inclusive of neural network are often used to overcome the difficulty in exact quantitation resulted from the cross-reactivity (86-90).

5. Conclusion and Outlook

In recent years, MAIA has attracted considerable interest due to its outstanding advantage in assay speed, cost and labor consuming. So far the spatial-resolved mode has been the most popular mode due to its high analyte throughput and large information amount. The further work needs to develop arrays with higher density and simpler preparation protocol using cheaper array detector. Most of the multilabel mode based methods focus on using of lanthanide chelates as labels and time-resolved fluorescent detection. More labels with higher signal resolution degree and less requirement to assay condition are urgently needed. Various resolution methods in time, space, substrates, reactants, labels and detection methods will be designed and developed for MAIA in the future. Military application and

environment monitor are anxious to miniaturized, integrated and portable MAIA system fit for field application. MAIA system with high sample throughput and rapid assay speed has great application potential in disease screen.

Acknowledgements

This research was financially supported by the National Science Funds for Distinguished Young Scholars (20325518) and Creative Research Groups (20521503), the Key Program (20535010) from the National Natural Science Foundation of China and the Science Foundation of Jiangsu (BS2006006, BS2006074).

References

1. Wilson, M. S., Nie, W. Y. (2006). Multiplex measurement of seven tumor markers using an electrochemical protein chip. *Anal. Chem*, 78: 6476-6483.
2. Morgan, C. R. (1966). Immunoassay of human insulin and growth hormone simultaneously using I-131 and I-125 tracers. *Proc. Soc. Exp. Biol. Med*, 123: 230-233.
3. Kricka, L. J. (1992). Multianalyte testing. *Clin. Chem*, 38: 327-328.
4. Moreno-Bondi, M. C., Alarie, J. P. and Vo-Dinh, T. (2003). Multi-analyte analysis system using an antibody-based biochip. *Anal. Bioanal. Chem*, 375: 120-124.
5. Chen, C. S., Durst, R. A. (2006). Salmonella spp. and Listeria monocytogenes with an array-based immunosorbent assay using universal protein G-liposomal nanovesicles. *Talanta*, 69: 232-238.
6. Song, S. P., Li, B., Hu, J. and Li, M. Q. (2004). Recent developments in single-cell analysis. *Anal. Chim. Acta*, 510: 147-138.

7. Belleville, E., Dufva, M., Aamand, J., Bruun, L., Clausen, L. and Christensen, C. B. V. (2004). Quantitative microarray pesticide analysis. *J. Immunol. Methods*, 286: 219-229.
8. Wadkins, R. M., Golden, J. P., Pritsiolas, L. M. and Ligler, F. S. (1998). Detection of multiple toxic agents using a planar array immunosensor. *Biosens. Bioelectron.*, 13: 407-415.
9. Christodoulides, N., Tran, M., Floriano, P. N., Rodriguez, M., Goodey, A., Ali, M., Neikirt, D. and McDevitt, J. T. (2002). A Microchip-based multianalyte assay system for the assessment of cardiac risk. *Anal. Chem.*, 74: 3030-3036.
10. Kido, H., Maquieira, A. and Hammock, B. D. (2000). Disc-based immunoassay microarrays. *Anal. Chim. Acta*, 411: 1-11.
11. Roda, A., Mirasoli, M., Venturoli, S., Cricca, M., Bonvicini, F., Baraldini, M., Pasini, P., Zerbin, M. and Musiani, M. (2002). Microtiter format for simultaneous multianalyte detection and development of a PCR-chemiluminescent enzyme immunoassay for typing human papillomavirus DNAs. *Clin. Chem.*, 48: 1654-1660.
12. Strasser, A., Dietrich, R., Usleber, E. and Märtlbauer, E. (2003). Immunochemical rapid test for multiresidue analysis of antimicrobial drugs in milk using monoclonal antibodies and hapten-glucose oxidase conjugates. *Anal. Chim. Acta*, 495: 11-19.
13. Huang, R. P., Huang, R. C., Fan, Y. and Lin, Y. (2001). Simultaneous detection of multiple cytokines from conditioned media and patient's sera by an antibody-based protein array system. *Anal. Biochem.*, 294: 55-62.
14. Knecht, B. G., Strasser, A., Dietrich, R., Märtlbauer, E., Niessner, R. and Weller, M. G. (2004). Automated microarray system for the simultaneous detection of antibiotics in milk. *Anal. Chem.*, 76: 646-654.
15. Weller, M. G., Schuetz, A. J., Winklmaier, M. and Niessner, R. (1999). Highly parallel affinity sensor for the detection of environmental contaminants in water. *Anal. Chim. Acta*, 393: 29-41.
16. Winklmaier, M., Schuetz, A. J., Weller, M. G. and Niessner, R. (1999). Immunochemical array for the identification of cross-reacting analytes. *Fresenius J. Anal. Chem.*, 363: 731-737.
17. Fall, B. I., Eberlein-König, B., Behrendt, H., Niessner, R., Ring, J. and Weller, M. G. (2003). Microarrays for the screening of allergen-specific IgE in human serum. *Anal. Chem.*, 75: 556-562.
18. Jiang, X. Y., Ng, J. M. K., Stroock, A. D., Dertinger, S. K. W. and Whitesides, G. M. (2003). A miniaturized, parallel, serially diluted immunoassay for analyzing multiple antigens. *J. Am. Chem. Soc.*, 125: 5294-5295.
19. Sapsford, K. E., Rasooly, A., Taitt, C. R. and Ligler, F. S. (2004). Detection of campylobacter and shigella species in food samples using an array biosensor. *Anal. Chem.*, 76: 433-440.
20. Delehanty, J. B., Ligler, F. S. (2002). A microarray immunoassay for simultaneous detection of proteins and bacteria. *Anal. Chem.*, 74: 5681-5687.
21. Rowe, C. A., Scruggs, S. B., Feldstein, M. J., Golden, J. P. and Ligler, F. S. (1999). An Array Immunosensor for simultaneous detection of clinical analytes. *Anal. Chem.*, 71: 433-439.

22. Golden, J. P., Taitt, C. R., Shriver-Lake, L. C., Shubin, Y. S. and Ligler, F. S. (2005). A portable automated multianalyte biosensor. *Talanta*, 65: 1078-1085.
23. Rowe-Taitt, C. A., Golden, J. P., Feldstein, M. J., Cras, J. J., Hoffman, K. E. and Ligler, F. S. (2000). Array biosensor for detection of biohazards. *Biosens. Bioelectron.*, 14: 785-794.
24. Rowe-Taitt, C. A., Hazzard, J. W., Hoffman, K. E., Cras, J. J., Golden, J. P. and Ligler, F. S. (2000). Simultaneous detection of six biohazardous agents using a planar waveguide array biosensor. *Biosens. Bioelectron.*, 15: 579-589.
25. Taitt, C. R., Anderson, G. P., Lingerfelt, B. M., Feldstein, M. J. And Ligler, F. S. (2002). Nine-Analyte Detection Using an Array-Based Biosensor. *Anal. Chem.*, 74: 6114-6120.
26. Rowe, C. A., Tender, L. M., Feldstein, M. J., Golden, J. P., Scruggs, S. B., MacCraith, B. D., Cras, J. J. And Ligler, F. S. (1999). Array biosensor for simultaneous identification of bacterial, viral, and protein analytes. *Anal. Chem.*, 71: 3846-3852.
27. Spasford, K. E., Ngundi, M. M., Moore, M. H., Lassman, M. E., Shriver-Lake, L. C., Taitt, C. R. and Ligler, F. S. (2006). Rapid detection of foodborne contaminants using an Array Biosensor. *Sens. Actuators B-Chem.*, 113: 599-607.
28. Barzen, C., Brecht, A. and Gauglitz, G. (2002). Optical multiple-analyte immunosensor for water pollution control. *Biosens. Bioelectron.*, 17: 289-295.
29. Klotz, A., Brecht, A., Barzen, C., Gauglitz, G., Harris, R. D., Quigley, G. R., Wilkinson, J.S. and Abuknesha, R. (1998). Immuno-fluorescence sensor for water analysis. *Sens. Actuators B-Chem.*, 51: 181-187.
30. Brecht, A., Klotz, A., Barzen, C., Gauglitz, G., Harris, R. D., Quigley, G. R., Wilkinson, J. S., Sztajn bok, P., Abuknesha, R., Gascün, J., Oubiña, A. and Barcelü, D. (1998). Optical immunoprobe development for multiresidue monitoring in water. *Anal. Chim. Acta*, 362: 69-79.
31. Rodriguez-Mozaz, S., de Alda, M. J. L. and Barceló, D. (2006). Fast and simultaneous monitoring of organic pollutants in a drinking water treatment plant by a multi-analyte biosensor followed by LC-MS validation. *Talanta*, 69: 377-384.
32. Fernández-Sánchez, C., McNeil, C. J., Rawson, K., Nilsson, O., Leung, H. Y. and Gnanapragasam, V. (2005). One-step immunostrip test for the simultaneous detection of free and total prostate specific antigen in serum. *J. Immunol. Methods*, 307: 1-12.
33. Zhang, C., Zhang, Y. and Wang, S. (2006). Development of multianalyte flow-through and lateral-flow assays using gold particles and horseradish peroxidase as tracers for the rapid determination of carbaryl and endosulfan in agricultural products. *J. Agric. Food Chem.*, 54: 2502-2507.
34. Yacoub-George, E., Meixner, L., Scheithauer, W., Koppi, A., Drost, S., Wolf, H., Danapel, C. and Feller, K. A. (2002). Chemiluminescence multichannel immunosensor for biodetection. *Anal. Chim. Acta*, 457: 3-12.
35. Koch, S., Wolf, H., Danapel, C. and Feller, K. A. (2000). Optical flow-cell multichannel immunosensor for the detection of biological warfare agents. *Biosens. Bioelectron.*, 14: 779-784.
36. Haasnoot, W., Cazemier, G., Koets, M. and van Amerongen, A. (2003). Single biosensor immunoassay for the detection of five aminoglycosides in reconstituted

- skimmed milk. *Anal. Chim. Acta*, 488: 53-60.
37. Chung, J. W., Bernhardt, R. and Pyun, J. C. (2006). Sequential analysis of multiple analytes using a surface plasmon resonance (SPR) biosensor. *J. Immunol. Methods*, 311: 178-188.
38. Mastichiadis, C., Kakabakos, S. E., Christofidis, I., Koupparis, M. A., Willetts, C. and Misiakos, K. (2002). Simultaneous determination of pesticides using a four-band disposable optical capillary immunosensor. *Anal. Chem* 74: 6064-6072.
39. Petrou, P. S., Kakabakos, S. E., Christofidis, I., Argitis, P. and Misiakos, K. (2002). Multi-analyte capillary immunosensor for the determination of hormones in human serum samples. *Biosens. Bioelectron*, 17: 261-268.
40. Piyasena, M. E., Buranda, T., Wu, Y., Huang, J. M., Sklar, L. A. and Lopez, G. P. (2004). Near-simultaneous and real-time detection of multiple analytes in affinity microcolumns. *Anal. Chem*, 76: 6266-6273.
41. Ogasawara, D., Hirano, Y., Yasukawa, T., Shiku, H., Kobori, K., Ushizawa, K., Kawabata, S. and Matsue, T. (2006). Electrochemical microdevice with separable electrode and antibody chips for simultaneous detection of pepsinogens 1 and 2. *Biosens. Bioelectron*, 21:1784-1790.
42. Wilson, M. S., Nie, W. Y. (2006). Electrochemical multianalyte immunoassays using an array-based sensor. *Anal. Chem*, 78: 2507-2513.
43. Wilson, M. S., Nie, W.Y. (2006). Multiplex measurement of seven tumor markers using an electrochemical protein chip. *Anal. Chem*, 78: 6476-6483.
44. Wilson, M. S. (2005). Electrochemical immunosensors for the simultaneous detection of Two Tumor Markers. *Anal. Chem*, 77: 1496-1502.
45. Kojima, K., Hiratsuka, A., Suzuki, H., Yano, K., Ikebukuro, K. and Karube, I. (2003). Electrochemical protein chip with arrayed immunosensors with antibodies immobilized in a plasma-polymerized film. *Anal. Chem*, 75: 1116-1122.
46. Pritchard, D. J., Morgan, H. and Cooper, J. M. (1995). Simultaneous determination of follicle stimulating hormone and luteinising hormone using a multianalyte immunosensor. *Anal. Chim. Acta*, 310: 251-256.
47. Dill, K., Montgomery, D. D., Ghindilis, A. L, Schlarzkopf, K. R., Ragsdale, S. R. and Oleinikov, A. V.(2004). Immunoassays based on electrochemical detection using microelectrode arrays. *Biosens. Bioelectron*, 20: 736-742.
48. Wu, J., Yan, F., Tang, J. H., Zhai, C. and Ju, H. X. (2007). A disposable multianalyte electrochemical immunosensor array for automated simultaneous determination of tumor markers. *Clin. Chem*, 53: 1495-1503.
49. Wu, J., Zhang, Z. J., Fu, Z. F. and Ju, H. X. (2007). A disposable two-throughput electrochemical immunosensor chip for simultaneous multianalyte determination of tumor markers. *Biosens. Bioelectron*, 23: 114-120.
50. Jiang, D. C., Tang, J., Liu, B. H., Yang, P. Y. and Kong, J. L. (2003). Ultrathin alumina sol-gel-derived films: allowing direct detection of the liver fibrosis markers by capacitance measurement. *Anal. Chem*, 75: 4578-4584.
51. Shi, M. H., Peng, Y. Y., Zhou, J., Liu, B. H., Huang, Y. P. and Kong, J. L. (2006). Immunoassays based on microelectrodes arrayed on a silicon chip for high

- throughput screening of liver fibrosis markers in human serum. *Biosens. Bioelectron.*, 21: 2210-2216.
52. Luo, Y., Chen, M., Wen, Q. J., Zhao, M., Zhang, B., Li, X. Y., Wang, F., Huang, Q., Yao, C. Y., Jiang, T. L., Cai, G. R. and Fu, W. L. (2006). Rapid and Simultaneous Quantification of 4 Urinary Proteins by Piezoelectric Quartz Crystal Microbalance Immunosensor Array. *Clin. Chem.*, 52: 2273-2280.
53. Wang, L. L., Fang, H., Zeng, Q. Y., Zhou, X. D., Fang, Y. X., and Hu, J. M. (2001). Detection of complement factors using piezoelectric immunosensor array. *J. Anal. Sci.*, 17: 358-362.
54. Michael, K. L., Taylor, L. C., Schultz, S. L. and Walt, D. R. (1998). Randomly ordered addressable high-density optical sensor arrays. *Anal. Chem.*, 70: 1242-1248.
55. Szurdoki, F., Michael, K. L. And Walt, D. R. (2001). A duplexed microsphere-based fluorescent immunoassay. *Anal. Biochem.*, 291: 219-228.
56. Rissin, D. M., Walt, D. R. (2006). Duplexed sandwich immunoassays on a fiber-optic microarray. *Anal. Chim. Acta.*, 564: 34-39.
57. Zhi, Z. L., Murakami, Y. J., Morita, Y., Hasan, Q. and Tamiya, E. (2003). Multianalyte immunoassay with self-assembled addressable microparticle array on a chip. *Anal. Biochem.*, 318: 236-243.
58. Zhi, Z. L., Morita, Y., Hasan, Q. and Tamiya, E. (2003). Micromachining microcarrier-based biomolecular encoding for miniaturized and multiplexed immunoassay. *Anal. Chem.*, 75: 4125-4131.
59. McBride, M. T., Gammon, S., Pitesky, M., O'Brien, T. W., Smith, T., Aldrich, J., Langlois, R. G., Colston, B. and Venkateswaran, K. S. (2003). Multiplexed liquid arrays for simultaneous detection of simulants of biological warfare agents. *Anal. Chem.*, 75: 1924-1930.
60. Ray, C. A., Bowsher, R. R., Smith, W. C., Devanarayan, V., Willey, M. B., Brandt, J. T. and Dean, R. A. (2005). Development, validation, and implementation of a multiplex immunoassay for the simultaneous determination of five cytokines in human serum. *J. Pharm. Biomed. Anal.*, 36: 1037-1044.
61. Fu, Z. F., Liu, H. and Ju, H. X. (2006). Flow-through multianalyte chemiluminescent immunosensing system with designed substrate zone-Resolved technique for sequential detection of tumor markers. *Anal. Chem.*, 79: 6999-7005.
62. Blake, C., Al-Bassam, M. N., Gould, B. J., Marks, V., Bridges, J. W. and Riley, C. (1982). Simultaneous enzyme immunoassay of two thyroid hormones. *Clin. Chem.*, 28: 1469-1473.
63. Porstmann, T., Nugel, E., Henklein, P., Dopel, H., Ronspeck, W., Pas P. and von Baehr, R. (1993). Two-colour combination enzyme-linked immunosorbent assay for the simultaneous detection of HBV and HIV infection. *J. Immunol. Methods* 158: 95-106.
64. Ihara, T., Mori, Y., Imamura, T., Mukae, M., Tanaka, S. and Jyo, A. (2006). Colorimetric multiplexed immunoassay using specific aggregation of antigenic peptide-modified luminous nanoparticles. *Anal. Chim. Acta.*, 578: 11-18.
65. Swartzman, E. E., Miraglia, S. J., Mellentin-Michelotti, J., Evangelista, L. And Yuan, P. M. (1999). A homogeneous and multiplexed immunoassay for high-throughput screening using fluorometric microvolume assay technology. *Anal. Biochem.*, 271: 143-151.

66. Goldman, E. R., Clapp, A. R., Anderson, G. P., Uyeda, T., Mauro, J. M., Medintz, I. L. and Mattoussi, H. (2004). Multiplexed toxin analysis using four colors of quantum dot fluororeagents. *Anal. Chem*, 76: 684-688.
67. Matsumoto, K., Yuan, J. L., Wang, G. L. And Kimura, H. (1999). Simultaneous determination of α fetoprotein and carcinoembryonic antigen in human serum by time-resolved fluoroimmunoassay. *Anal. Biochem*, 276: 81-87.
68. Wu, F. B., Han, S. Q., Xu, T. And He, Y. F. (2003). Sensitive time-resolved fluoroimmunoassay for simultaneous detection of serum thyroid-stimulating hormone and total thyroxin with Eu and Sm as labels. *Anal. Biochem*, 314: 87-96.
69. Bookout, J. T., Joaquim, T. R., Magin, K. M., Rogan, G. L. and Lirette, R. P. (2000). Development of a dual-label time-resolved fluorometric immunoassay for the simultaneous detection of two recombinant proteins in potato. *J. Agric. Food Chem*, 48: 5868.
70. Aggerbeck, H., Nørgaard-Pedersen, B. and Heron, I. (1996). Simultaneous quantitation of diphtheria and tetanus antibodies by double antigen, time-resolved fluorescence immunoassay. *J. Immunol. Methods*, 190: 171-183.
71. Ito, K., Oda, M., Tsuji, A. and Maeda, M. (1999). Simultaneous determination of alpha-fetoprotein, human chorionic gonadotropin and estriol in serum of pregnant women by time-resolved fluoroimmunoassay. *J. Pharm. Biomed. Anal.*, 20: 169-178.
72. Bordes, A. L., Limoges, B., Brossier, P. and Degrand, C. (1997). Simultaneous homogeneous immunoassay of phenytoin and phenobarbital using a Nafion-loaded carbon paste electrode and two redox cationic labels. *Anal. Chim. Acta*, 356: 195-203.
73. Liu, G. D., Wang, J., Kim, J., Jan, M. R. and Collins, G. E. (2004). Electrochemical coding for multiplexed immunoassays of proteins. *Anal. Chem*, 76: 7126-7130.
74. Hayes, F. J., Halsall, H. B. And Heineman, W. R. (1994). Simultaneous immunoassay using electrochemical detection of metal ion labels. *Anal. Chem*, 66: 1860-1865.
75. Zhang, S. C., Zhang, C., Xing, Z. and Zhang, X.R. (2004). Simultaneous determination of α fetoprotein and free β -human chorionic gonadotropin by element-tagged immunoassay with detection by inductively coupled plasma mass spectrometry. *Clin. Chem*, 50: 1214-1221.
76. Hu, S. H., Zhang, S. C., Hu, Z. C., Xing, Z. and Zhang, X. R. (2007). Detection of multiple proteins on one spot by laser ablation inductively coupled plasma mass spectrometry and application to immunomicroarray with element-tagged antibodies. *Anal. Chem*, 79: 923-926.
77. Gutcho, S., Mansbach, L. (1977). Simultaneous radioassay of serum vitamin B12 and folic acid. *Clin. Chem*, 23: 1609-1614.
78. Wlans, F. H., Dev, J., Jr., Powell, M. M. and Heald, J. I. (1986). Evaluation of simultaneous measurement of lutropin and follitropin with the simulTROPIN radioimmunoassay kit. *Clin. Chem*, 32: 887-890.
79. Fu, Z. F., Yang, Z. J., Tang, J. H., Liu, H., Yang, F. and Ju, H. X. (2007). Channel and substrate zone two-dimensional resolution for chemiluminescent multiplex immunoassay. *Anal. Chem*, 79: 7376-7382.
80. Chen, F. T. A., Evangelista, R. A. (1994). Feasibility studies for simultaneous

- immunochemical multianalyte drug assay by capillary electrophoresis with laser-induced fluorescence. *Clin. Chem*, 40: 1819-1822.
81. Caslavská, J., Allemann, D. and Thormann, W. (1999). Analysis of urinary drugs of abuse by a multianalyte capillary electrophoretic immunoassay. *J. Chromatogr. A*, 838: 197-211.
82. German, I., Kennedy, R. T. J. (2000). Rapid simultaneous determination of glucagon and insulin by capillary electrophoresis immunoassays. *Chromatogr. B*, 742: 353-362.
83. Haake, H. M., de Best, L., Irth, H., Abuknesha, R. and Brecht, A. (2000). Label-free biochemical detection coupled on-line to liquid chromatography. *Anal. Chem*, 72: 3635-3641.
84. Roda, A., Mirasoli, M., Melucci, D. and Reschiglian, P. (2005). Toward multianalyte immunoassays: a flow-assisted, solid-Phase format with chemiluminescence detection. *Clin. Chem*, 51: 1993-1995.
85. Zhou, Y., Zhang, Y. H., Lau, C. W. And Lu, J. Z. (2006). Sequential determination of two proteins by temperature-triggered homogeneous chemiluminescent immunoassay. *Anal. Chem*, 78: 5920-5924.
86. Jones, G., Wortberg, M., Hammock, B. D. and Rocke, D. M. (1996). A procedure for the immunoanalysis of samples containing one or more members of a group of cross-reacting analytes. *Anal. Chim. Acta*, 336: 175-183.
87. Reder, S., Dieterle, F., Jansen, H., Alcock, S. And Gauglitz, G. (2003). Multi-analyte assay for triazines using cross-reactive antibodies and neural networks. *Biosens. Bioelectron*, 19: 447-455.
88. Piehler, J., Brecht, A., Giersch, T., Kramer, K., Hock, B. and Gauglitz, G. (1997). Affinity characterization of monoclonal and recombinant antibodies for multianalyte detection with an optical transducer. *Sens. Actuators B-Chem*, 39: 432-437.
89. Samsonova, J. V., Rubtsova, M. Y., Kiseleva, A. V., Ezhov, A. A. and Egorov, A. M. (1999). Chemiluminescent multiassay of pesticides with horseradish peroxidase as a label. *Biosens. Bioelectron*, 14: 273-281.
90. Bhand, S., Surugiu, I., Dzgoev, A., Ramanathan, K., Sundaram, P. V. and Danielsson, B. (2005). Immuno-arrays for multianalyte analysis of chlorotriazines. *Talanta*, 65: 331-336.

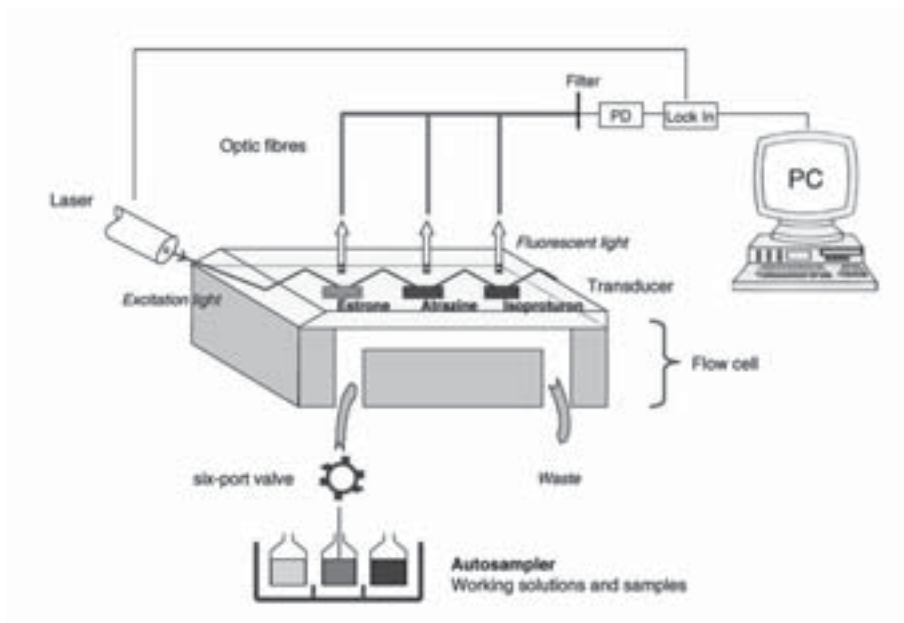


Fig 1 : Scheme of flow-injection immunosensor used for detection of multiple pollutants in river water.

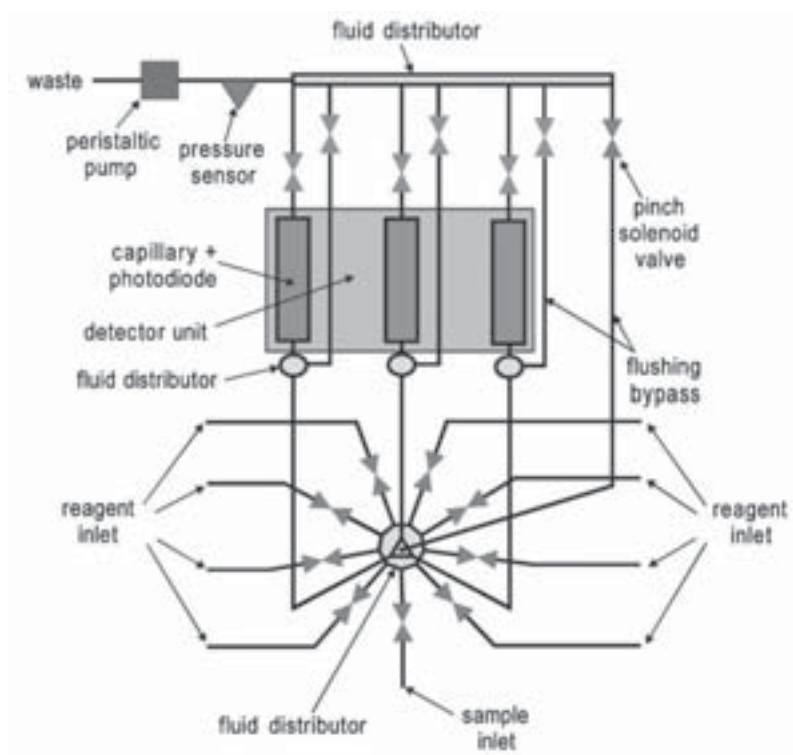


Fig 2 : Scheme representing the arrangement of the fluidics components of the CL multichannel immunosensor for biological warfare agents.

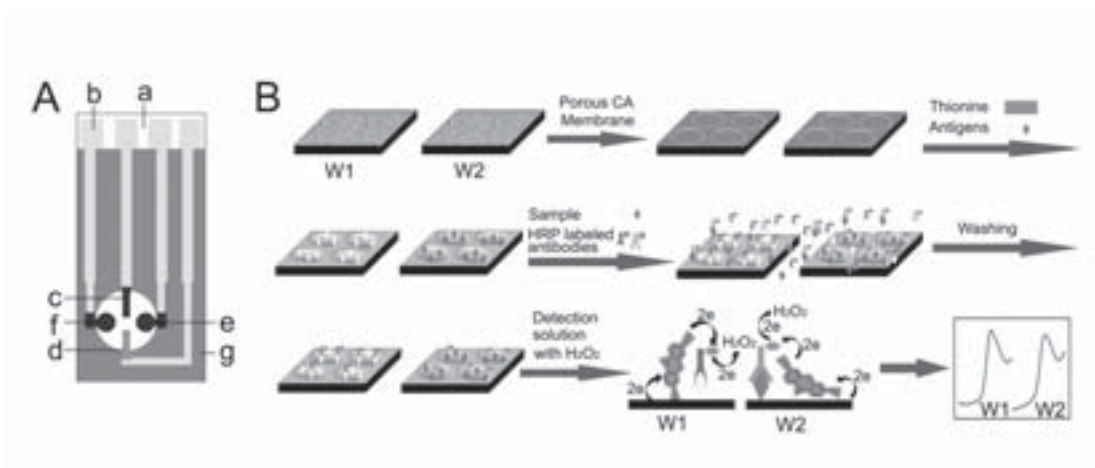


Fig 3 : Schematic diagrams of (A) screen-printed four-electrode system and (B) preparation of immunosensor array and MAIA procedure: (a) Nylon sheet, (b) silver ink, (c) graphite auxiliary electrode, (d) Ag/AgCl reference electrode, (e) W1, (f) W2 and (g) insulating dielectric.

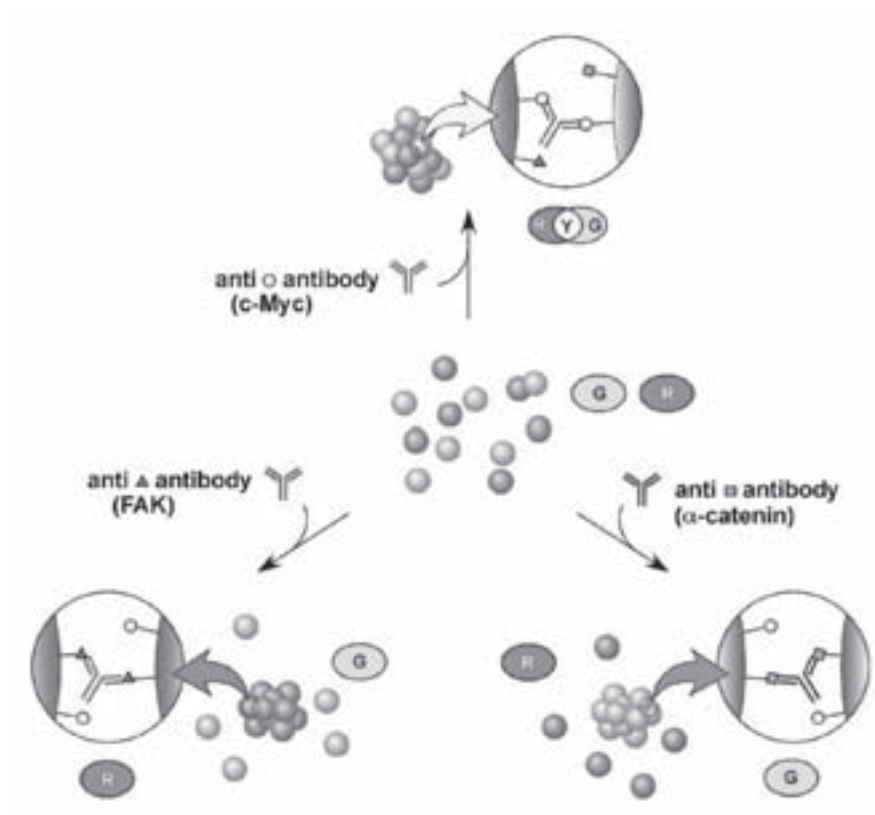


Fig 4 : Schematic illustration of the MAIA using selective aggregation of antigenic peptide-modified nanospheres.

Fig 5 : Multiprotein electrochemical stripping immunoassay protocol using different inorganic nanocrystal tracers: (A) introduction of antibody-immobilized magnetic beads, (B) capture of the antigens to the antibodies-immobilized magnetic beads, (C) capture of the nanocrystal-labeled secondary antibodies and formation of sandwich immunocomplexes, (D) dissolution of nanocrystals and electrochemical stripping detection.

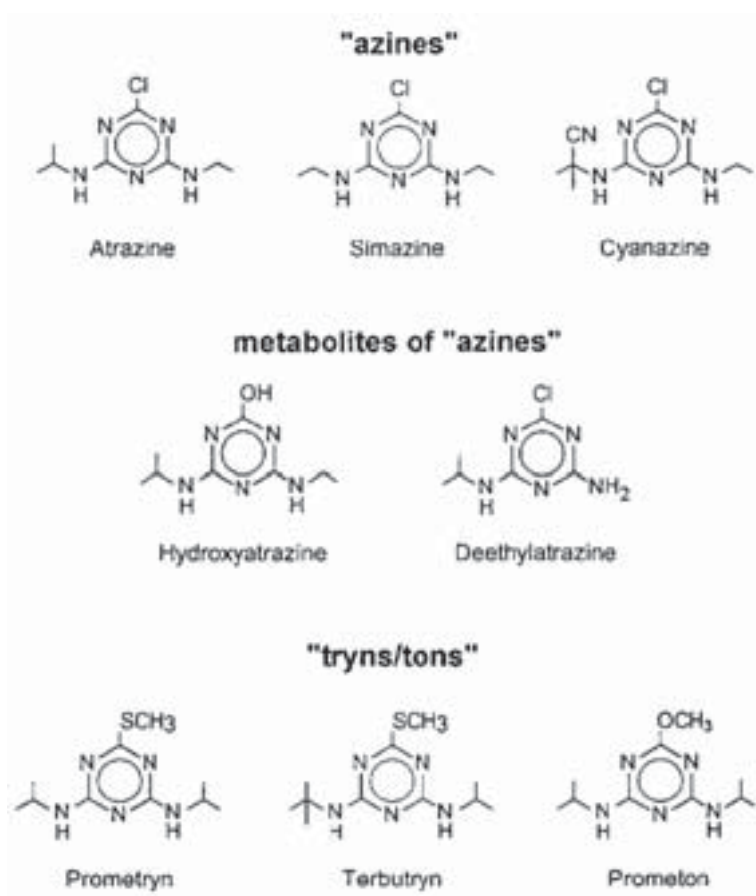
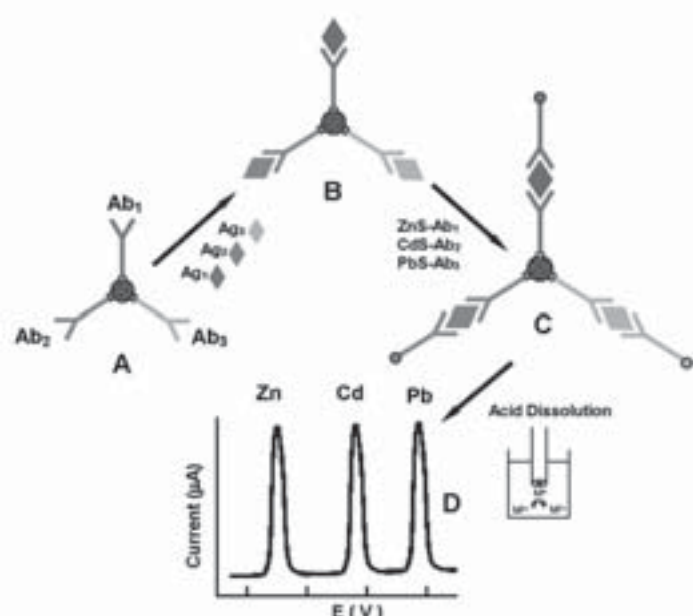


Fig 6 : Some *s*-triazines and their metabolites with similar structures.

Effective drug targeting by Erythrocytes as Carrier Systems

V.S. Gopal, A. Ranjith Kumar, A.N. Usha, A. Karthik, N. Udupa*

Manipal College of Pharmaceutical Sciences
Manipal University, Manipal, 576 104, Karnataka

* For correspondence - n.udupa@manipal.edu

Abstract

Carrier erythrocytes, resealed erythrocytes loaded by a drug or other therapeutic agents, have been exploited extensively in recent years for both temporally and spatially controlled delivery of a wide variety of drugs and other bioactive agents owing to their remarkable degree of biocompatibility, biodegradability and a series of other potential advantages. Biopharmaceuticals, therapeutically significant peptides and proteins, nucleic acid-based biologicals, antigens and vaccines, are among the recently focused pharmaceuticals for being delivered using carrier erythrocytes. In this article, the potential applications of erythrocytes in drug delivery have been reviewed with a particular stress on the studies and laboratory experiences on successful erythrocyte loading and characterization of the different classes of drugs.

Keywords

Erythrocyte, Carrier erythrocytes, Cellular carriers, Resealed erythrocytes, Carrier RBCs.

Introduction

Drug delivery is now entering quite an exciting and challenging era. Significant high costs involved in the development of new drug molecule has compelled scientists all over the world to search for alternative ways of administering the existing drug molecules with enhanced effectiveness. Improper drug administration inside the biological system not only causes distress to other body tissues but also

demands more therapeutic molecules to elicit the appropriate response. Among the various carriers used for targeting drugs to various body tissues, the cellular carriers meet several criteria desirable in clinical applications, among the most important being biocompatibility of carrier and its degradation products. Leucocytes, platelets, erythrocytes, nanoerythrocytes, hepatocytes, and fibroblasts etc. have been proposed as cellular carrier systems (1, 2). Among these, the erythrocytes have been the most investigated and have found to possess greater potential in drug delivery. Therapeutic uses of a variety of drug carrier systems have significant impact on the treatment and potential cure of many chronic diseases, including cancer, diabetes mellitus, rheumatoid arthritis, HIV infection, and drug addiction.

Erythrocytes are natural products of the body, biodegradable in nature, isolation of these is easy and large amount of drug can be loaded in small volume of cells, non immunogenic in action and can be targeted to disease tissue or organ, prolong the systemic activity of the drug while residing for a longer time in the body (3), prevent the premature degradation, inactivation and excretion of proteins and enzymes, act as a carrier for number of drugs, target the drugs within the reticuloendothelial system (RES) as well non RES organs/sites. Moreover, the possibility of targeting carrier erythrocytes to non-RES organs has been exploited in recent years, e.g., using homing devices such as IgG or IgM. Also these cells are non-immunogenic and biodegradable; they freely circulate throughout the body and

offer ease of preparation; they have the capacity to carry large amounts of drug; and can behave as a slow-release long-acting system (4). Also, as aging erythrocytes are normally phagocytized by cells of the reticuloendothelial system, thus, these cells could serve as a natural target for delivery of their payload to these organs. Potential clinical indications for “RES targeting” include iron over-storage diseases (5), parasitic diseases (6), hepatic tumors (7), and lysosomal storage diseases. Erythrocytes, also known as red blood cells, have been extensively studied for their potential carrier capabilities for the delivery of drugs and drug-loaded microspheres. Such drug-loaded carrier erythrocytes are prepared simply by collecting blood samples from the organism of interest, separating erythrocytes from plasma, entrapping drug in the erythrocytes, and resealing the resultant cellular carriers. Hence, these carriers are called resealed erythrocytes. Upon re injection, the drug-loaded erythrocytes serve as slow circulating depots and target the drugs to a reticuloendothelial system (RES).

Morphology and physiology of erythrocytes

Erythrocytes are the most abundant cells in the human body (5.4 million cells/mm³ blood in a healthy male and 4.8 million cells/mm³ blood in a healthy female). These cells were described in human blood samples by Dutch Scientist Lee Van Hock in 1674. In the 19th century, Hope Seyler identified hemoglobin and its crucial role in oxygen delivery to various parts of the body. Erythrocytes are biconcave discs with an average diameter of 7.8μm, a thickness of 2.5μm in periphery, 1μm in the center, and a volume of 85–91 μm³. The flexible, biconcave shape enables erythrocytes to squeeze through narrow capillaries, which may be only 3μm wide. Mature erythrocytes are quite simple in structure (8), they lack a nucleus and other organelles. Their plasma membrane encloses hemoglobin, a heme-containing protein that is responsible for O₂–CO₂ binding inside the erythrocytes (9). The main role of erythrocytes is the transport of O₂ from the

lungs to tissues and the CO₂ produced in tissues back to lungs. Thus, erythrocytes are a highly specialized O₂ carrier system in the body. Because a nucleus is absent, all the intracellular space is available for O₂ transport.

Erythrocytes live only about 120 days because of wear and tear on their plasma membranes as they squeeze through the narrow blood capillaries. Worn-out erythrocytes are removed from circulation and destroyed in the spleen and liver (RES), and the breakdown products are recycled. The process of erythrocyte formation within the body is known as erythropoiesis (10). In a mature human being, erythrocytes are produced in red bone marrow under the regulation of a hemopoietic hormone called erythropoietin.

Source and isolation of erythrocytes

Various types of mammalian erythrocytes have been used for drug delivery, including erythrocytes of mice, cattle, pigs, dogs, sheep, goats, monkeys, chicken, rats, and rabbits. To isolate erythrocytes, blood is collected in heparinized tubes by venipuncture (11).

Fresh blood is typically used for loading purposes because the encapsulation efficiency of the erythrocytes isolated from fresh blood is higher than that of the aged blood. Freshly collected blood is immediately frozen to 4 °C and stored, it can be used for a period of two days. The erythrocytes are then harvested and washed by centrifugation. The washed cells are suspended in buffer solutions at various hematocrit values as desired and are often stored in acid–citrate–dextrose buffer at 4 °C for a period of 48 h before use (12).

Advantages of erythrocytes as drug carriers (13)

1. These are biocompatible, particularly when autologous cells are used, hence no possibility of triggered immune response and circulate throughout the body.

2. These are biodegradable carriers with no generation of toxic products, relatively inert in intracellular environment and wide variety of drugs that can be loaded.
3. These carriers prevent degradation of the loaded drug from inactivation by endogenous chemicals.
4. These carriers can be used for modification of pharmacokinetic and pharmacodynamic parameters of drug and attains steady-state plasma concentration thereby decreases fluctuations in blood concentration. The incorporated drug can be released in zero-order kinetics

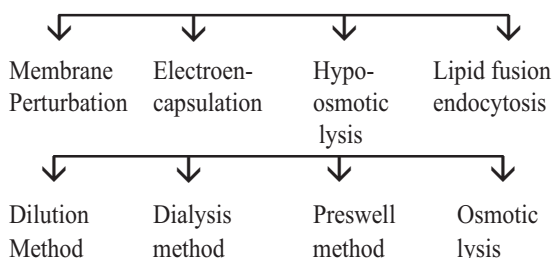
Erythrocytes can be used as carriers in two ways (14)

1. Targeting particular tissue/organ
2. For continuous or prolonged release of drugs.

For targeting, only the erythrocyte membrane is used. This is obtained by splitting the cell in hypotonic solution and after introducing the drug into the cells, allowing them to reseal into spheres. Such erythrocytes are called Red cell ghosts. Ghosts do not remain in the circulation for a long time as they are quickly sequestered and rapidly phagocytosed by the reticulo endothelial cells in the liver and spleen. The disadvantage of using ghosts is that they can be targeted only to those tissues which contain phagocytic cells (liver and spleen) and not to all other tissues in the body alternatively, erythrocytes can be used as a continuous or prolonged release system, which provides prolonged drug action. There are different methods for encapsulation of drugs within erythrocytes. They remain in the circulation for prolonged periods of time (up to 120 days) and release the entrapped drug at a slow and steady rate.

Various methods of preparation of resealed erythrocytes

Methods of Drug loading in resealed Erythrocytes



When erythrocytes are osmotically lysed and then resealed, there is an exchange of intracellular and extracellular solutes. Therefore, a drug added during the lysis procedures will be encapsulated within the membrane envelope of erythrocytes.

Methods of drug loading (15)

Several methods can be used to load drugs or other bioactive compounds in erythrocytes, including physical (electrical pulse method) osmosis-based systems, and chemical methods (chemical perturbation of the erythrocytes membrane). Irrespective of the method used, the optimal characteristics for the successful entrapment of the compound requires the drug to have a considerable degree of water solubility, resistance against degradation within erythrocytes, lack of physical or chemical interaction with erythrocyte membrane, and well-defined pharmacokinetic and pharmacodynamic properties. The comparison of different types of methods of drug entrapment is shown table 1. Schematic representation of entrapment of drug into erythrocytes is given in figure 1.

Hypotonic hemolysis (16)

This method is based on the ability of erythrocytes to undergo reversible swelling in a hypotonic solution. Erythrocytes have an exceptional capability for reversible shape changes with or without accompanying volume change and for reversible deformation under stress. An increase in volume leads to an initial

change in the shape from biconcave to spherical. This change is attributable to the absence of superfluous membrane; hence the surface area of the cell is fixed. The cells assume a spherical shape to accommodate additional volume while keeping the surface area constant. The volume gain is ~25–50%. The cells can maintain their integrity up to a tonicity of ~150 mosm/kg, above which the membrane ruptures, releasing the cellular contents. At this point (just before cell lysis), some transient pores of 200–500 Å are generated on the membrane. After cell lysis, cellular contents are depleted. The remnant is called an erythrocyte ghost.

The principle of using these ruptured erythrocytes as drug carriers is based on the fact that the ruptured membranes can be resealed by restoring isotonic conditions. Upon incubation, the cells resume their original biconcave shape and recover original impermeability.

Use of red cell loader (17)

Novel method for entrapment of non-diffusible drugs into erythrocytes. Piece of equipment called a “red cell loader”. With as little as 50 mL of a blood sample, different biologically active compounds were entrapped into erythrocytes within a period of 2h at room temperature. The process is based on two sequential hypotonic dilutions of washed erythrocytes followed by concentration with a hemofilter and an isotonic resealing of the cells. There was ~30% drug loading with 35–50% cell recovery. The processed erythrocytes had normal survival *in vivo*. The same cells could be used for targeting by improving their recognition by tissue macrophages.

Hypotonic dilution (18)

Hypotonic dilution was the first method investigated for the encapsulation of chemicals into erythrocytes and is the simplest and fastest. In this method, a volume of packed erythrocytes

is diluted with 2–20 volumes of aqueous solution of a drug. The solution tonicity is then restored by adding a hypertonic buffer. The resultant mixture is then centrifuged, the supernatant is discarded, and the pellet is washed with isotonic buffer solution. The major drawbacks of this method include low entrapment efficiency and a considerable loss of hemoglobin and other cell components. This reduces the circulation half life of the loaded cells. These cells are readily phagocytosed by RES macrophages and hence can be used for targeting RES organs. Hypotonic dilution is used for loading enzymes such as β galactosidase and β glucosidase, asparaginase, and arginase, as well as bronchodilators such as salbutamol.

Hypotonic preswelling (19)

This method was developed by Rechsteiner in 1975 and was modified by Jenner et al. for drug loading. The technique is based upon initial controlled swelling in a hypotonic buffered solution. This mixture is centrifuged at low g values. The supernatant is discarded and the cell fraction is brought to the lysis point by adding 100–120 μ L portions of an aqueous solution of the drug to be encapsulated.

The mixture is centrifuged between the drug-addition steps. The lysis point is detected by the disappearance of a distinct boundary between the cell fraction and the supernatant upon centrifugation. The tonicity of a cell mixture is restored at the lysis point by adding a calculated amount of hypertonic buffer. Then, the cell suspension is incubated at 37° C to re anneal the resealed erythrocytes. Such cells have a circulation half life comparable to that of normal cells. This method is simpler and faster than other methods, causing minimum damage to cells. Drugs encapsulated in erythrocytes using this method include propranolol, methotrexate, insulin, metronidazole, levothyroxine, enalaprilat, and isoniazid.

Hypotonic dialysis (20)

Several methods are based on the principle that semipermeable dialysis membrane maximizes the intracellular:extracellular volume ratio for macromolecules during lysis and resealing. In the process, an isotonic, buffered suspension of erythrocytes with a hematocrit value of 70–80 is prepared and placed in a conventional dialysis tube immersed in 10–20 volumes of a hypotonic buffer. The medium is agitated slowly for 2 h. The tonicity of the dialysis tube is restored by directly adding a calculated amount of a hypertonic buffer to the surrounding medium or by replacing the surrounding medium by isotonic buffer. The drug to be loaded can be added by either dissolving the drug in isotonic cell suspending buffer inside a dialysis bag at the beginning of the experiment or by adding the drug to a dialysis bag after the stirring is complete. In this method, the erythrocyte suspension and the drug to be loaded were placed in the blood compartment and the hypotonic buffer was placed in a receptor compartment. This led to the concept of “continuous flow dialysis,” which has been used by several other researchers.

This method has been used for loading enzymes such as β galactosidase, glucoserebrosidase, asparaginase, inositol hexaphosphatase, as well as drugs such as gentamicin, adriamycin, pentamidine and furamycin, interlukin-2, desferroxamine, and human recombinant erythropoietin.

Isotonic osmotic lysis (21)

This method, also known as the osmotic pulse method, involves isotonic hemolysis that is achieved by physical or chemical means. The isotonic solutions may or may not be isoionic. If erythrocytes are incubated in solutions of a substance with high membrane permeability, the solute will diffuse into the cells because of the concentration gradient. This process is followed by an influx of water to maintain osmotic

equilibrium. Chemicals such as urea solution, polyethylene glycol, and ammonium chloride have been used for isotonic hemolysis. However, this method also is not immune to changes in membrane structure composition. In 1987, Franco et al. developed a method that involved suspending erythrocytes in an isotonic solution of dimethyl sulfoxide (DMSO). The suspension was diluted with an isotonic-buffered drug solution. After the cells were separated, they were resealed at 37 °C.

Chemical perturbation of the membrane (22)

This method is based on the increase in membrane permeability of erythrocytes when the cells are exposed to certain chemicals. In 1973, Deuticke et al showed that the permeability of erythrocytic membrane increases upon exposure to polyene antibiotic such as amphotericin B. In 1980, this method was used successfully by Kitao and Hattori to entrap the antineoplastic drug daunomycinin human and mouse erythrocytes. Lin et al used halothane for the same purpose. However, these methods induce irreversible destructive changes in the cell membrane and hence are not very popular.

Electro-insertion or electroencapsulation (23)

In 1973, Zimmermann tried an electrical pulse method to encapsulate bioactive molecules. Also known as electroporation, the method is based on the observation that electrical shock brings about irreversible changes in an erythrocyte membrane. In 1977, Tsong and Kinosita suggested the use of transient electrolysis to generate desirable membrane permeability for drug loading. The erythrocyte membrane is opened by a dielectric breakdown. Subsequently, the pores can be resealed by incubation at 37 °C in an isotonic medium. The procedure involves suspending erythrocytes in an isotonic buffer in an electrical discharge chamber. A capacitor in an external circuit is charged to a definite voltage and then discharged within a definite time interval through cell suspension to produce a square-wave

potential. The optimum intensity of an electric field is between 1–10 kW/cm and optimal discharge time is between 20–160 μ s. An inverse relationship exists between the electric-field intensity and the discharge time. The compound to be entrapped is added to the medium in which the cells are suspended from the commencement of the experiment. The characteristic pore diameter created in the membrane depends upon the intensity of electric field, the discharge time, and the ionic strength of suspending medium. The colloidal macromolecules contents of the cell may lead to cell lysis because of the increase in osmotic pressure. This process can be prevented by adding large molecules (e.g., tetrasaccharide stachyose and bovine serum albumin) and ribonucleose.

One advantage of this method is a more uniform distribution of loaded cells in comparison with osmotic methods. The main drawbacks are the need for special instrumentation and the sophistication of the process. Entrapment efficiency of this method is >35%, and the life span of the resealed cells in circulation is comparable with that of normal cells.

Various compounds such as sucroseurease, methotrexate, isoniazid, DNA fragments, and latex particles of diameter 0.2 μ m can be entrapped within erythrocytes by this method. Mangal and Kaur achieved sustained release of a drug entrapped in erythrocytes with the use of electroporation.

Entrapment by endocytosis (24)

This method was reported by Schrier et al. in 1975. Endocytosis involves the addition of one volume of washed erythrocytes to nine volumes of buffer containing 2.5 mM ATP, 2.5 mM MgCl₂, and 1mM CaCl₂, followed by incubation for 2 min at room temperature. The pores created by this method are resealed by using 154 mM of NaCl and incubation at 37 °C for 2 min. The entrapment of material occurs by endocytosis. The vesicle membrane separates endocytosed

material from cytoplasm thus protecting it from the erythrocytes and vice-versa. The various candidates entrapped by this method include primaquine and related 8-amino-quinolines, vinblastine, chlorpromazine and related phenothiazines, hydrocortisone, propranolol, tetracaine, and vitamin A.

Loading by electric cell fusion (25)

This method involves the initial loading of drug molecules into erythrocyte ghosts followed by adhesion of these cells to target cells. The fusion is accentuated by the application of an electric pulse, which causes the release of an entrapped molecule. An example of this method is loading a cell-specific monoclonal antibody into an erythrocyte ghost. An antibody against a specific surface protein of target cells can be chemically cross-linked to drug-loaded cells that would direct these cells to desired cells.

Loading by lipid fusion (26)

Lipid vesicles containing a drug can be directly fused to human erythrocytes, which lead to an exchange with a lipid-entrapped drug. This technique was used for entrapping inositol monophosphate to improve the oxygen carrying capacity of cells. However, the entrapment efficiency of this method is very low (~1%).

***In vitro* characterization**

The *in vivo* performance of resealed erythrocytes is affected to a great extent by their biological properties. Hence, *in vitro* characterization forms an important part of studies involving such cellular carriers.

Physical characterization (27)

Shape, surface morphology, vesicle size and size distribution of drug loaded erythrocytes can be studied by using transmission electron microscopy, scanning electron microscopy (Figure 2 and 3), phase contrast microscopy, optical microscopy (28). Drug release from the erythrocytes can be carried using diffusion cell

method. Surface charge of the erythrocytes can be measured by zeta potential measurement.

Cellular characterization (29)

Percentage Hb content is determined by deproteinization of cell membrane followed by hemoglobin assay. Percentage cell recovery is carried out by Neubaur's chamber and hematological analyzer. Osmotic fragility test involves stepwise incubation with isotonic to hypotonic saline solutions and determination of drug and hemoglobin assay. Osmotic shock is determined by dilution with distilled water and estimation of drug and hemoglobin. Turbulent shock is determined by Passage of cell suspension through 30- gauge hypodermic needle at 10 mL/min flow rate and estimation of residual drug and hemoglobin, vigorous shaking followed by hemoglobin estimation. Erythrocyte sedimentation rate by ESR methods.

Biological characterization (30)

Biological characterization of the developed erythrocytes includes sterility test, pyrogenicity test, LAL test and toxicity tests. The morphology of erythrocytes decides their life span after administration. Light microscopy reveals no observable change in resealed cells but in few cases spherical erythrocytes (spherocytes) are detected. Scanning electron microscopic studies will show that a majority of the cells maintain their biconcave discoid shapes after the loading procedure, and few stomatocytes—a form of spherocytes. In some cases, cells of smaller size (microcyte) are also observed.

Shape change (deformability) is another factor that affects the life span of the cells. This parameter evaluates the ease of passage of erythrocytes through narrow capillaries and the RES. It determines the rheological behavior of the cells and depends on the viscoelasticity of the cell membrane, viscosity of the cell contents, and the cellular surface-to-volume ratio. The deformability is measured by passage time of

definite volume of cells through capillary of 4 μm diameter or polycarbonate filter with average pore size of 45 μm . Another indirect approach is to evaluate chlorpromazine induced shape changes turbidimetrically.

The osmotic fragility of resealed erythrocytes is an indicator of the possible changes in cell membrane integrity and the resistance of these cells to osmotic pressure of the suspension medium. The test is carried out by suspending cells in media of varying sodium chloride concentration and determining the hemoglobin released. In most cases, osmotic fragility of resealed cells is higher than that of the normal cells because of increased intracellular osmotic pressure.

The turbulence fragility is yet another characteristic that depends upon changes in the integrity of cellular membrane and reflects resistance of loaded cells against hemolysis resulting from turbulent flow within circulation. It is determined by the passage of cell suspension through needles with smaller internal diameter (e.g., 30 gauges) or vigorously shaking the cell suspension. In both cases, hemoglobin and drug released after the procedure are determined. The turbulent fragility of resealed cells is found to be higher.

Routine clinical hematological tests also can be carried out for drug-loaded cells, including mean corpuscular volume, mean corpuscular hemoglobin, mean corpuscular hemoglobin content.

Studies have shown that the average size and hemoglobin content of resealed cells is lower than that of normal cells.

Drug release kinetics

The most important parameters for evaluation of resealed erythrocytes are the drug release pattern. Hemoglobin is also invariably released because drug release involves the loss of cell membrane integrity indicating hemolysis. On the basis of

the various *in vitro* release experiments carried out on these cells, three general drug release patterns are observed:

- The rate of drug release is considerably higher than that of hemoglobin. In other words, drug diffuses readily. Such a pattern is shown by lipophilic drugs, including methotrexate, phenytoin, dexamethasone, primpquin, and vitamin B12. Cell lysis is not essential for the release of such drugs.
- The rate of drug release is comparable to that of hemoglobin. This indicates that cell lysis is essential for drug release and drug can not be released by mere diffusion. Polar drugs such as gentamicin, heparin, and enalaprilat, and enzymes such as asparaginase, peptides, including urogasterone and l-lysine-l-phenylalanine follow such pattern.
- The rate of drug release lies between the above mentioned two extremes; for example, propranolol, isoniazid, metronidazole, and recombinant human erythropoietin.

The two factors that determine the drug release pattern are size and polarity of the drug molecule. The release rate can be modified by cross-linking cell membrane with glutaraldehyde, which results in a slower drug release. This can also be achieved by entrapping biodegradable prodrug such as o-acetyl propranolol, o-pivaloyl propranolol, cortisol-21-phosphate, prednisolone-21-sodium succinate, and cytosine arabinoside monophosphate. The complexation of a drug with macromolecules such as dextran and albumin also retard the release rate.

Mechanism of release of resealed erythrocytes (31)

- Phagocytosis
- Diffusion through the membrane of cell
- Using a specific transport system

The rate of diffusion depends upon the rate at which a particular molecule penetrates through

a lipid bilayer. Many substances enter cells by a specific membrane protein system because the carriers are proteins with many properties analogous to that of enzymes, including specificity e.g. nucleotides and nucleosides. Release of drugs from erythrocytes is rapid followed by sustained release profile and rate of exit is proportional to the instantaneous intracellular drug concentration (first order kinetics). By incorporating polymer into erythrocytes, the release pattern may be modified. The drug, however, could be resealed from macrophages after phagocytosis if the linkage is susceptible to lysosomal enzymes.

***In vitro* storage (32)**

The success of resealed erythrocytes as a drug delivery system depends to a greater extent on their *in vitro* storage. Preparing drug-loaded erythrocytes on a large scale and maintaining their survival and drug content can be achieved by using suitable storage methods. However, the lack of reliable and practical storage methods has been a limiting factor for the wide-spread clinical use of the carrier erythrocytes.

The most common storage media include Hank's balanced salt solution and acid-citrate-dextrose at 4 °C. Cells remain viable in terms of their physiologic and carrier characteristics for at least 2 weeks at this temperature. The addition of calcium-chelating agents or the purine nucleosides improve circulation survival time of cells upon reinjection.

Exposure of resealed erythrocytes to membrane stabilizing agents such as dimethyl sulfoxide, dimethyl,3,3-di-thio-bispropionamide, glutaraldehyde, toluene-2-4-diisocyanate followed by lyophilization or sintered glass filtration has been reported to enhance their stability upon storage. The resultant powder was stable for at least one month without any detectable changes. But the major disadvantage of this method is the presence of appreciable amount of membrane stabilizers in bound form

that remarkably reduces circulation survival time. Other reported methods for improving storage stability include encapsulation of a prodrug that undergoes conversion to the parent drug only at body temperature, high glycerol freezing technique, and reversible immobilization in alginate or gelatin gels.

Crosslinking, stability and *in-vivo* survival of resealed erythrocytes (33)

The cells treated with dimethyl sulphoxide (DMSO), toluene 2, 4-di-isocyanate (TDI) and gluteraldehyde are even resistant to sonication, freezing and thawing. Chemically cross linking of erythrocytes renders a yield of 55-97% of non-lysed cells. An attempt was made to get drug loaded cells in lyophilized form. The dried powder was filled in amber color glass vials and stored at 4°C for one month. Improvement in shelf-life of the carrier erythrocytes was achieved by storing the cells in powder form ready for reconstitution at 4°C. This is important in the large scale manufacturing of drug loaded erythrocytes.

***In vivo* life span (34)**

The efficacy of resealed erythrocytes is determined mainly by their survival time in circulation upon reinjection. For the purpose of sustained action, a longer life span is required, although for delivery to target-specific RES organs, rapid phagocytosis and hence a shorter life span is desirable. The life span of resealed erythrocytes depends upon its size, shape, and surface electrical charge as well as the extent of hemoglobin and other cell constituents lost during the loading process.

The various methods used to determine *in vivo* survival time include labeling of cells by ⁵¹Cr or fluorescent markers such as fluorescein isothiocyanate or entrapment of ¹⁴C sucrose or gentamicin.

The circulation survival kinetics of resealed erythrocytes show typical bimodal behavior with

a rapid loss of cells during the first 24 h after injection, followed by a slow decline phase with a half life on the order of days or weeks. The early loss accounts for ~15–65% loss of total injected cells. The erythrocytic carriers constructed of red blood cells of mice, cattle, pigs, dogs, sheep, goats, and monkeys exhibit a comparable circulation profile with that of normal unloaded erythrocytes. On the other hand, resealed erythrocytes prepared from red blood cells of rabbits, chickens, and rats exhibit relatively poor circulation profile.

Applications of resealed erythrocytes (35)

Resealed erythrocytes have several possible applications in various fields of human and veterinary medicine. Such cells could be used as circulating carriers to disseminate a drug within a prolonged period of time in circulation or in target-specific organs, including the liver, spleen, and lymph nodes. A majority of the drug delivery studies using drug-loaded erythrocytes are in the preclinical phase. In a few clinical studies, successful results were obtained.

Slow drug release (36)

Erythrocytes have been used as circulating depots for the sustained delivery of antineoplastics, antiparasitics, veterinary antiamoebics, vitamins, steroids, antibiotics, and cardiovascular drugs.

Drug targeting (37)

Ideally, drug delivery should be site-specific and target-oriented to exhibit maximal therapeutic index with minimum adverse effects. Resealed erythrocytes can act as drug carriers and targeting tools as well. Surface-modified erythrocytes are used to target organs of mononuclear phagocytic system/ reticuloendothelial system because the changes in the membrane are recognized by macrophages. However, resealed erythrocytes also can be used to target organs other than those of RES.

Targeting RES organs (38)

Damaged erythrocytes are rapidly cleared from circulation by phagocytic Kupffer cells in liver and spleen. Resealed erythrocytes, by modifying their membranes, can therefore be used to target the liver and spleen. The various approaches to modify the surface characteristics of erythrocytes include Surface modification with antibodies, gluteraldehyde, sialic acid, sulphhydryl and Surface chemical cross-linking e.g. delivery of ¹²⁵I-labeled carbonicanhydrase loaded in erythrocytes cross-linked with sulfosuccinimidyl propionate.

Targeting the liver- Enzyme deficiency/ replacement therapy (39)

Many metabolic disorders related to deficient or missing enzymes can be treated by injecting these enzymes. However, the problems of exogenous enzyme therapy include a shorter circulation half life of enzymes, allergic reactions, and toxic manifestations.

These problems can be successfully overcome by administering the enzymes as resealed erythrocytes. The enzymes used include β glucosidase, β glucuronidase, β galactosidase. The disease caused by an accumulation of glucocerebrosides in the liver and spleen can be treated by glucocerebrosidase- loaded erythrocytes.

Treatment of hepatic tumors (40)

Hepatic tumors are one of the most prevalent types of cancer. Antineoplastic drugs such as methotrexate, bleomycin, asparaginase and adriamycin have been successfully delivered by erythrocytes. Agents such as daunorubicin diffuse rapidly from the cells upon loading and hence pose a problem. This problem can be overcome by covalently linking daunorubicin to the erythrocytic membrane using gluteraldehyde or cisaconitic acid as a spacer. The resealed erythrocytes loaded with carboplatin show localization in liver.

Treatment of parasitic diseases

The ability of resealed erythrocytes to selectively accumulate within RES organs make them useful tool during the delivery of antiparasitic agents. Parasitic diseases that involve harboring parasites in the RES organs can be successfully controlled by this method. Results were favorable in studies involving animal models for erythrocytes loaded with antimalarial, antileishmanial and antiamebic drugs.

Removal of RES iron overload

Desferrioxamine-loaded erythrocytes have been used to treat excess iron accumulated because of multiple transfusions to thalassemic patients. Targeting this drug to the RES is very beneficial because the aged erythrocytes are destroyed in RES organs, which results in an accumulation of iron in these organs.

Removal of toxic agents

Cannon et al. reported inhibition of cyanide intoxication with murine carrier erythrocytes containing bovine rhodanase and sodium thiosulfate. Antagonization of organophosphorus intoxication by resealed erythrocytes containing a recombinant phosphodiesterase also has been reported.

Targeting organs other than those of RES

Recently, resealed erythrocytes have been used to target organs outside the RES. The various approaches include Entrapment of paramagnetic particles, photosensitive material along with the drug and Antibody attachment to erythrocyte membrane to get specificity of action.

Zimmermann proposed that the entrapment of small paramagnetic particles into erythrocytes might allow their localization to a particular location under the influence of an external magnetic field. The loading of ferrofluids (colloidal suspension of magnetite) has been reported by Sprandel et al. Jain and Vyas reported entrapment of the anti-inflammatory drugs

diclofenac sodium and ibuprofen in magnetoresponsive erythrocytes. Photosensitized erythrocytes have been studied as a phototriggered carrier and delivery system for methotrexate in cancer treatment. Chiarantini et al. have reported in vitro targeting of erythrocytes to cytotoxic T-cells by coupling of Thy-1.2 monoclonal antibody.

Price et al. reported delivery of colloidal particles and erythrocytes to tissue through microvessel ruptures created by targeted microbubble destruction with ultrasound. IV fluorescent erythrocytes were delivered to the interstitium of rat skeletal muscle through microvessel ruptures by insonifying microbubbles *in vivo*. This technique provides a noninvasive means for delivering resealed erythrocytes across the endothelial carrier to the target tissue. Other approaches for targeting organs outside the RES include the preparation of carrier erythrocytes fused to thermoresponsive liposomes and their localization using an external thermal source, intraperitoneal injection of resealed erythrocytes for drug targeting to peritoneal macrophages, and lectin pretreatment of resealed cells loaded with antineoplastic drugs to improve targeting tumor cells.

Delivery of antiviral agents

Several reports have been cited in the literature about antiviral agents entrapped in resealed erythrocytes for effective delivery and targeting. Because most antiviral drugs are nucleotides or nucleoside analogs, their entrapment and exit through the membrane needs careful consideration. Nucleosides are rapidly transported across the membrane whereas nucleotides are not, and thus exhibiting prolonged release profiles. The release of nucleotides requires conversion of these moieties to purine or pyrimidine bases. Resealed erythrocytes have been used to deliver deoxycytidine derivatives, recombinant herpes simplex virus type 1 (HSV-1) glycoprotein B, azidothymidine derivatives,

azathioprene, acyclovir, and fludarabine phosphate.

Enzyme therapy

Enzymes are widely used in clinical practice as replacement therapies to treat diseases associated with their deficiency (e.g., Gaucher's disease, galactosuria), degradation of toxic compounds secondary to some kind of poisoning (cyanide, organophosphorus), and as drugs. The problems involved in the direct injection of enzymes into the body have been cited. One method to overcome these problems is the use of enzyme-loaded erythrocytes. These cells then release enzymes into circulation upon hemolysis act as a "circulating bioreactors" in which substrates enter into the cell, interact with enzymes, and generate products or accumulate enzymes in RES upon hemolysis for future catalysis.

The first report of successful clinical trials of the resealed erythrocytes loaded with enzymes for replacement therapy is that of β glucoserebrosidase for the treatment of Gaucher's disease. The disease is characterized by inborn deficiency of lysosomal β glucoserebrosidase in cells of RES thereby leading to accumulation of β glucoserebrosides in macrophages of the RES.

The most important application of resealed erythrocytes in enzyme therapy is that of asparaginase loading for the treatment of pediatric neoplasms. This enzyme degrades asparagine, an amino acid vital for cells. This treatment prevents remission of pediatric acute lymphocytic leukemia. There are reports of improved intensity and duration of action in animal models as well as humans.

To treat lead poisoning, the concentration of β aminolevulinic acid dehydrogenase (ALA-D) in erythrocytes decreases. This leads to an accumulation of β aminolevulinic acid in tissues, blood, and urine. This state leads to acute porphyria and CNS-related problems. An injection

of resealed erythrocytes loaded with ALA-D to lead intoxicated animal significantly reduces toxic manifestations. Other enzymes used for loading resealed erythrocytes include urease, galactose-1-phosphate uridyl transferase, uricase and acetaldehyde dehydrogenase.

Improvement in oxygen delivery to tissues

Hemoglobin is the protein responsible for the oxygen-carrying capacity of erythrocytes. Under normal conditions, 95% of hemoglobin is saturated with oxygen in the lungs, whereas under physiologic conditions in peripheral blood stream only ~25% of oxygenated hemoglobin becomes deoxygenated. Thus, the major fraction of oxygen bound to hemoglobin is recirculated with venous blood to the lungs. The use of this bound fraction has been suggested for the treatment of oxygen deficiency. 2, 3-Diphosphoglycerate (2,3-DPG) is a natural effector of hemoglobin. The binding affinity of hemoglobin for oxygen changes reversibly with changes in intracellular concentration of 2, 3-DPG. This compensates for changes in the oxygen pressure outside of the body, as the affinity of 2, 3-DPG to oxygen is much higher than that of hemoglobin.

Other organic polyphosphates can serve as allosteric effectors of hemoglobin with binding affinities higher than those of 2, 3-DPG and can compete with 2, 3-DPG for binding to hemoglobin. Inositol hexophosphate (IHP) is one of the strongest effectors of this type. However, because of its ionization at physiologic pH, it cannot enter erythrocytes. Hence, it is entrapped by the electroporation process.

Upon encapsulation, IHP irreversibly binds to hemoglobin, thereby decreasing the oxygen affinity to hemoglobin and subsequent shift of oxygen binding isotherm to the right. As a result, the oxygen pressure corresponding to 50% of the total binding capacity of hemoglobin to oxygen (P₅₀ value) increases from 26–27 mm Hg to >50 mm Hg. In the presence of IHP encapsulated in erythrocytes, the difference between the oxygen

bound fraction of hemoglobin in lungs and tissues increases, thereby increasing the oxygen concentration in tissues. Also, the extent of carbamate formed in the N-terminal amine group of β chain of hemoglobin decreases, which is compensated by an uptake of H⁺ and CO₂ that leads to increased formation of bicarbonate ion.

Intravenous injection of IHP-loaded erythrocytes to piglets led to a decrease in cardiac output with a constant oxygen consumption by animals. This indicates that because of an increased extraction ratio of oxygen by tissues, a given amount of oxygen can be delivered in lower blood flow. In addition, these erythrocytes reduce ejection fraction, left ventricular diastolic volume, and heart rate. An isolated perfused-heart model showed reduction in coronary blood flow with increased oxygen consumption by myocardium upon administration of IHP-loaded erythrocytes. The same results are reported when intact animal models were used.

An application of IHP-loaded erythrocytes for improved oxygen supply is beneficial under the following conditions, such as high altitude conditions where the partial pressure of oxygen is low, reduction in the number of alveoli, where exchange surface of the lungs is decreased, increased resistance to oxygen diffusion in the lungs, reduction in oxygen transport capacity, mutation or chemical modification, which involves a decrease in oxygen affinity for hemoglobin, increased radiosensitivity of radiation-sensitive tumors, restoration of oxygen-delivery capacity of stored blood and ischemia of myocardium, brain, or other tissues.

Microinjection of macromolecules (41)

Biological functions of macromolecules such as DNA, RNA, and proteins are exploited for various cell biological applications.

Hence, various methods are used to entrap these macromolecules into cultured cells (e.g., microinjection). A relatively simple structure and

a lack of complex cellular components (e.g., nucleus) in erythrocytes make them good candidates for the entrapment of macromolecules. In microinjection, erythrocytes are used as microsyringes for injection to the host cells.

The microinjection process involves culturing host eukaryotic cells *in vitro*. The cells are coated with fusogenic agent and then suspended with erythrocytes loaded with the compound of interest in an isotonic medium. Sendai virus (hemagglutinating virus of Japan, HVJ) or its glycoproteins or polyethylene glycol have been used as fusogenic agents. The fusogen causes fusion of cosuspended erythrocytes and eukaryotic cells. Thus, the contents of resealed erythrocytes and the compound of interest are transferred to host cell. This procedure has been used to microinject DNA fragments, arginase, proteins, nucleic acids, ferritin, latex particles, bovine and human serum albumin, and enzyme thymidine kinase to various eukaryotic cells.

Advantages of this method include quantitative injection of materials into cells, simultaneous introduction of several materials into a large number of cells, minimal damage to the cell, avoidance of degradation effects of lysosomal enzymes and simplicity of the technique. Disadvantages include a need for a larger size of fused cells, thus making them amenable to RES clearance, adverse effects of fusogens and unpredictable effects on cell resulting from the co-introduction of various components. Hence, this method is limited to mainly cell biological applications rather than drug delivery.

Novel approaches

Erythroosomes

These are specially engineered vesicular systems that are chemically cross-linked to human erythrocytes support upon which a lipid bilayer is coated (42). This process is achieved by modifying a reverse-phase evaporation technique. These vesicles have been proposed as

useful encapsulation systems for macromolecular drugs.

Nanoerythroosomes

These are prepared by extrusion of erythrocyte ghosts to produce small vesicles with an average diameter of 100 nm (43). Daunorubicin was covalently conjugated to nanoerythroosomes using gluteraldehyde spacer. This complex was more active than free daunorubicin alone, both *in vitro* and *in vivo*.

Conclusion

The use of resealed erythrocytes looks promising for a safe and effective delivery of various drugs for passive and active targeting. However, the concept needs further optimization to become a routine drug delivery system. The same concept also can be extended to the delivery of biopharmaceuticals and much remains to be explored regarding the potential of resealed erythrocytes.

References

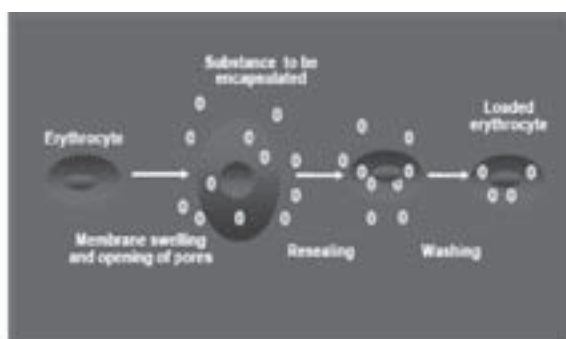
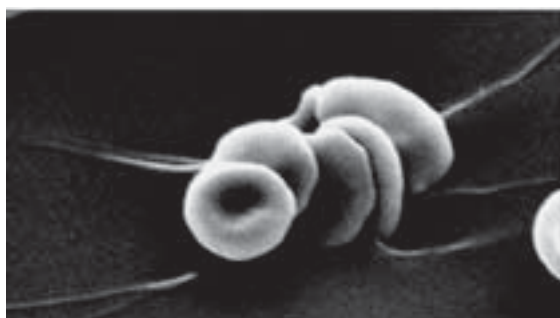
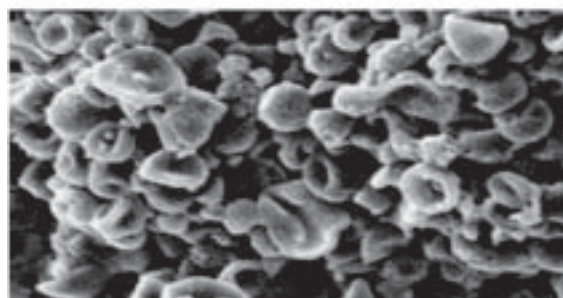
1. Gothoskar, A.V. (2004). Resealed erythrocytes: a Review. Pharm Tech. March. 1-6, Fraternal, A.
2. Rossi, L. and Magnani, M. (1996). Encapsulation, Metabolism, and Release of 2-Fluoro-Ara-AMP from Human Erythrocytes. Biochim. Biophys. Acta. 1291 (2): 149–154.
3. Lejeune, A., Poyet, P., Gaudreault, R.C., Gicquaud, C. (1997). Nanoerythroosomes, A New Derivative of Erythrocyte Ghost: III. Is Phagocytosis Involved in the Mechanism of Action?. Anticancer Res. 17: 5A.
4. Al-Achi, A. and Boroujerdi, M. (1990). Pharmacokinetics and tissue uptake of doxorubicin associated with erythrocyte-membrane: erythrocytes-ghosts vs. erythrocytes-vesicles. Dev. Ind. Pharm. 16: 2199–2219.
5. Jain, S. and Jain, N.K. (1997). Engineered Erythrocytes as a Drug Delivery System. Indian J. Pharm. Sci. 59: 275–281.

6. Jain, S., Jain, S.K., Dixit, V.K. (1995). Erythrocytes Based Delivery of Isoniazid: Preparation and In Vitro Characterization. *Indian Drugs* 32: 471–476.
7. Guyton, C.A. and Hall, J.E. (1996). Red Blood Cells, Anemia and Polycythemia,” in *Textbook of Medical Physiology* (W.B. Saunders, Philadelphia, PA.), pp. 425–433.
8. Jain, S., Jain, S.K., Dixit, V.K. (1997). Magnetically Guided Rat Erythrocytes Bearing Isoniazid: Preparation, Characterization, and Evaluation. *Drug Dev. Ind. Pharm.* 23: 999–1006.
9. Torotra, G.J. and Grabowski, S.R. (1993). The Cardiovascular System: The Blood,” in *Principles of Anatomy and Physiology* (Harper Collins College Publishers, New York, NY, 7th ed.), pp. 566–590
10. Jain, S.K. and Vyas, S.P. (1994). Magnetically Responsive Diclofenac Sodium- Loaded Erythrocytes: Preparation and In Vitro Characterization, *J. Microencapsul.* 11 (2): 141–151.
11. Gaudreault, B., Bellemare, Lacroix, J. (1989). Erythrocyte Membrane- Bound Daunorubicin as a Delivery System in Anticancer Treatment. *Anticancer Res.* 9 (4): 1201-5.
12. Banker, G.S., Rhodes, C.T. (2002). *Modern Pharmaceutics*. Marcel Dekker Inc., New York.
13. Lewis, D.A. (1984). Red Blood Cells for Drug Delivery. *Pharm. J.* 233: 384–385.
14. Mitchell, D.H., James, G.T., and Kruse, C.A. (1990). Bioactivity of Electric Field-Pulsed Human Recombinant Interleukin-2 and Its Encapsulation into Erythrocyte Carriers. *Biotechnol. Appl. Biochem.* 12 (3): 264–275.
15. Pitt, E., Johnson, C.M., Lewis, D.A., Jenner, D.A., Offord, R.E. (1983). Encapsulation of Drugs in Intact Erythrocytes: An Intravenous Delivery System. *Biochem. Pharmacol.* 22: 3359–3368.
16. Alvarez, F.J., Jordán, J.A., Calleja, P., Lotero, L.A., Olmos, G., Díez, J.C., Tejedor, M.C. (1998). Cross-Linking Treatment of Loaded Erythrocytes Increases delivery of Encapsulated Substance to Macrophages. *Biotechnol. Appl. Biochem.* 27 (pt 2): 139–143.
17. Gutierrez Millan, C., Zarzuelo Castaneda, A., Sayalero Marinero, M.L., Lanao, J.M., (2004). Factors associated with the performance of carrier erythrocytes obtained by hypotonic dialysis. *Blood Cells Mol. Dis.* 33: 132–140.
18. Tajerzadeh, H. and Hamidi, M. (2000). Evaluation of the Hypotonic Preswelling Method for Encapsulation of Enalaprilat in Human Intact Erythrocytes. *Drug Dev. Ind. Pharm.* 26: 1247–1257.
19. Alpar, H.O. and Irwin, W.J. (1987). Some Unique Applications of Erythrocytes as Carrier Systems. *Adv. Biosci. (Series)* 67:1–9.
20. Hamidi, M., Tajerzadeh, H., (2003). Carrier erythrocytes: an overview. *Drug Deliv.* 10: 9–20.
21. Jaitely, V., Kanaujia, P., Venkatesan, N., Jain, S., Vyas, S.P. (1996). Resealed erythrocytes: carrier potentials and biomedical application. *Indian Drugs* 33: 549–589.
22. Pei, L., Omburo, G., McGuinn, W.D., Petrikovics, I., Dave, K., Raushel, F.M., Wild, J.R., DeLoach, J.R., Way, J.L. (1994). Encapsulation of Phosphotriesterase within Murine Erythrocytes. *Toxicol. Appl. Pharmacol.* 124 (2): 296–301.
23. Li, L.H., Hensen, M.L., Zhao, Y.L., Hui, S.W. (1996). Electrofusion between Heterogeneous-Sized Mammalian Cells in a Pellet: Potential Applications in Drug Delivery and Hybridoma Formation. *Biophys J.* 71 (1): 479–486.
24. Alvarez-Guerra, M. Nazaret, C. and Garay, R.P. (1998). The Erythrocyte Na, K, Cl Co Transporter and Its Circulating Inhibitor in Dahl Salt- Sensitive rats. *J Hypertens.* 10: 1499–1504. 100.

25. Hamidi, M. and Tajerzadeh, H. (2003). Carrier Erythrocytes: An Overview. *Drug Delivery* 10: 9–20.
26. Hamidi, M., Tajerzadeh, H., Dehpour, A.R., Ejtemaee-Mehr, S. (2001). ACE Inhibition in Rabbits Upon Administration of Enalaprilat-Loaded Intact Erythrocytes. *J.Pharm. Pharmacol.* 53: 1281–1289.
27. Hamidi, M., Tajerzadeh, H., Dehpour, A.R., Rouini, M.R., Ejtemaee-Mehr, S. (2001). In Vitro Characterization of Human Intact Erythrocytes Loaded by Enalaprilat. *Drug Delivery* 8: 231–237.
28. Hamidi, M., Zarei, N., Zarrin, A.H., Mohammadi-Samani, S. (2007). Preparation and in vitro characterization of carrier erythrocytes for vaccine delivery. *Int. J. Pharm.* 338: 70–78.
29. Magnani, M., Bianchi, M., Rossi, L., Stocchi, V. (1989). Acetaldehyde Dehydrogenase-Loaded Erythrocytes as Bioreactors for Removal of Blood Acetaldehyde, Alcoholism. *Clin. Exp. Res.* 13: 849–859.
30. Magnani, M. and Rossi, L. (1998). Erythrocyte Engineering for Drug Delivery and Targeting. *Biotechnol. Appl. Biochem.* 28: 1–13.
31. Moorjani, M., Lejeune, A., Gicquaud, C., Lacroix, J., Poyet, P., Gaudreault, R.C. (1996). Nanoerythrocytes, A New Derivative of Erythrocyte Ghost II: Identification of the Mechanism of Action. *Anticancer Res.* 16 (5A): 2831–2836.
32. Talwar, N. and Jain, N.K, (1992). Erythrocytes as Carriers of Primaquin Preparation: Characterization and Evaluation. *J. Controlled Release.* 20: 133–142.
33. Talwar, N., and Jain, N.K. (1992). Erythrocytes as Carriers of Metronidazole: In-Vitro Characterization. *Drug Dev. Ind. Pharm.* 18: 1799–1812.
34. Mangal, P.C., and Kaur, A. (1991). Electroporation of Red Blood Cell Membrane and its Use as a Drug Carrier System. *Ind. J. Biochem. Biophys.* 28 (3): 219–221.
35. Price, R. J., Skyba, D.M., Kaul, S., Skalak, T.C. (1998). Delivery of Colloidal Particles and Red Blood Cells to Tissue through Microvessel Ruptures Created by Targeted Microbubble Destruction with Ultrasound. *Circulation* 98 (13): 1264–1267.
36. Rossi, L., Serafini, S., Pierige, F., Antonelli, A., Cerasi, A., Fraternali, A., Chiarantini, L. and Magnani, M. (2005). Erythrocyte-based delivery. *Exp. Opin. Deliv.* 2: 311–322.
37. Bhaskaran, S. and Dhir, S.S (1995). Resealed Erythrocytes as Carriers of Salbutamol Sulphate. *Indian J. Pharm. Sci.* 57: 240–242.
38. Schrier, S.L., Junga, I., Johnson, M. (1975). Energized Endocytosis in Human Erythrocyte Ghosts. *J. Clin. Invest.* 56 (1): 8–22.
39. Vyas, S.P. and Khar, R.K. (2002). Resealed Erythrocytes in Targeted and Controlled Drug Delivery: Novel Carrier Systems (CBS Publishers and Distributors, India), 87–416.
40. DeLoach, 1983. R. Encapsulation of Exogenous Agents in Erythrocytes and the Circulating Survival of Carrier Erythrocytes. *J. Appl. Biochem.* 5 (3): 149–157.
41. Kravtsoff, R., Ropars, C., Laguerre, M., Muh, J.P., Chassaigne, M. (1990). Erythrocytes as Carriers for L-Asparaginase: Methodological and Mouse In-Vivo Studies. *J. Pharm. Pharmacol.* 42: 473–476.
42. Vyas, S.P. and Dixit, V.K. (1999). *Pharmaceutical Biotechnology 1* (CBS Publishers & Distributors, New Delhi), 655.
43. Jaitely, V., Kanaujia, P., Vyas, S.P. (1996). Resealed Erythrocytes: Drug Carrier Potentials and Biomedical Applications. *Indian Drugs* 33: 589–594.

Table 1. Comparison of various hypo-osmotic lysis methods

Method	% loading	Advantages	Disadvantages
Dilution method	20-40%	Fastest and simplest especially for low molecular weight drugs	Entrapment efficiency is less
Dialysis	30-45%	Better in vivo survival of erythrocytes better structural integrity of membrane	Time consuming heterogenous size distribution of resealed erythrocytes
Preswell dilution	30-90%	Good retention of cytoplasm constituents and good survival in vivo	—
Isotonic osmotic lysis	—	Better in vivo surveillance	Impermeable only to large molecules, process is time consuming

**Fig 1.** Schematic representation of entrapment of drug into erythrocytes**Fig 2.** SEM photograph of unloaded erythrocytes (magnification of 5000)**Fig 3.** SEM photograph of drug-encapsulated erythrocytes prepared by hypotonic preswelling method (magnification of 3500)

Screening of supports for *Kluyveromyces marxianus* var. *bulgaricus* inulinase immobilization

F.C. Paula¹, M.L. Cazetta¹, R.Monti² and J. Contiero^{1,*}

¹Department of Biochemistry and Microbiology, Biological Sciences Institute, São Paulo State University-Unesp, 13506-900 - Av 24A, 1515 Rio Claro, São Paulo, Brasil.

²Department of Food and Nutrition, Faculty of Pharmaceutical Sciences, São Paulo State University-Unesp, 13506-900 - Av 24A, 1515 Rio Claro, São Paulo, Brasil.

* For correspondence: jconti@rc.unesp.br

Abstract

Some relatively low-cost supports were assessed for the immobilization of inulinase produced by the yeast strain *Kluyveromyces marxianus* var. *bulgaricus*. Crude enzyme in the culture supernatant was immobilized on various solid supports: activated carbon, diatomite, hen egg shell, Amberlite, porous silica and gelatin. The best performance was obtained in the gelatin-water support after treatment with glutaraldehyde as a cross-linking reagent, which showed an immobilization yield of 82.60 % for inulinase specific activity.

Keywords

Inulinase. *Kluyveromyces marxianus*, Fructose, Immobilization, Gelatin support.

Introduction

The inulinases are 2,1- α -D-fructan fructanohydrolases (EC 3.2.1.7), which hydrolyze inulin to practically pure fructose (13, 2). Fructose is a GRAS (Generally Recognized as Safe under U.S. FDA regulations) sweetener that enhances flavor, color and product stability (10) and is

considered as a safe alternative to sucrose. Fructose metabolism bypasses some of the metabolic pathway of glucose and therefore does not require insulin (18). Furthermore, fructose increases iron adsorption in children and has a higher sweetening capacity and lower glycemic index than sucrose. Owing to its beneficial effects, fructose is fast emerging as an important ingredient in the food and drug industries (6).

Inulinases are usually thermostable and commercially available for industrial use in fructose syrup production (5). However, there are two major problems associated with industrial application: at ambient temperature, inulin has a limited solubility and there is a good chance that microbial contamination will occur. Therefore, inulinase preparations have been immobilized by several processes on various supports, so as to improve the thermostability of the enzymes (6).

Yeasts of the genus *Kluyveromyces* show a high capacity to produce inulinase (15) with activity against both inulin and sucrose (8). Conversion of sucrose to high quality invert syrups is currently performed with strong cationic resins (5). However, the chemical

approach is associated with some drawbacks, namely formation of unwanted by-products and color forming compounds that lower product yield and require more demanding downstream processing (16).

Inulinase hydrolysis is becoming recognized as an alternative procedure in fructose syrup production (6). This approach is particularly effective if an immobilized biocatalyst is used and such systems have been described by several authors, employing immobilized inulinase (4, 9, 19, 20; 1, 23, 24). A cheap and simple, but effective, immobilization method would provide a key asset, if an experimental set-up amenable to scale-up were envisaged (11). Thus, this study was designed to screen relatively cheap solid supports for the immobilization of inulinase produced by yeast strain *Kluyveromyces marxianus* var. *bulgaricus*.

Materials and Methods

Microorganism

The yeast strain *Kluyveromyces marxianus* var. *bulgaricus* ATCC 16045 used in this study was obtained from the Department of Food Engineering, UNICAMP, Brazil.

Fed-batch culture

The yeast *K. marxianus* var. *bulgaricus* was grown in 2 L of a fermentation medium containing (w/v) 1% sucrose, 0.5% yeast extract, 1% peptone, 0.5% KH_2PO_4 , 0.15% NH_4Cl , 0.12% KCl and 0.07% $\text{MgSO}_4 \cdot 7\text{H}_2\text{O}$. The inoculum was grown in a rotary incubator shaker for 16 h at 30 °C and 180 rpm, in 200 mL of the fermentation medium. The culture was fed with a 20% sucrose solution and maintained at 30 °C and pH 5.0

for 72 h, the pH being controlled automatically with 1M KOH. The shaking and aeration rates were gradually increased up to 600 rpm and 1.0 vvm, respectively, during this period.

Enzyme preparations

Preparation of crude enzyme

The fermented broth was centrifuged at 5600g for 20 min. The supernatant obtained was used as crude enzyme for activity and protein assays and enzyme immobilization.

Partial purification of crude extract

The crude enzyme was partially purified on a column (23 x 1.4 cm) containing 15 g of activated charcoal particles, at a flow rate of 15 mL/h at room temperature. The filtrate was used for enzyme immobilization on porous silica beads.

Enzyme and protein assays

The inulinase activity was assayed, as detailed in Suzuki, Ozawa & Maeda (21), by determining the reducing sugars formed during incubation of soluble or immobilized enzyme in a solution of 2% sucrose in 0.05 M citrate-phosphate buffer (pH 4.0), with the reagent 3,5-dinitrosalicylic acid, as described by Miller (17). Glucose was used as a standard. One inulinase unit (IU) was defined as the amount of enzyme that released 1.0 μmol of reducing sugar per min under the above conditions. Protein content was measured as described by Lowry *et al* (14), using bovine serum albumin as standard. The protein content for the immobilized enzyme was calculated from the protein concentration

of the initial solution and the final concentration of unbound protein. The immobilization yield was calculated as the ratio of the specific activity of immobilized enzyme to that of the soluble enzyme.

Enzyme immobilization

Activated charcoal

The enzyme solution (2 mL containing 7.6 mg of protein) was incubated with 300 mg of activated carbon particles for 3 h, at room temperature. The same procedure was carried out after ethanol treatment of the charcoal to remove manufacturing impurities.

Diatomite

The crude enzyme (2 mL containing 7.6 mg of protein) was incubated with 300 mg of diatomite for 3 h, at room temperature.

Hen egg shell

The enzyme solution was immobilized on hen egg shell with and without subsequent glutaraldehyde treatment, as described by Chatterjee *et al* (3), with some modifications. The dried triturated egg shell (500 mg) was added to 10 mL of crude enzyme (containing 38 mg of protein) with constant stirring for 48 h, at 25 °C. The residue after centrifugation (5600g for 10 min) was repeatedly washed with 0.05 M citrate-phosphate buffer at pH 4.0 until no protein was detected in the washings.

Amberlite

The crude enzyme was immobilized on Amberlite XAD-2 (Sigma-Aldrich Co.) by both adsorption and covalent coupling. In the adsorption method, the enzyme solution (2 mL containing 7.6 mg of protein) was

incubated with 100 mg of Amberlite XAD-2 for 3 h, at 25 °C. The second method, immobilization by covalent coupling, has been described by Weetall (22) and involves: a) amination of the inert support with silane coupling reagent (0.5% γ -aminopropyltriethoxysilane), b) activation with 2.5 % (v/v) glutaraldehyde and c) incubation with inulinase solution (20 mg of protein per g of support).

Porous silica beads

Both the crude and the partially purified enzymes were immobilized on porous silica beads, using the procedure of Weetall (22).

Gelatin

The immobilization was carried out as described by Chatterjee *et al.* (3), with some modifications. Gelatin (500 mg) was dissolved in 5 mL of water at 50 °C or 0.05 M citrate-phosphate buffer at pH 4.0, and thereafter allowed to cool to room temperature. To this, 0.5 mL and 1 mL (containing 1.69 mg and 3.38 mg protein, respectively) of crude enzyme was added with constant stirring. After the suspension had set to a gel, it was covered with 10 mL glutaraldehyde (2.5 %) for 30 min. To remove excess glutaraldehyde, the resultant gel was washed with distilled water and then cut into small pieces. Finally, the gel was suspended in 0.05 M citrate-phosphate buffer at pH 4.0.

Results and Discussion

Immobilization of inulinase

With the aim of identifying a suitable solid support for the immobilization of inulinase, attempts were made to immobilize the crude

enzyme from *K. marxianus* var. *bulgaricus* on various supports (Table 1). Under the experimental conditions described here, the immobilization yield was highest on gelatin-water (82.60 %). The immobilization on untreated and ethanol-treated activated charcoal gave low yields (2.25% and 3.04%, respectively). The remaining methods screened were not successful either because no protein binding occurred or because the immobilization process resulted in activity loss.

Crude enzyme immobilization on porous silica beads resulted in no activity retention on this support. After purifying partially the crude enzyme on an activated charcoal column, the specific activity was thus increased 9.09-fold to 137.32 IU/mg protein according Table 2 and the enzyme was then immobilized on porous silica beads, giving an immobilization yield of 16.98 %.

Table 1

Table 2

Various supports have been used for inulinase immobilization. Gill *et al* (7) immobilized the purified inulinase from *Aspergillus fumigatus* on chitin, casein and sodium alginate. The same authors reported retention of the enzyme on the anion exchangers DEAE-Sephacel (yield 100%), QAE-Sephadex (100%), Dowex (63%), Amberlite (39%) and also the affinity matrix of concanavalin A linked to amino-activated silica beads (100 %). The inulinase from *Aspergillus ficuum* was immobilized on porous glass beads of various porosities by Ettalibi & Baratti (5), with a range of activity retention from 70 to 77%. On the other hand,

inulinase from *Kluyveromyces fragilis* showed 22.5% and 54% activity retention when immobilized on tygon tube and aminoethyl cellulose, respectively (12), whereas 30-40% of the inulinase from *Fusarium oxysporum* was retained on DEAE-cellulose (9).

Reusability of immobilized inulinase

The highest immobilization yield was observed on the gelatin-water support. Although alternative gelatin preparations were tested, replacing the water with citrate-phosphate buffer and doubling the amount of enzyme solution, neither of these alternatives increased the immobilization yield. Since gelatin is cheaper than the other supports, it is the most suitable for the economic viability of this process. Therefore, the inulinase immobilized on gelatin-water was tested in a batch reactor to assess its reusability (Table 3). The trials were carried out over four reaction cycles. After 24 h (batch 1), the bioconversion medium was replaced with fresh medium and a new bioconversion cycle allowed to proceed for a further 24 h, with great success. The degree of sucrose conversion was maintained over 96% in all four reaction cycles and the inulinase activity remained unchanged.

Table 3

Storage Stability of immobilized inulinase

After 34 days of storage in cold conditions, the inulinase immobilized on gelatin-water lost 9.80% of its initial enzyme activity, whereas the soluble inulinase lost 22.50% over the same interval.

To conclude, these results suggest that inulinase immobilization on gelatin, a low cost support, could be used in commercial processes for production of high purity fructose syrups.

Acknowledgements

The authors acknowledge CNPq Agency for the financial support.

References

1. Catana, R.; Ferreira, B.S.; Cabral, J.M.S.; Fernandes, P. Immobilization of inulinase for sucrose hydrolysis. **Food Chemistry**, Oxford, v. 91, p. 517-520, 2005.
2. Cazzeta, M. L., Martins, P. M. M., Monti, R., & Contiero, J. (2005). Yacon (*Polymnia sanchifolia*) extract as a substrate to produce inulinase by *Kluyveromyces marxianus* var. *bulgaricus*. *Journal of Food Engineering*, 66: 301-305.
3. Chatterjee, U., Kumar, A., & Sanwal, G. G. (1990). Goat liver catalase immobilized on various solid supports. *Journal of Fermentation and Bioengineering*, 70: 429-430.
4. Ettalibi, M., & Baratti, J. C. (1992). Immobilization of *Aspergillus ficuum* inulinases on porous glass. *Biocatalysis*, 5: 175-182.
5. Ettalibi, M., & Baratti, J. C. (2001). Sucrose hydrolysis by thermostable immobilized inulinases from *Aspergillus ficuum*. *Enzyme Microbial Technology*, 28: 596-601.
6. Gill, P. K., Manhas, R. K., & Singh, P. (2006a). Purification and properties of a heat-stable exoinulinase isoform from *Aspergillus fumigatus*. *Bioresource Technology*, 97: 894-902.
7. Gill, P. K., Manhas, R. K., & Singh, P. (2006b). Hydrolysis of inulin by immobilized thermostable extracellular exoinulinase from *Aspergillus fumigatus*. *Journal of Food Engineering*, 76: 369-375.
8. Guiraud, J. P., & Galzy, P. (1990). Inulin Conversion by Yeasts. In: Verachtert, H., & De Mot, R. (Eds), *Yeast: Biotechnology and Biocatalysis*, (pp. 255-296). Marcel Dekker, New York.
9. Gupta, A. K., Kaur, M., Kaur, N., & Singh, R. (1992). A comparison of properties of inulinases of *Fusarium oxysporum* immobilized on various supports. *Journal of Chemical Technology and Biotechnology*, 53: 293-296.
10. Hanover, A. W., & White, J. (1993). Manufacturing, composition and applications of fructose. *American Journal of Clinical Nutrition*, 5 (Suppl.) 724S-732S.
11. Katchalski-Katzir, E., & Kraemer, D. M. (2000). Eupergit® C, a carrier for immobilization of enzymes of industrial potential. *Journal of Molecular Catalysis B*, 10: 157-176.
12. Kim, W. Y., Byun, S. M., & Uhm, T. B. (1982). Hydrolysis of inulin from Jerusalem artichoke by inulinase immobilized on amino ethyl cellulose. *Enzyme Microbial and Technology*, 4: 239-244.
13. Kushi, R.T.; Monti, R.; Contiero, (2000) J. Production, purification and

- characterization of an extracellular inulinase from *Kluyveromyces marxianus* var. *bulgaricus*. *Journal of Industrial Microbiology and Biotechnology*, Hampshire, v. 25, p. 63-69.
14. Lowry, O. H., Rosenbrough, N. J., Farr, A. L., & Randall, R. J. (1951). Protein measurement with folin-phenol reagent. *The Journal of Biological Chemistry*, 193: 265-275.
 15. Manzoni, M., & Cavazzoni, V. (1988). Extracellular inulinase from four yeasts. *Lebensmittel-Wissenschaft und Technologie*, 21: 271-274.
 16. Matsumoto, K., & Yamazaki, H. (1986). Production of fructose syrups. US Patent US4613377.
 17. Miller, G. L. (1959). Use of dinitrosalicylic acid reagent for determination of reducing sugars. *Analytical Chemistry*, 31: 426-429.
 18. Millo, H., & Werman, M. J. (2000). Hepatic fructose-metabolizing enzymes and related metabolites: Role of dietary copper and gender. *Journal of Nutritional Biochemistry*, 11: 374-381.
 19. Nakamura, T., Ogata, Y., Shitara, A., Nakamura, A., & Ohta, K. (1995). Continuous production of fructose syrups from inulin by immobilized inulinase from *Aspergillus niger* mutant 817. *Journal of Fermentation and Bioengineering*, 80: 164-169.
 20. Rocha, J. R., Catana, R., Ferreira, B. S., Cabral, J. M. S., & Fernandes, P. (2006). Design and characterisation of an enzyme system for inulin hydrolysis. *Food Chemistry*, 95: 77-82.
 21. Suzuki, H., Ozawa, Y., & Maeda, H. (1988). Studies of water-insoluble yeast invertase. *Agricultural and Biological Chemistry*, 30: 807-812.
 22. Weetall, H. H. (1993). Preparation of immobilized proteins covalently coupled through silane coupling agents to inorganic supports. *Applied Biochemistry and Biotechnology*, 41: 157-188.
 23. Wenling, W., Huiying, W. W. L., & Shiyuan, W. (1999). Continuous preparation of fructose syrups from Jerusalem artichoke tuber using immobilized intracellular inulinase from *Kluyveromyces* sp. Y-85. *Process Biochemistry*, 34: 643-646.
 24. Yun, J. W., Park, J. P., Song, J. P., Lee, C. Y., Kim, J. H., & Song, S. K. (2000). Continuous production of inulo-oligosaccharides from chicory juice by immobilized endoinulinase. *Bioprocess Engineering*, 22: 189-194.

Table 1 : Immobilization of inulinase on different solid supports

Support	Immobilized protein (mg)	Immobilized activity (IU) ^a	Retention of activity (IU) ^b	Immobilization yield (%)
Activated charcoal	6.95	39.48	2.4	2.25
Activated charcoal-ethanol	6.52	28.39	3.00	3.04
Diatomite	nd	nd	nd	nd
Hen egg shell	nd	nd	nd	nd
Hen egg shell-glutaraldehyde	nd	nd	nd	nd
Amberlite-absorption	2.20	24.26	nd	nd
Amberlite-covalent coupling	nd	nd	nd	nd
Porous silica beads-crude enzyme	nd	nd	nd	nd
Porous silica beads-partially purified inulinase	1.8	427.99	41.98	16.98
Gelatin-water (1.69 mg of protein)	1.69	27.30	22.54	82.60
Gelatin-citrate-phosphate buffer (1.69 mg of protein)	1.69	27.30	10.36	37.96
Gelatin-water (3.38 mg of protein)	3.38	27.30	15.48	56.72

^a Theoretical activity (calculated as difference between initial soluble activity and activity found in washings).

^b Immobilized activity experimentally measured. nd –not detected

Table 2 : Partial purification of *K. marxianus* var. *bulgaricus* on activated charcoal

Purification step	Enzyme activity (UA/mL)	Protein (mg/mL)	Specific activity (UA/mg)	Yield (%)	Purification factor (x)
Crude broth	57.42	3.80	15.11	100.00	1.00
Filtred broth on activated charcoal	42.57	0.31	137.32	74.14	9.09

Table 3: Reusability of the gelatin-immobilized inulinase (the bioconversion medium contained 10 mL of 1% sucrose solution prepared with 0.05M citrate-phosphate buffer, pH 4.0, at 45 °C)

Batch	Residual activity (%)	Sucrose conversion (%)
1(24 h)	100	100
2(48 h)	100	99.94
3(72 h)	100	99.03
4(96 h)	100	96.97

Correct identification of wood-inhabiting fungi by ITS analysis

Annette Naumann #, Mónica Navarro-González #, Olivia Sánchez-Hernández #,
Patrik J. Hoegger # and Ursula Kües #*

Georg-August-University Göttingen Buisgen-Institute
Section Molecular Wood Biotechnology and Technical Mycology
Buisgenweg 2, D-37077 Göttingen

These authors contributed equally to the study

* For correspondence - ukuees@gwdg.de

Abstract

In this study, we established ITS sequences from 20 strong wood degraders from different fungal genera and from 15 strains of the coprini which are occasionally found on wood. These sequences were used in blast searches to evaluate their species identity. ITS sequences confirmed for 25 strains previous morphological species determination. ITS sequences from *Coprinopsis scobicola* were determined for the first time from DNA of two different strains. Finally, eight strains were found assigned to a wrong species or assignments were uncertain. We present problems encountered in fungal identification by molecular data, such as difficulties in previous morphological identification, occurrence of contaminations or mixing-up of strains in fungal culture collections, and wrong entries in the NCBI GenBank sequence dataset. A long-term target of ITS sequencing of wood-inhabiting fungi is to establish a specific database that can be either used for blast searches or in ITS barcoding for species identification. We present first studies in ITS barcoding of coprini.

Key words

Wood degraders, Coprinoid mushrooms, misidentifications, phylogenetic analysis, barcoding

Introduction

Wood is threatened by various types of fungal damage. Blue stain fungi grow within parenchymatic cells in wood and live from storage products within these cells. They do not influence dimensional properties and stability of the wood. However, infestation by blue stain fungi makes wood unattractive for use because of melanin in the fungal cell walls that gleams in dirty blue-greyish colours through the wood. Furthermore, moulds might grow on the surface of wood spoiling its looks as well as being a hygienic problem by abundant production of asexual spores. Other fungi attack the wood structure by degrading cell wall compounds. Three major kinds of fungal decay are distinguished. White rot fungi degrade the lignin in the plant cell walls while brown rots and soft rots preferentially degrade cellulose and hemicellulose. As a result of such decay, stability of the wood is affected in early stages until the decay is completed leaving white strings of cellulosic materials in case of white rot, brown cubicles of lignin in case of brown rot and the middle lamellae in case of soft rot (1).

Under certain environmental conditions such as higher levels of humidity and when in contact with soil, wood in service is in danger to be infested by destructive fungi. Early detection of fungi can be crucial, e.g. for rescuing houses in

case of a dry rot infestation in a wooden construction or for avoiding health problems such as spore allergies in case of moulds on wood. In living trees, early detection can help to decide upon measures to be taken against fungal pathogens. Early detection of harmful wood-inhabiting fungi implies in the best possible case also species identification [discussed further in references (2), (3) and (4)]. Traditionally, species identification has been done in late stages of infestation when sexual fruiting bodies occur or asexual spores are produced on the surface of infested wood (5). This, however, does not exclude that there are other species present in the wood not producing any obvious morphological structures. Such fungi might be isolated from wood on suitable artificial medium for further evaluation of mycelial cultures. Despite that not all fungi might be growing in culture or species might be overgrown by others during the isolation process (6), identification by mycelial growth characters is very difficult or often impossible to perform even for a trained mycologist (7). Modern molecular biology offers more accurate ways of identification. Very common is to apply sequencing of PCR (polymerase chain reaction)-amplified ITS (internal transcribed spacer) fragments, non-coding regions localized in between ribosomal RNA genes (rDNA). rRNA gene clusters are conserved within species, but differ in sequence between species with the degree of differences reflecting distance of relation between organisms [(1), (4), (Fig. 1)]. PCR-amplification of ITS sequences can be applied on isolated fungal cultures but also on DNA obtained from wood samples without prior fungal strain isolation (8)-(12), our unpublished results]. In such a way, any bias by loss of species due to non- or unequal growth on artificial medium during fungal isolation is overcome.

Although wood-inhabiting fungi are often deleterious for wood as such, there are various biotechnological applications for such fungi [(1), (13)]. A variety of species are used in mushroom

production on lignocellulosic waste materials from agriculture and forestry (14). Particularly the white rot fungi are sources of enzymes such as cellulases, hemicellulases, peroxidases, laccases, and others used in various types of industry. Furthermore, such fungi are appointed in bioremediation of contaminated soils, purification of industrial effluents, etc. [(15), (16)]. Also in biotechnology, it is of interest to unequivocally identify the species for an exact definition of the fungal material applied in a process.

Whilst analysis of ITS sequences is technically easy, there are, however, also problems related to this molecular approach. Established sequences are usually submitted to public databases such as the NCBI GenBank (<http://www.ncbi.nlm.nih.gov/>) or the EMBL Nucleotide Sequence Database (<http://www.ebi.ac.uk/embl/>). These databases are open to submissions by everybody, with the consequence that up to 20% of sequence entries within a group of fungi may be faulty [(4), (17)]. Reasons for this can be that a species name has been assigned by ITS sequence identity to a formerly wrongly assigned species, that a parallel mycological identification by morphological characters was wrong, that another mycelium has been isolated unnoticed from a morphologically assigned fungal structure taken non-sterile from nature, that unseen contaminations occurred in isolates in culture, or that fungal cultures were accidentally mixed up in a laboratory. Searchable experts' sequence databases with controlled data entries are therefore required [(1), (4)].

In this paper, we present case studies on ITS sequences obtained from fungal cultures for the long-term goal to establish a large sequence database on wood-inhabiting fungi.

Material and Methods

Fungal strains and culture conditions: Fungi were routinely grown at 25°C or 28°C on 2%

malt extract (agar) with the exception of *Coprinopsis cinerea* strains that were cultured at 37°C. Aerial mycelia were scraped from the surface of the agar for chromosomal DNA isolation by established methods [(18), (19)]. Origins of fungal strains used in this study for ITS sequencing are given in the footnotes of Table 1 and 2.

Coprinoid mushrooms collected from the wild were morphologically identified according to the keys by Uljé (20) and Orton and Watling (21). Inner tissues from mushroom stipes were used to establish further fungal cultures for DNA isolation and barcoding by ITS sequence amplification. *Coprinus comatus* strains 1-2004, 2-2004, MN-23, MN-24 and MN-25 were mycelial isolates obtained from stipe tissues from independent mushrooms collected in 2004 and 2006 on the grounds of the North Campus of the Georg-August-University Göttingen. *Coprinellus micaceus* strain MN-7 was isolated from a colony of fruiting bodies found in year 2006 on the grounds of the Georg-August-University Hospital in the bifurcation of a forked *Robinia pseudoacacia* tree breaching through its bark.

ITS sequence characterization: PCR was performed with ca 5 ng DNA of a fungal isolate in a total volume of 25 µl containing 10 mM Tris pH 8.8, 50 mM KCl, 0.1% Triton X-100, 1.5 mM MgCl₂, 0.2 mM dNTPs (Fermentas, St. Leon-Rot, Germany), each 0.4 µM of primer ITS1 [5'-TCCGTAGGTGAACCTGCGG-3' (22)] and primer ITS4 [5'-TCCTCCGCTTATTGATATGC-3', (22)], and 1 U of *Taq* DNA polymerase. PCR conditions were 2 min initial denaturation at 94 °C, followed by 35 cycles of 30 s at 94 °C, 30 s at 55 °C, and 30 s at 72 °C, and a final extension at 72 °C for 10 min. 20 µl per PCR reaction were precipitated with isopropanol and resuspended in 20 µl H₂O. Restriction enzyme digests and agarose gel electrophoresis of purified DNAs were performed by standard methods (23). For cycle sequencing reactions, 2 µl of the purified

DNA were mixed with BigDye Terminator v3.1 (Applied Biosystems, Darmstadt, Germany) applying a quarter of the reagents recommended by the manufacturer and either primer ITS1 or ITS4. After cycling following the manufacturer's instructions, the reaction products were purified by sodium acetate/ethanol precipitation and washing with 70% ethanol and subsequently run on an ABI PRISM 3100 Genetic Analyzer (Applied Biosystems). Obtained sequences were compared against the nucleotide entries in the NCBI GenBank by using search tool blastn (<http://www.ncbi.nlm.nih.gov/>). Identity values were taken either from the blastn results or from alignments performed by the tool for blasting two sequences bl2seq (<http://www.ncbi.nlm.nih.gov/>). For phylogenetic analysis, appropriate sequences were taken from the NCBI database and aligned with sequences established in this study using ClustalX (<http://www-igbmc.u-strasbg.fr/BioInfo/ClustalX/Top.html>) and GeneDoc version 2.6.002 (<http://www.psc.edu/biomed/genedoc/>). Phylogenetic trees of the nucleotide sequence alignments were calculated by the neighbour joining method of the programme MEGA version 3.1 (24).

Results and Discussion

Evaluating correct species assignment in a selection of wood-rotting fungi

ITS sequences were determined from 20 strains of strong fungal wood-decayers. The ITS sequences of fifteen of them matched perfectly or nearly perfectly to sequences published in NCBI GenBank for strains registered under the same species names (Table 1). In the special cases of *Polyporus brumalis* FBI 5 and *Trametes versicolor* 051130.2, each two sequences were established that distinguished by a 1 bp insertion (Table 1). Such restricted nucleotide polymorphism within one strain is not uncommon in higher basidiomycetes [(25)-(27), Hoegger et al. unpublished]. It is also quite often observed be-

tween strains of a same species [(28)-(30)]. Species identification by ITS sequences is thus not always relying on 100% sequence identity but can include a certain degree of variation [(30), Table 1] that however might indicate ongoing speciation in diverging morphotaxons [(31), (32)].

The five further cases of ITS sequences established in this study are discussed in the following:

Pleurotus ostreatus var. *florida* N001 is a commercial mushroom production strain used in genetic characterisation of the genome of the species (33). The ITS sequence of the strain is presented for the first time. It is 100% identical to region 61-654 of sequence AY540322 from a fungus identified as *Pleurotus floridanus*. *P. floridanus* is considered a synonym for *P. ostreatus* (34).

For *Gloeophyllum odoratum*, an ITS sequence was so far not present in the NCBI database. In blastn searches, the most similar sequence to the ITS sequence of strain *G. odoratum* 050601.3 was therefore from *Gloeophyllum abietinum* (AJ420947) with 86% identity.

The ITS sequence from *Trametes zonata* 921011.17 was 99% identical to an ITS sequence from a strain called *Trametes versicolor* 3633 (AY840580) and 98% identical to an ITS sequence from a strain called *Trametes ochracea* PRM 900601 (AY684177). *T. ochracea* is a synonym of *T. zonata* (35). Tomšovský et al. (36) recently published a first extensive phylogenetic analysis of the genus *Trametes*. The ITS sequence of their *T. versicolor* voucher strain PRM 900594 (AY684179) showed 98% identity to our sequence. Many of the GenBank entries involving the genus *Trametes* are mislabelled. There are several *T. versicolor* ITS sequences wrongly attributed to other fungal genera (4) but by the difficult morphological definitions of *Trametes*

fruiting bodies there are also various ITS sequences assigned within the genus to a wrong species. The high level of identity of ITS sequences from different *Trametes* species makes species definition in this genus difficult. A thorough analysis of ITS sequences in larger numbers of *Trametes* isolates is in progress (Hoegger et al. unpublished).

The ITS sequence of a strain from the institute's collection labeled *Coniophora arida* FBI 516 was 99% identical to region 30-677 of the ITS sequence from *Coniophora puteana* strain EBW 15 [(AJ344110), (37)]. Fig. 2 shows that in a phylogenetic tree of *C. arida* and *C. puteana* ITS sequences taken from GenBank, the two species clearly distinguish from each other. The species concept within *Coniophora* is difficult since there are few and unstable morphological characteristics, especially for mycelia but also for fruiting bodies [(1), (7), (38)]. Present species identification is therefore based on molecular methods by comparing ITS sequences with those of standard strains [(1), (32), (37)]. In conclusion, by the clustering of the strain from our institute's collection with the *C. puteana* reference strains (Fig. 2), we suggest to rename our strain *C. puteana*. Regions 54-470 and 598-648 of the ITS sequence of our strain showed only 91% and 88% identity, respectively to regions 91-510 and 583-630 of the reference strain MUCL 30844 of *C. arida* (AJ345007).

The most complicated case links to the strain FBI 52 from our institute's collection labelled *Trichaptum abietinum* (*Hirschioporus abietinus*). Originally obtained as *H. abietinus* CBS 376.68 from the CBS culture collection (Centraalbureau voor Schimmelcultures), this strain has been stored for decades in our institute's collection. In blastn searches of the ITS sequence of this strain, perfect or nearly perfect hits (98-100% identity) were obtained with a number of sequences that should represent either *Entrophospora* sp., *Ceratobasidium stevensii*,

Thanatephorus cucumeris (or its anamorph *Rhizoctonia solani*) or *Bjerkandera* strains. The one assignment (AY035664) of a soil fungus from a community of arbuscular mycorrhizal fungi to *Entrophospora* sp. (39) is easily identified as being wrong by the fact that the genus *Entrophospora* belongs to the phylum Glomeromycota that is evolutionary distantly related to fungi from the phylum Basidiomycota in the subkingdom Dikarya (40). A number of NCBI GenBank submissions labelled *T. cucumeris* or with the anamorph name *Rhizoctonia* (AF455419, AF455435, AF455438, AF455459, AF455461, AF455463, AJ000198, AJ276054, AY443531, DQ117961, DQ278948, DQ426512, DQ426519, DQ426529) as well as one submission labelled *Ceratobasidium stevensii* (AJ427405) from the same fungal family Ceratobasidiaceae of the Basidiomycota have also to be considered as wrongly assigned. This mislabelling likely goes back to sequence AJ000198 obtained from a strain T4 (IMI 360314, sequenced also in another laboratory: DQ278948) listed as *Rhizoctonia solani* isolated from rice from Ghana (41). Johanson et al. (41) noted at the time of first analysis that this sequence was highly dissimilar to sequences from *Rhizoctonia* labelled strains from other sources. The other sequences were obtained later in history from sequences amplified by PCR from air in hospital laboratory environment (DQ426512, DQ426519, DQ426529), nasal mucus (42) and leaf material from *Ipomea asarifolia* (43) and from fungi from root material of orchids (44). The ITS sequence from the single strain labelled *C. stevensii* came from a fungus that has been isolated from a twig of an apple tree (AJ427405). The final large group of about 20 sequences with high similarity to our ITS sequence represents the genus *Bjerkandera*. Among these are at least three sequences from independent isolates that were identified morphologically as *Bjerkandera* [(45), (46), DQ060096]. From strain *Bjerkandera adusta* VH57 (AB096737) in addition the sequence from the 28S rDNA gene is known that

matches with 98% identity that of strain *B. adusta* DAOM 215869 [(45), (47), (48)]. Morphological identification of at least four different strains argues strongly for correct assignments. These and some other *Bjerkandera* sequences were extracted from the NCBI GenBank and used to construct the phylogenetic tree shown in Fig. 3. Two of the sequences had only 95-96% identity to the sequence of our strain and were obviously from the same species (*Bjerkandera fumosa* according to AJ006673) closely related to *B. adusta* (Fig. 3). The only entry labelled *T. abietinum* (U63474) showing a high degree identity to our sequence (96%) was also included and two other *T. abietinum* labelled entries not hit in the blastn search by our ITS sequence. When comparing each two sequences in the direct alignment, the ITS sequence of our strain matched only in each two short stretches to the sequences U63475 (190-353 with 96% identity and 540-572 with 96% identity) and AY781273 (190-353 with 98% identity and 510-533 with 95% identity). Finally, ITS sequences from *Trametes versicolor* (AY354226), *Ganoderma tsuga* (DQ206985) and *Polyporus squamosus* (DQ267123) from the Polyporales were included in the phylogenetic analysis and the ITS sequence from *Schizophyllum commune* (AF249390) from the Agaricales was used as an outgroup (Fig. 2). The sequence submitted under U63474 clearly clustered with *Bjerkandera* sequences, although in an own short branch, whereas the sequences of the two other *T. abietinum*-labelled species grouped further away from the sequences of the three other genera of the Polyporales (Fig. 2). Grouping with *B. adusta* has been noted before and interpreted as likely misidentification or mislabelling of the respective strain (49). The ITS sequence established in this study for strain FBI 52 implies that there has been also an error with this strain. *T. abietinum* CBS 376.68 is also known as DAOM 72245A. Ko & Jung (50) analyzed the mitochondrial small subunit ribosomal DNA of DAOM 72245A and found it to cluster with those of other *T. abietinum* strains.

It is thus likely, that a mislabelling has happened at some point in the past in case of strain FBI 52. The ITS analysis implies that the strain in our collection should be relabelled as *B. adusta*.

Evaluating ITS sequences from coprini

Coprini present a group of approximately 200 different species that, with a few exceptions, are very difficult to distinguish from each other by morphological means. Coprini have been compiled in one genus *Coprinus* until recently, when molecular data divided them into four new genera belonging to the Psathyrellaceae (*Coprinopsis* with an estimated 100 species, *Coprinellus* with more than 40 species and *Parasola* with currently 18 defined species) and the Agaricaceae (*Coprinus* with just three species), respectively (51). Most species grow on dung and plant litter in soil but about a third of the species has been observed growing also on (decaying) wood (Navarro-González, PhD thesis in preparation). A collection of coprini obtained from different sources (Table 2) for testing of growth behaviour on wood (Navarro-González, PhD thesis in preparation) were subjected in this study to an analysis of ITS sequences.

ITS sequences verified species identity of two *C. comatus* strains, of a *Coprinellus radians* strain, 3 *Coprinellus xanthothrix* strains, and a *Coprinopsis cinerea* strain (Table 2). ITS sequences for *Coprinopsis scobicola* were so far not available and we provide new ITS sequences from two monokaryotic strains well established in mating type analysis of *C. scobicola* [(52)-(53)]. Misidentified within the family of the Psathyrellaceae were obviously the strains labelled as *Coprinellus disseminatus* C50, *Parasola plicatilis* C65, and *Coprinopsis atramentaria* C67. The first two should present two different further to be defined species from the genus *Coprinellus*, the third one a further to

be defined species from the genus *Coprinopsis* (Table 2, Fig. 4).

Mushrooms of the related species *Coprinopsis lagopus* and *Coprinopsis lagopides* are very difficult to distinguish and misidentifications are easily possible (20). The ITS sequences of the *Coprinopsis* strains labelled *C. lagopus* C215 and *C. lagopides* C262 are both related to the NCBI sequence AF345815 assigned to *C. lagopides* and poorly to the NCBI sequence AF345813 assigned to *C. lagopus* (Table 2, Fig. 4). Since further background on the sequences AF345815 and AF345813 is not available, at the current state a complete species designation to the two tested strains is better left open until a more thorough analysis on the two species with several different isolates has been made.

Finally, the snow mould used as *Coprinopsis psychromorbida* in microbiological practicals to demonstrate growth at low temperatures (2-4°C, optimum at 15°C) turned out to be an unknown basidiomycete with clamp cells at its hyphal septa. The only highly similar sequence (98 % identity) in the NCBI database is from an uncultured basidiomycete from forest soil (AY969953). The next similar sequence is from *Athelia bombacina* (ABU85795) (86% identity) belonging to the family of Atheliaceae in the Atheliales (Table 2, Fig. 4).

ITS in molecular barcoding of coprini

Once ITS sequences have been established and positions of recognition sites of restriction enzymes deduced from these sequences, the information can be used as barcodes in species identification (54), eliminating the need for further tedious sequencing and allowing also less equipped laboratories without modern sequencers an easy access to molecular species identifications. In the following, we describe examples of barcoding of new isolates of *C. comatus* and *Coprinellus micaceus*.

The edible *C. comatus* (Fig. 5 A to C) able to grow on wood (Navarro-González, PhD thesis in preparation) is not as easily mixed up with other coprini by the large size and the characteristic elongated-ovoid shape of the mushroom cap, the floccose, shaggy scales on the cap surface, a white annulus on the stipe upon opening the cap and an elastic cord suspended in the stipe that is not found in coprini belonging to the Psathyrellaceae (21). PCR-amplified ITS fragments of new isolates from *C. comatus* mushrooms collected at different times and places on the grounds of the North Campus of the Georg-August-University Göttingen and a PCR-amplified ITS fragment of the *C. comatus* strain C108 were digested with restriction enzymes *Hinf*I and *Hha*I (Fig. 5 E and F). All showed the same banding patterns. Within the error range of the agarose gels, the size of the DNA fragments obtained corresponded well with the expected sizes (Fig. 5 D). The ITS sequence of the closest related species, *Coprinus sterquilinus* (AF345821), is identical in size to the ITS fragment of *C. comatus* strains. *Hinf*I and *Hha*I digests can however clearly distinguish these two species by the fact that in the *C. sterquilinus* sequence the first *Hinf*I site is missing (not shown).

Other genera of the coprini containing many more species than the newly defined genus *Coprinus* are more difficult to categorize. Fig. 6 shows an analysis of a strain isolated from easy to recognize fruiting bodies of the tree-pathogenic species *C. micaceus*. The *Hha*I restriction pattern of its ITS sequence is identical to that of strain C56 (Fig. 6C) that according to ITS sequencing (Table 2) likely presents a *C. flocculosus* strain. In contrast, the *Hinf*I digests distinguish these two species (Fig. 6B). An evaluation of ITS sequences of other species of the genus showed that *Hha*I and *Hinf*I digests are not always sufficient to distinguish *C. flocculosus* from other species such as *Coprinellus verrucispermus* and e.g. *Coprinellus radians* from species such as *Coprinellus xanthothrix* on

agarose gels (Fig. 7). Whilst these four species divide into two groups due to a restriction site for *Hha*I shared only between *C. flocculosus* and *C. verrucispermus*, a third digest for example with enzyme *Dpn*I is required to resolve the otherwise alike species (Fig. 7). In contrast, *C. micaceus* is easily recognized from the other species by a *Hinf*I site shared only with *C. disseminatus* that in turn is characterized by multiple *Hha*I and *Hinf*I sites (Fig. 7). *Coprinellus curtus* (of which currently only a partial ITS sequence is available – AY461834) is distinct from all discussed species by lack of *Hinf*I and/or *Hha*I sites (Fig. 7). Considering only 7 different species is a start of barcoding different members of the genus *Coprinellus* through restriction enzyme analysis of PCR-amplified ITS fragments. It is to be expected that in barcoding of the over 40 species of the genus, further enzymes will have to be incorporated in such ITS analysis.

Conclusion

In this study, we established the ITS sequences from collections of fungal strains of wood-inhabiting species and of a collection of coprini, of which several also occur on wood (Navarro-González, PhD thesis in preparation). To the best of our knowledge, in 71 % of the cases (25 of totally 35 sequences), ITS sequences confirmed species names assigned previously to the isolates. For one species (*C. scobicola*), ITS sequences were determined for the first time making use of different two strains. Two different strains (*Bjerkandera* sp. and an unidentified snow mould) were assigned to a wrong genus and in the six other cases left, strains were assigned to a wrong species within a genus (considering in case of *Coprinellus* sp. C65 the traditional genus *Coprinus*) or assignments were uncertain.

Our study documents the difficulty of correct identifications of fungal species by molecular means due to various types of errors that can oc-

cur in the process (e.g. wrong morphological identification of a species, mixing up cultures in stock collections, assigning names to strains by wrong entries in the sequences databases). Once introduced into the databases, such mistakes are carried on and tend to multiply.

To avoid mistakes in molecular identification, correct linkage between morphological characteristics and DNA sequences are required and in best cases, fungal voucher strains have been deposited in a suitable strain collection allowing at any time a control (55). Since wrong entries in public databases cannot be avoided by the principle that submitting of sequences is open to everyone, separate databases controlled by experts are required as already founded for mycorrhizal species and certain groups of food-inhabiting fungi (4). With enough numbers of species entries, such databases can then on the one hand be used for blast searching of sequences. On the other hand, such data are open to be used with suitable computer programs in the technically easier to perform barcoding of species.

Acknowledgements

We are very grateful to M.P. Challen, O. Holdenrieder, T.Y. James, S. Peddireddi, L. Ramírez, D. Rigling, K. Voigt, and H.A.B. Wösten for supplying fungal strains for our studies. We thank Alexandra Dolynska for excellent technical work performed in frame of EFRE grant 2001.085 from the European Fund for Regional Development. AN holds a grant "Eigene Stelle" (NA 749/1-1) awarded by the DFG (Deutsche Forschungsgemeinschaft) for establishing new methods for detection and identification of fungi in wood. MN was financially supported by a PhD scholarship (170607) awarded by CONACYT (Mexico). In frame of a grant (0330551) for analyzing fungal behaviour on beech and grand fir wood to UK, the BMBF (Bundesministerium für Bildung und Forschung) supports a long-term database project on fungal

ITS sequences. The laboratory Molecular Wood Biotechnology was established by funds from the DBU (Deutsche Bundesstiftung Umwelt).

References

1. Schmidt, O. (2006). Wood and Tree Fungi. Springer, Berlin, Germany.
2. Naumann, A., Navarro-González, M., Peddireddi, S., Kües, U. & Polle, A. (2005). Fourier transform infrared (FTIR) microscopy and imaging. Detection of fungi in wood. *Fungal Genetics and Biology*, 42: 829-835.
3. Naumann, A., Peddireddi, S., Kües, U. & Polle, A. (2007). Fourier transform microscopy in wood analysis. In: *Wood Production, Wood Technology and Biotechnological Impacts* (Kües, U., ed.), Universitätsverlag Göttingen, Göttingen, Germany.
4. Hoegger, P.J. & Kües, U. (2007). Molecular detection of fungi in wood. In: *Wood Production, Wood Technology and Biotechnological Impacts* (Kües, U., ed.), Universitätsverlag Göttingen, Göttingen, Germany.
5. Schwarze, F.W.M.R., Engels, J. & Mattheck, C. (2000). *Fungal Strategies of Wood Decay in Trees*. Springer, Berlin, Germany.
6. Johannesson, H. & Stenlid, J. (1999). Molecular identification of wood inhabiting fungi in an unmanaged *Picea abies* forest in Sweden. *Forest Ecology and Management*, 115: 203-211.
7. Stalpers, J.A. (1978). Identification of wood-inhabiting Aphyllophorales in pure culture. *Studies in Mycology* No. 16. Centraalbureau voor Schimmelcultures, Baarn, The Netherlands.
8. Schulze, S. (2000). Rapid silica matrix binding-based isolation of DNA from various wood-rotting and mycorrhizal basidiomycete fungi suitable for the

- detection by multiplex PCR. *Journal of Plant Diseases and Protection*, 107: 664-671.
9. Pennanen, T., Paavolainen, L. & Hantula, J. (2001). Rapid PCR-based method for the direct analysis of fungal communities in complex environmental samples. *Soil Biology & Biochemistry*, 33: 697-699.
 10. Adair, S., Kim, S.H. & Breuil, C. (2002). A molecular approach for early monitoring of decay basidiomycetes in wood chips. *FEMS Microbiology Letters*, 211: 117-122.
 11. Jellison, J., Jasalavich, C. & Ostrofsky, A. (2003). Detecting and identifying wood decay fungi using DNA analysis. *Wood Deterioration and Preservation, ACS Symposium Series*, 845: 346-357.
 12. Yen, T.B., Six, D.L. & Burke, E.J. (2006). Evaluation of rapid DNA extraction and identification of *Phellinus pini* associated with *Pinus contorta* by rDNA assay. *Forest Products Journal*, 56: 107-110.
 13. Mai, C., Kües, U. & Militz, H. (2004). Biotechnology in the wood industry. *Applied Microbiology and Biotechnology*, 63: 477-494.
 14. Rühl, M. & Kües, U. (2007). Mushroom production. In: *Wood Production, Wood Technology and Biotechnological Impacts* (Kües, U., ed.), Universitätsverlag Göttingen, Göttingen, Germany.
 15. Hoegger, P.J., Majcherczyk, A., Dwivedi, R., Kilaru, S., Svobodová, K. & Kües, U. (2007). Enzymes in wood degradation. In: *Wood Production, Wood Technology and Biotechnological Impacts* (Kües, U., ed.), Universitätsverlag Göttingen, Göttingen, Germany.
 16. Rühl, M., Kilaru, S., Hoegger, P.J., Kharazipour, A. & Kües, U. (2007). Production of laccases for the wood industry. In: *Wood Production, Wood Technology and Biotechnological Impacts* (Kües, U., ed.), Universitätsverlag Göttingen, Göttingen, Germany.
 17. Bridge, P.D., Roberts, P.J., Spooner, B.M. & Panchal, G. (2003). On the unreliability of published DNA sequences. *New Phytologist*, 160: 43-48.
 18. Zolan, M.E. & Pukkila P.J. (1986). Inheritance of DNA methylation in *Coprinus cinereus*. *Molecular and Cellular Biology*, 6: 195-200.
 19. Liu, D., Coloe, S., Baird, R. & Pedersen, J. (2000). Rapid mini-preparation of fungal DNA for PCR. *Journal of Clinical Microbiology*, 38: 471.
 20. Uljé, C.B. (2003). All about inkcaps. <http://www.homepages.hetnet.nl/~idakees/>
 21. Orton, P.D. & Watling, R. (1979). *British fungus flora. Agarics and Boleti 2. Coprinaceae Part 1: Coprinus*. Her Majesty's Stationary Office, Edinburg, U.K.
 22. White, T.J., Bruns, T., Lee, S. & Taylor, J.W. (1990). Amplification and direct sequencing of fungal ribosomal RNA genes for phylogenetics. In: *PCR Protocols: A Guide to Methods and Applications* (Innis, M.A., Gelfand, D.H., Sninsky, J.J. & White, T.J., eds.), Academic Press Inc., New York, pp. 315-322.
 23. Sambrook, J. & Russell, D.W. (2001). *Molecular Cloning. A Laboratory Manual*. 3rd Edn. Cold Spring Harbor Laboratory Press, Cold Spring Harbor, N.Y.
 24. Kumar, S., Tamura, K. & Nei, M. (2004). MEGA3: Integrated software for molecular evolutionary genetics analysis and sequence alignment. *Briefings in Bioinformatics*, 5: 150-163.
 25. Aanen, D.K., Kuyper, T.W. & Hoekstra, R.F. (2001). A widely distributed ITS polymorphism within a biological species of the ectomycorrhizal fungus *Hebeloma*

- velutipes*. Mycological Research, 105: 284-290.
26. Okabe, I. & Matsumoto, N. (2003). Phylogenetic relationships of *Sclerotium rolfsii* (teleomorph *Athelia rolfsii*) and *S. delphinii* based on ITS sequences. Mycological Research, 107: 165-168.
 27. Wang, D.M. & Yao, Y.J. (2005). Intrastrain internal transcribed spacer heterogeneity in *Ganoderma* species. Canadian Journal of Microbiology, 51: 113-121.
 28. Kauserud, H. & Schumacher, T. (2003). Ribosomal DNA variation, recombination and inheritance in the basidiomycete *Trichaptum abietinum*: Implications for reticulate evolution. Heredity, 91: 163-172.
 29. Schmidt, O. & Moreth, U. (2003). Molecular identity of species and isolates of internal pore fungi *Antrodia* spp. and *Oligoporus placenta*. Holzforschung, 57: 120-126.
 30. Högberg, N. & Land, C.J. (2004). Identification of *Serpula lacrymans* and other decay fungi in construction timber by sequencing of ribosomal DNA. Holzforschung, 58: 199-204.
 31. Kauserud, H., Hofton, T.H. & Saetre, G.P. (2007). Pronounced ecological separation between two closely related lineages of the polyporous fungus *Gloeoporus taxicola*. Mycological Research, 111: 778-786.
 32. Kauserud, H., Svegård, I.B., Decock, C. & Hallenberg, N. (2007). Hybridization among cryptic species of the cellar fungus *Coniophora puteana* (Basidiomycota). Molecular Ecology, 16: 389-399.
 33. Larraya, L.M., Perez, G., Peñas, M.M., Baars, J.J.P., Mikosch, T.S.P., Pisabarro, A.G. & Ramírez, L. (1999). Molecular karyotype of the white rot fungus *Pleurotus ostreatus*. Applied and Environmental Microbiology, 65: 3413-3417.
 34. Lechner, B.E., Wright, J.E. & Albertó, E. (2004). The genus *Pleurotus* in Argentina. Mycologia, 96: 845-858.
 35. Nobles, M.K. (1948). Studies in forest pathology. VI. Identification of cultures of wood-rotting fungi. Canadian Journal of Research, 26: 281-431.
 36. Tomšovský, M., Kolořík, M., Pažoutová, S. & Homolka, L. (2006). Molecular phylogeny of European Trametes (Basidiomycetes, Polyporales) species based on LSU and ITS (nrDNA) sequences. Nova Hedwigia, 82: 269-280.
 37. Schmidt, O., Grimm, K. & Moreth, U. (2002). Molecular identity of species and isolates of the *Coniophora* cellar fungi. Holzforschung, 56: 563-571.
 38. Ginns, J. (1982). A monograph of the genus *Coniophora* (Aphylllophorales, Basidiomycetes). Opera Botanica, 61: 1-61.
 39. Janza, J., Mozafar, A., Anken, T., Ruh, R., Sanders, I.R. & Frossard, E. (2002). Diversity and structure of AMF communities as affected by tillage. Mycorrhiza, 12: 225-234.
 40. Hibbett, D.S., Binder, M., Bischoff, J.F., Blackwell, M., Cannon, P.F., Eriksson, O.E., Huhndorf, S., James, T., Kirk, P.M., Lücking, R., Lumbsch, H.T., Lutzoni, F., Matheny, P.B., McLaughlin, D.J., Powell, M.J., Redhead, S., Schoch, C.L., Spatafora, J.W., Stalpers, J.A., Vilgalys, R., Aime, M.C., Aptroot, A., Bauer, R., Begerow, D., Benny, G.L., Castlebury, L.A., Crous, P.W., Dai, Y.-C., Gams, W., Geiser, D.M., Griffith, G.W., Gueidan, C., Hawksworth, D.L., Hestmark, G., Hosaka, K., Humber, R.A., Hyde, K.D., Ironside, J.E., Kõljalg, U., Kurtzman, C.P., Larsson, K.-H., Lichtwardt, R., Longcore, J., Miądlikowska, J., Miller, A., Moncalvo, J.-M., Mozley-Standridge, S., Oberwinkler, F., Parmasto, E., Reeb, V., Rogers, J.D., Roux, C., Ryvarden, L., Sampaio, J.P.,

- Schüßler, A., Sugiyama, J., Thorn, R.G., Tibell, L., Untereiner, W.A., Walker, C., Wang, Z., Weir, A., Weiss, M., White, M.M., Winka, K., Yao, Y.-J. & Zhang, N. (2007). A higher-level phylogenetic classification of the fungi. *Mycological Research*, 111: 509-547.
41. Johanson, A., Turner, H.C., McKay, G.J. & Brown, A.E. (1998). A PCR-based method to distinguish fungi of the rice sheath-blight complex, *Rhizoctonia solani*, *R. oryzae* and *R. oryzae-sativae*. *FEMS Microbiology Letters*, 162: 289-294.
42. Buzina, W., Braun, H., Freudenschuss, K., Lackner, A. & Stammberger, H. (2003). Fungal biodiversity as found in nasal mucus. *Medical Mycology*, 41: 149-161.
43. Steiner, U., Ahimsa-Müller, M.A., Markert, A., Kucht, S., Gross, J., Kauf, N., Kuzma, M., Zych, M., Lamshoft, M., Furmanowa, M., Knoop, V., Drewke, C. & Leistner, E. (2006). Molecular characterization of a seed transmitted clavicipitaceous fungus occurring on dicotyledoneous plants (Convolvulaceae). *Planta*, 224: 533-544.
44. Otero, J.T., Ackerman, J.D. & Bayman, P. (2004). Differences in mycorrhizal preferences between two tropical orchids. *Molecular Ecology*, 13, 2393-2404.
45. Sato, A., Watanabe, Y., Nugroho, N.B., Chrisnayanti, E., Natusion, U.J., Koesnandar & Nishida, H. (2003). Screening for dioxin-degrading basidiomycetes from temperate and tropical forests. *World Journal of Microbiology & Biotechnology*, 19: 763-766.
46. Romero, M.L., Terrazas, E., van Bavel, B. & Mattiasson, B. (2006). Degradation of toxaphene by *Bjerkandera* sp. strain BOL13 using waste biomass as a substrate. *Applied Microbiology and Biotechnology*, 71: 549-554.
47. Hibbett, D.S., Gilbert, L.B. & Donoghue, M.J. (2000). Evolutionary instability of ectomycorrhizal symbioses in basidiomycetes. *Nature*, 407: 506-508.
48. Hibbett, D.S., Pine, E.M., Langer, E., Langer, G. & Donoghue, M.J. (1997). Evolution of gilled mushrooms and puffballs inferred from ribosomal DNA sequences. *Proceedings of the National Academy of Sciences USA*, 94: 12002-12006.
49. Ko, K.S., Hong, S.G. & Jung, H.S. (1997). Phylogenetic analysis of *Trichaptum* based on nuclear 18S, 5.8S and ITS ribosomal DNA sequences. *Mycologia*, 89: 727-734.
50. Ko, K.S., Jung, H.S. (1999). Molecular phylogeny of *Trametes* and related species. *Antonie van Leeuwenhoek*, 75: 191-199.
51. Redhead, S.A., Vilgalys, R., Moncalvo, J.M., Johnson, J. and Hopple, J.S. Jr. (2001). *Coprinus* Pers. and the disposition of *Coprinus* species *sensu lato*. *Taxon*, 50: 203-241.
52. Elliott, T.J. & Challen, M.P. (1993) Genetic ratios in secondarily homothallic basidiomycetes. *Experimental Mycology*, 7: 170-174.
53. Kües, U., James, T.Y., Vilgalys, R. & Challen, M.P. (2001). The chromosomal region containing *pab-1*, *mip*, and the *A* mating type locus of the secondarily homothallic homobasidiomycete *Coprinus bilanatus*. *Current Genetics*, 39: 16-24.
54. Frøslev, T.G., Jeppesen, T.S., Læssøe, T. & Kjølner, R. (2007). Molecular phylogenetics and delimitation of species in *Cortinari* section *Calochroi* (Basidiomycota, Agaricales) in Europe. *Molecular Phylogenetics and Evolution*, 44: 217-227.
- Ryan, M.J. & Smith, D. (2004). Fungal genetic resource centres and the genomic challenge. *Mycological Research*, 198: 1351-1362.
55. Elliott, T.J. & Challen, M.P. (1993) Genetic ratios in secondarily homothallic basidiomycetes. *Experimental Mycology*, 7: 170-174.

Table 1 : Strains of wood-rotting fungi analyzed by ITS sequencing

Strain as originally named #	Fragment length in bp ⁺	Hits in NCBI GenBank			Gen Bank accession number/new species name *
		Accession number (region)	Species	% Identity	
Basidiomycota/Agaricales					
<i>Armillaria gallica</i> 910224.1 ¹	750	AY190248 (55-805)	<i>Armillaria gallica</i>	99	EU140578
<i>Armillaria mellea</i> 901010.3 ¹	782	AF163581 (36-819)	<i>Armillaria mellea</i>	98	EU162047
<i>Pleurotus ostreatus</i> N001 ²	594	AY540322 (61-654)	<i>Pleurotus floridanus</i>	100	EU162048
<i>Schizophyllum commune</i> 4-39 x 4-40 ³	563	AF348142 (71-633)	<i>Schizophyllum commune</i>	100	EU162049
Basidiomycota/Boletales					
<i>Coniophora arida</i> FBI 516 ⁴	648	AJ344110 (40-687)	<i>Coniophora puteana</i>	99	EU162050/ <i>Coniophora</i> sp.
<i>Serpula lacrymans</i> FSU 2886 ⁵	538	AF335275 (75-612)	<i>Serpula lacrymans</i>	100	EU162051
Basidiomycota/Polyporales					
<i>Antrodia serialis</i> 910310.8 ¹	561	AJ345010 (37-594)	<i>Antrodia serialis</i>	99	EU162052
<i>Ganoderma adspersum</i> FBI 59 (CBS 351.74) ⁴	570	EF060012 (10-579)	<i>Ganoderma adspersum</i>	100	EU162053
<i>Gloeophyllum odoratum</i> 050601.3 ¹	509	AJ420947 (219-521)	<i>Gloeophyllum abietinum</i>	86	EU162054
<i>Gloeophyllum sepiarium</i> 041118.30 ¹	559	AJ420946 (31-589)	<i>Gloeophyllum sepiarium</i>	99	EU162055
<i>Fomes fomentarius</i> 980706.7 ¹	565	AY354213 (531-2)	<i>Fomes fomentarius</i>	99	EU162056
<i>Trichaptum abietinum</i> (<i>Hirschioporus abietinus</i>) FBI 52 ⁴	572	DQ060096 (50-622)	<i>Bjerkandera</i> sp.	99	EU162066/ <i>Bjerkandera</i> sp.
<i>Polyporus brumalis</i> FBI 5 (CBS 470.72) ⁴	558	AF516525 (36-593)	<i>Bjerkandera adusta</i>	99	
	559		<i>Polyporus brumalis</i>	99	EU162059 (sequence 1) EU162060 (sequence 2)
<i>Trametes gibbosa</i> 911030.1 ¹	577	AY684176 (8-568)	<i>Trametes gibbosa</i>	100	EU162057
<i>Trametes hirsuta</i> 911020.11 ¹	551	AY684170 (4-553)	<i>Trametes hirsuta</i>	99	EU162058

<i>Trametes versicolor</i> 051130.2 ¹	550	AY684179 (8-558)	<i>Trametes versicolor</i>	98	EU162061 (sequence 1)
	551			98	EU162062 (sequence 2)
<i>Trametes zonata</i> 921011.17 ¹	562	AY840580 (31-591)	<i>Trametes versicolor</i>	99	EU162063
		AY684177 (6-564)	<i>Trametes ochracea</i>	98	
		AY684179 (8-569)	<i>Trametes versicolor</i>	98	
Basidiomycota/Russulales					
<i>Heterobasidion annosum</i> (sensu stricto, P-type) 851007.1 ¹	588	X70027 (19-605)	<i>Heterobasidion annosum</i> (sensu stricto, P-type)	99	EU162064
<i>Heterobasidion annosum</i> S-type Steg#216 ⁶	576	X74923 (26-600)	<i>Heterobasidion parviporum</i> (<i>H. annosum</i> S-type)	99	EU162065/ <i>Heterobasidion parviporum</i>
Ascomycota/Xylariales					
<i>Ustulina deusta</i> 910506.1 ¹	578	AF201718 (60-638)	<i>Ustulina deusta</i>	99	EU162067

Origins of Strains

Origins of strains: ¹ isolated by O. Holdenrieder (Zurich); ² obtained from L. Ramírez (Pamplona); ³ monokaryons 4-39 and 4-40 were obtained from H. Wösten (Utrecht) and mated by S. Peddireddi (Göttingen); ⁴ from the culture collection of the Institute of Forest Botany (FBI) in Göttingen (now Büsngen-Institute); ⁵ obtained from K. Voigt (Pilz-Referenz-Zentrum Jena), ⁶ obtained from D. Rigling (WSL, Birmensdorf).

+ Note that a few nucleotides at the ends of the ITS fragments can be missing due to poor labelling in the sequencing reactions of PCR-amplified fragments.

* Species names were newly assigned according to the results from the comparison with ITS sequences deposited in the NCBI GenBank.

Table 2 : Coprini analyzed by ITS sequencing

Strain as originally named #	Fragment length in bp +	Hits in NCBI GenBank			Gen Bank accession number/new species name *
		Accession number (region)	Species	% Identity	
Basidiomycota/Agaricales/Agaricaceae					
<i>Coprinus comatus</i> C53 ¹	579	AY176346 (53-633)	<i>Coprinus comatus</i>	98	EU168100
<i>Coprinus comatus</i> C108 ¹	595	AY176346 (34-631)	<i>Coprinus comatus</i>	97	EU168101
Basidiomycota/Agaricales/ Psathyrellaceae					
<i>Coprinellus disseminatus</i> C50 ¹	367	AY969507 (45-412)	Uncultured basidiomycete	99	EU168102 <i>Coprinellus</i> sp. C50
		AY461838 (59-416)	<i>Coprinellus disseminatus</i>	94	
		DQ093648 (629-245)	<i>Coprinellus disseminatus</i>	93	
<i>Coprinellus radians</i> C22 ¹	617	AY461815 (25-640)	<i>Coprinellus radians</i>	98	EU168103
<i>Coprinellus xanthothrix</i> C144 ¹	462	AF361228 (44-501)	<i>Coprinopsis xanthothrix</i>	98	EU168104
<i>Coprinellus xanthothrix</i> C398 ¹	568	AF361228 (2-571)	<i>Coprinopsis xanthothrix</i>	98	EU168105
<i>Coprinellus xanthothrix</i> C482 ¹	624	AF361228 (22-645)	<i>Coprinopsis xanthothrix</i>	100	EU168106
<i>Parasola plicatilis</i> C65 ¹	399	AF345818 (142-536)	<i>Coprinellus flocculosus</i>	98	EU168107 <i>Coprinellus</i> sp. C65 (<i>flocculosus</i> ?)
		AF345817 (31-609)	<i>Coprinopsis stercorea</i>	97	EU168108 <i>Coprinopsis</i> sp. C67
<i>Coprinopsis atramentarius</i> C67 ¹	586	DQ486694 (20-599)	<i>Coprinopsis atramentaria</i>	93	
<i>Coprinopsis cinerea</i> C344 ¹	621	AY461825 (56-677)	<i>Coprinopsis cinerea</i>	99	EU168109
<i>Coprinopsis lagopus</i> C215 ¹	525	AF345815 (108-633)	<i>Coprinopsis lagopides</i>	99	EU168110 <i>Coprinopsis</i> sp. C215 (<i>lagopides</i> ?)
		DQ093649 (187-665)	<i>Coprinus</i> sp.	98	
		AF345813 (153-638)	<i>Coprinopsis lagopus</i>	85	

<i>Coprinopsis lagopides</i> C262 ¹	614	DQ093649	<i>Coprinus</i> sp.	99	EU168111
		(50-664)			
		AF345815	<i>Coprinopsis lagopides</i>	96, 97	<i>Coprinopsis</i> sp. C262
		(22-144, 146-623)			
		AF345813	<i>Coprinopsis lagopus</i>	83	
		(28-620)			
<i>Coprinopsis scobicola</i> Cb1 ²	608	AB097564	<i>Coprinopsis neolagopus</i>	92	EU168112
		(27-632)			
<i>Coprinopsis scobicola</i> Cb2 ²	524	AB097564	<i>Coprinopsis neolagopus</i>	92	EU168113
		(73-596)			
<i>Coprinopsis psychromorbida</i> ³	622	AY969953	Uncultured basidiomycete	98	EU168114
		(31-652)			Unidentified snow mold
		U85795	<i>Athelia bombacina</i>	86	
		(92-718)			

Origins of strains

- # Origins of strains: ¹ obtained from T. James (Duke University); ² obtained from M. Challen (Wellesbourne); ³ from O. Holdenrieder via the fungal collection of the Institute for Microbiology, ETH Zurich
- + Note that a few nucleotides at the ends of the ITS fragments can be missing due to poor labelling in the sequencing reactions of PCR-amplified fragments.
- * Species names were newly assigned according to the results from the comparison with ITS sequences deposited in the NCBI GenBank.

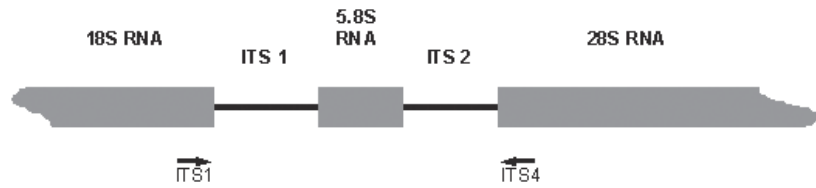


Fig. 1: Sector from an rDNA cluster with a partial 18S rRNA gene, ITS 1, a 5.8S rRNA gene, ITS 2, and a partial 28S rRNA gene. The positions and directions of primers ITS1 and ITS4 are marked to indicate the region to be amplified in ITS analysis.

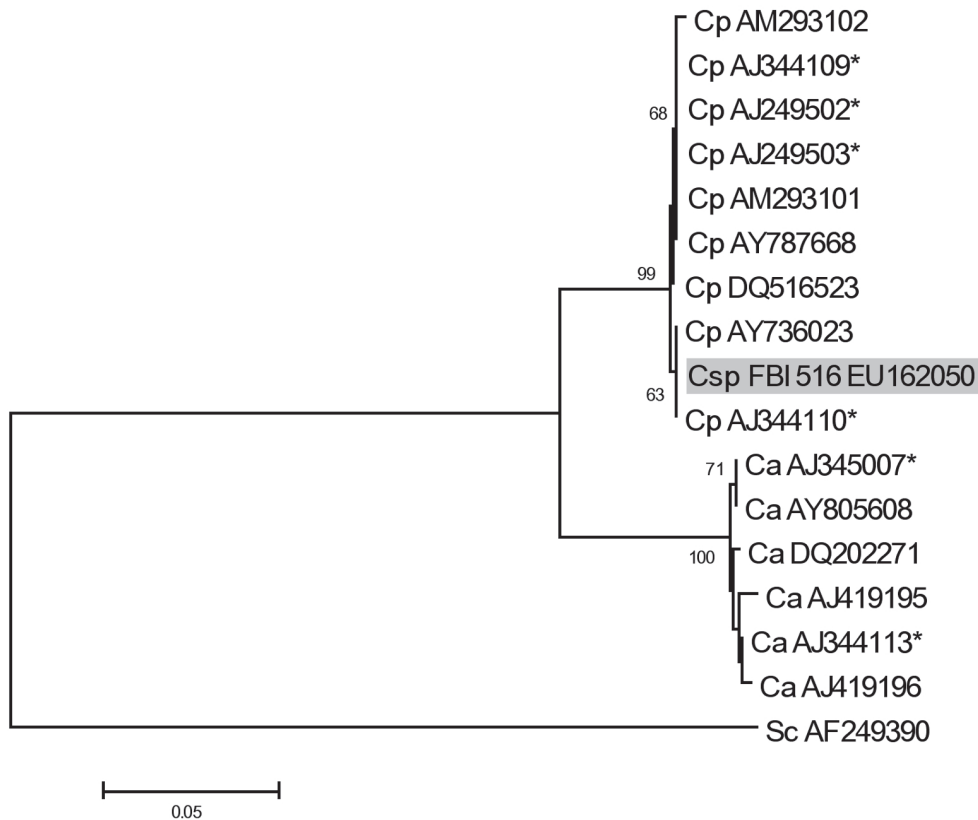


Fig. 2: Phylogenetic tree of ITS sequences from the genus *Coniophora* from the Boletales. Cp = ITS sequences from strains marked with *Coniophora puteana*, Ca = ITS sequences from strains marked as *Coniophora arida*. Codes indicate NCBI GenBank accession numbers. Stars mark the ITS sequences from reference strains of Schmidt et al. (37). Strain FBI 516 listed so far as *C. arida* (marked in grey) has now been renamed *C. sp.* (Csp FBI 516). The *Schizophyllum commune* sequence (Sc AF249390) served in this analysis as outgroup. Bootstrap values (500 replications) above 50 are shown at tree branchings. The scale bar defines the number of nucleotide substitutions per site.

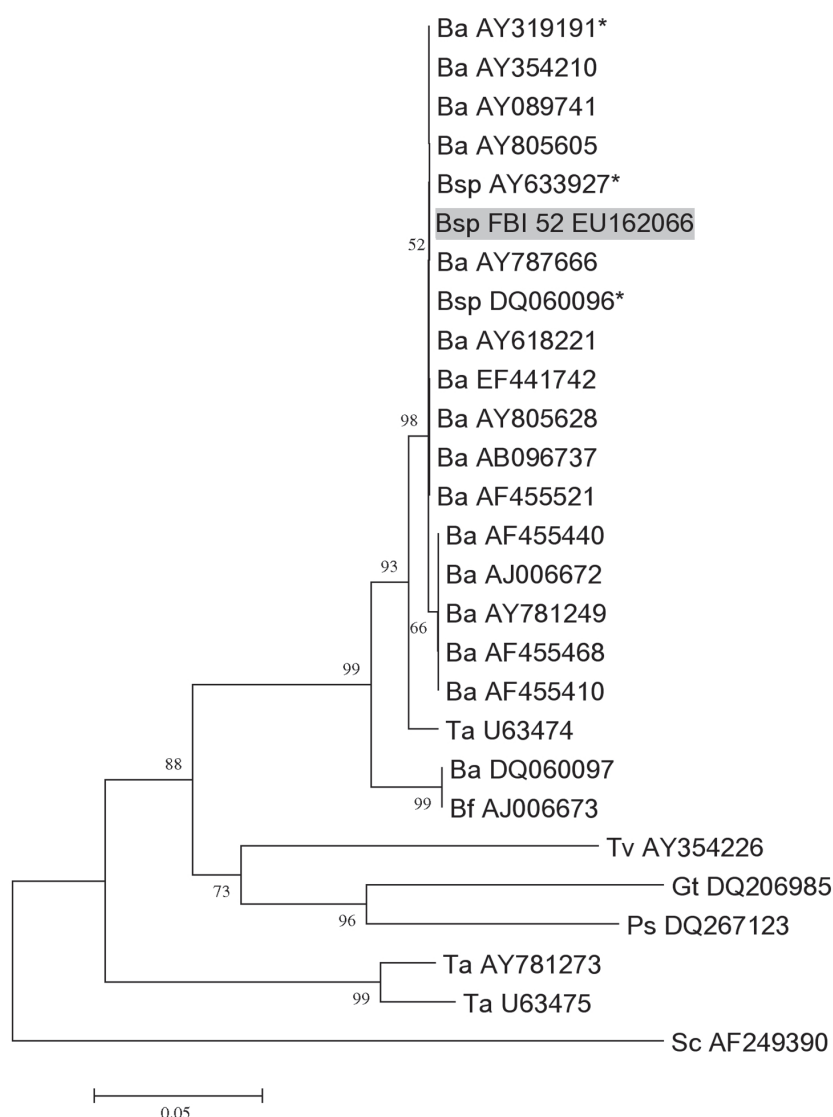


Fig. 3: Phylogenetic tree of species from the Polyporales. Ba = ITS sequences from strains marked with *Bjerkandera adusta*, Bf = ITS sequence from a strain marked with *Bjerkandera fumosa*, Bsp = ITS sequences from strains marked with *Bjerkandera* sp., Gt = ITS sequence from a strain marked with *Ganoderma tsuga*, Ps = ITS sequence from a strain marked with *Polyporus squamosus*, Ta = ITS sequences from strains marked with *Trichaptum abietinum*, Tv = ITS sequence from a strain marked with *Trametes versicolor*. Codes indicate NCBI GenBank accession numbers. Stars mark the ITS sequences from *Bjerkandera* strains that were morphologically defined. Strain FBI 52 listed so far as *T. abietinum* (marked in grey) has now been renamed *B. sp.* (Bsp FBI 52). The *Schizophyllum commune* sequence (Sc AF249390) served in this analysis as outgroup. Bootstrap values (500 replications) above 50 are shown at tree branchings. The scale bar defines the number of nucleotide substitutions per site.

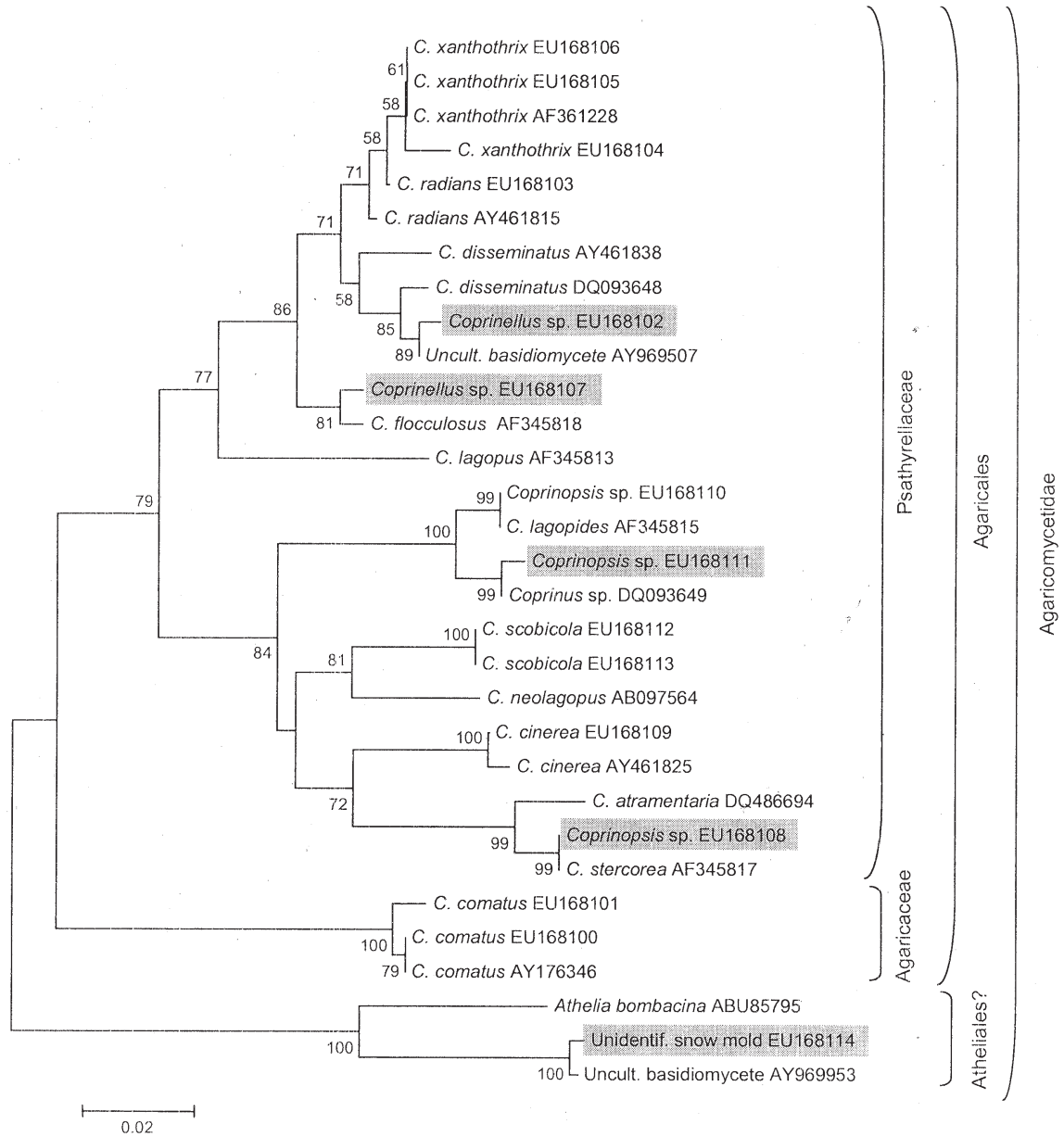


Fig. 4: Phylogenetic tree of coprini. Codes indicate NCBI GenBank accession numbers. Strains marked in grey are those from this study that were assigned to a wrong species name. The *Athelia bombacina* sequence (ABU85795) served in this analysis as outgroup. Bootstrap values (500 replications) above 50 are shown at tree branchings. The scale bar defines the number of nucleotide substitutions per site.

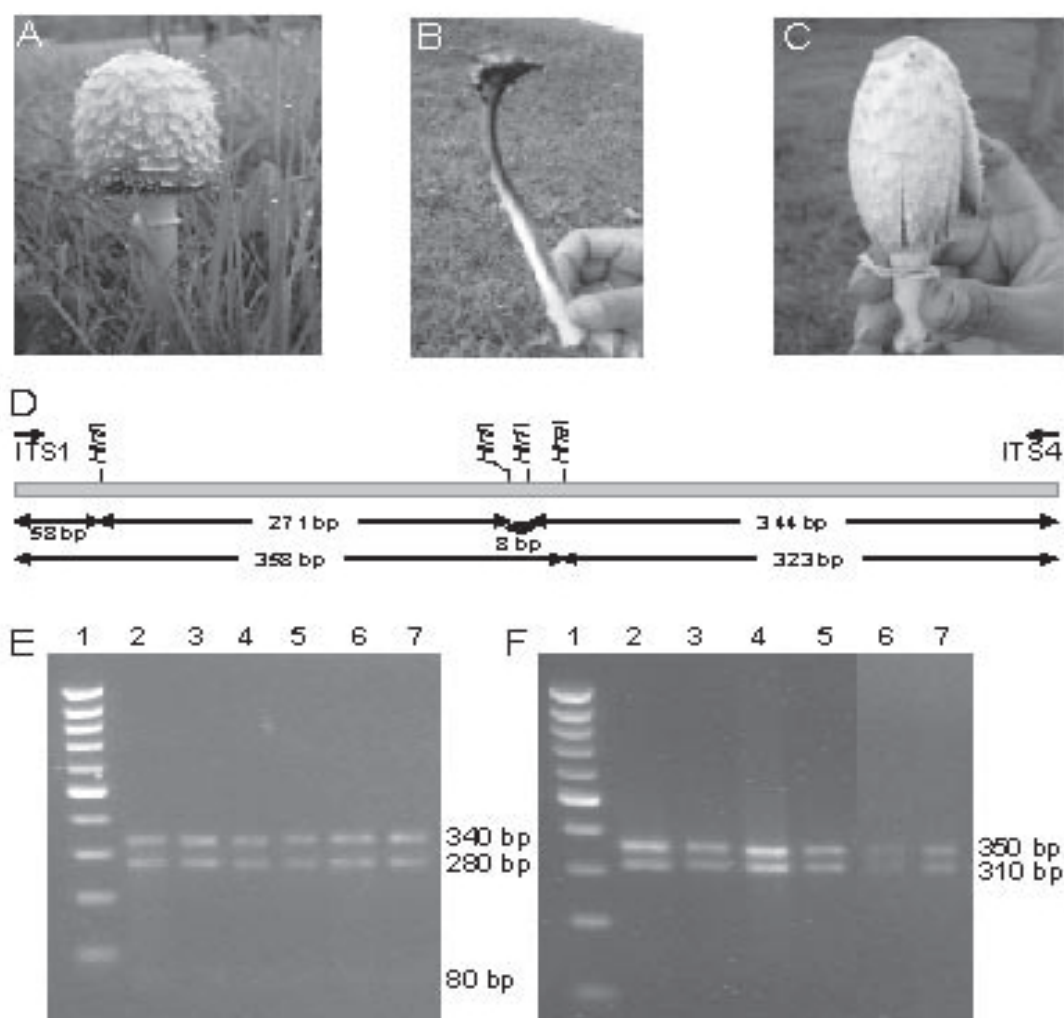


Fig. 5: Analysis of ITS sequences from *Coprinus comatus*: Fruiting bodies of *C. comatus* collected in year 2006 on the grounds of the North Campus of the Georg-August-University of Göttingen used to isolate strains MN-23 (A), MN-24 (B) and MN-25 (C) from stipe tissues. Physical map of the fragment with the internal transcribed spacer 1, the 5.8S rRNA gene, and the internal transcribed spacer 2 from *C. comatus* chromosomal DNA (AF345803) plus added ITS1 and ITS4 primer sequences (D). Sizes of fragments expected to be obtained in digests with restriction enzymes *HinfI* and *HhaI* are indicated. Restriction digests of PCR-amplified fragments with *HinfI* (E) and *HhaI* (F). Lane 1: size marker (1 kb ladder); lane 2 to 7: DNA amplified with primers ITS1 and ITS4 from genomic DNA of *C. comatus* C108, 1-2004, 2-2004, MN-23, MN-24, and MN-25, respectively.

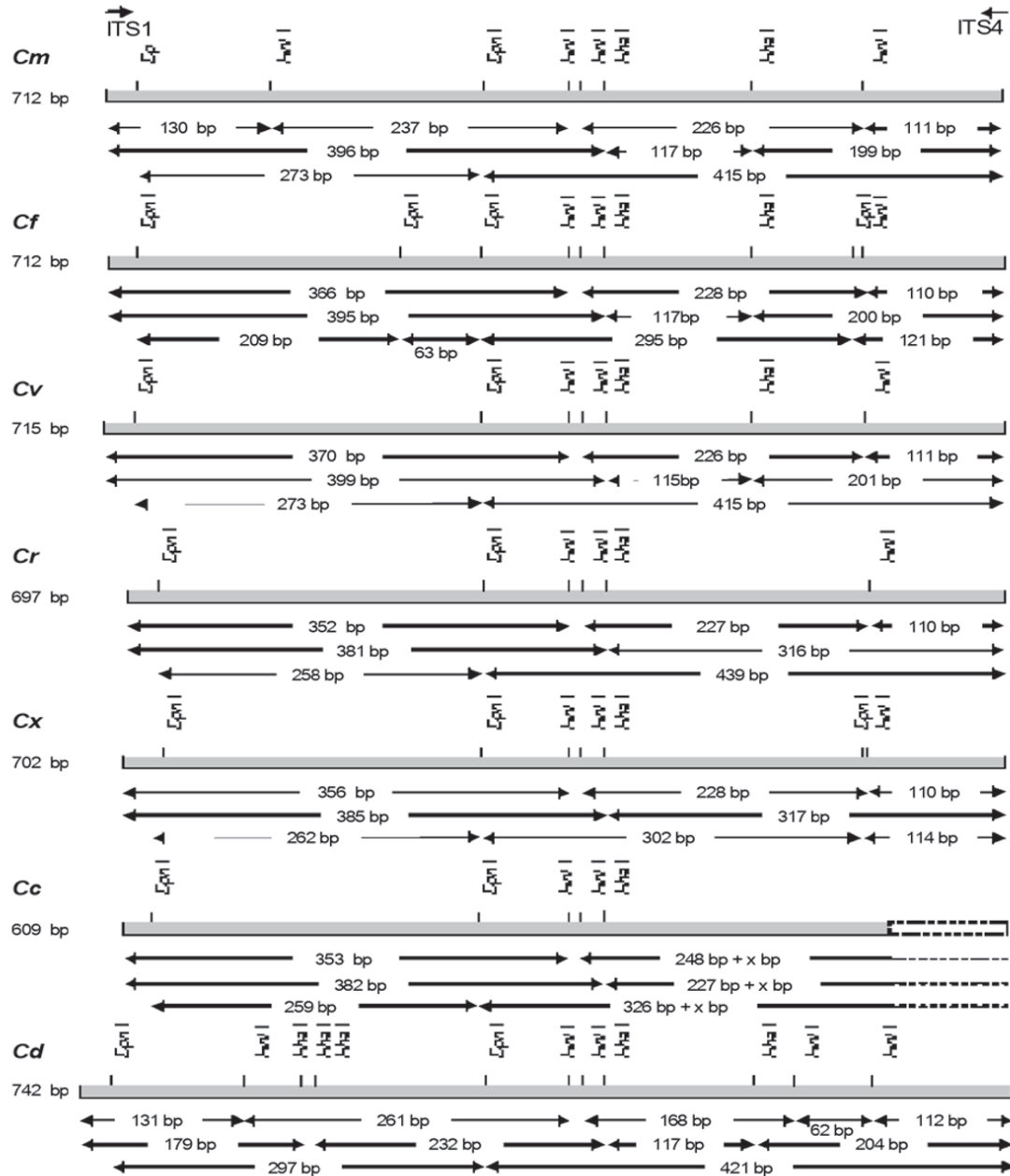


Fig. 7: Physical maps of ITS fragments of *Coprinellus micaceus* (*Cm*, AF345808), *Coprinellus flocculosus* (*Cf*, AF345818), *Coprinellus verrucispermus* (*Cv*, AY521250), *Coprinellus radians* (*Cr*, AF345822), *Coprinellus xanthothrix* (*Cx*, AF361228), *Coprinellus curtus* (*Cc*, AY46181834; incomplete sequence!), and *Coprinellus disseminatus* (*Cd*, AF345809) showing positions of restriction sites for enzymes *Hinf*I, *Hha*I, and *Dpn*I.

Studies on the influence of penetration enhancers on *in vitro* permeation of carvedilol across rat abdominal skin

G. Ramesh, Vamshi Vishnu Y, Kishan V and Madhusudan Rao Y*

Centre for Biopharmaceutics and Pharmacokinetics, University College of Pharmaceutical Sciences, Kakatiya University, Warangal- 506 009 (A.P)

* For correspondence - ymrao123@yahoo.com

Abstract

The aim of the investigation was to study the effect of penetration enhancers on the *in vitro* permeation of carvedilol across excised rat abdominal skin and to select suitable penetration enhancer. Terpenes menthol, camphor, d-limonene and carvone; surfactants, Transcutol and Labrasol at 5 % w/v, were used as penetration enhancers in the study. Skin permeation studies were conducted in Franz diffusion cells using excised rat abdominal skin. Solutions containing 5 % w/v camphor showed maximum permeation (451.20 $\mu\text{g}^?$) in 24 hr with a flux of 5.23 $\mu\text{g}/\text{hr}/\text{cm}^2$ and was significantly different ($p < 0.05$) to flux obtained with other permeation enhancers. Control (phosphate buffer saline, pH 7.4 containing 40 % v/v polyethylene glycol) sample showed lowest permeation (59.18 $\mu\text{g}^?$), with a flux of 0.67 $\mu\text{g}/\text{hr}/\text{cm}^2$. The flux of carvedilol obtained from the solutions containing camphor, Transcutol, d-limonene, carvone, Labrasol and menthol (5 % w/v) were 7.81, 7.26, 6.52, 5.91, 4.21 and 2.28 times higher than that observed with control, respectively. The flux obtained with camphor was significantly higher ($p < 0.05$) than the fluxes obtained with other penetration enhancers. The present study suggests that camphor, Transcutol and d-limonene at 5 % w/v level may be used as penetration enhancers in the development of transdermal drug delivery systems.

Key words

Carvedilol, Terpenes, Transcutol, Labrasol, Rat skin.

Introduction

Carvedilol is a non-selective β -adrenergic antagonist widely used in the treatment of mild to moderate essential hypertension and stable angina pectoris. It also possesses antioxidant and antiproliferative effects. That may enhance its ability to combat the deleterious effects of sympathetic nervous system activities in heart failure (1). It is well absorbed followed by oral administration. The systemic availability is approximately 25-35 % because of high first pass metabolism (2). To reduce its high first pass metabolism and enhance its bioavailability other routes of administration such as buccal (3), have been reported. The biological properties of carvedilol such as high first pass metabolism, low dose, need for long term treatment and repetitive dosing make this drug an interesting candidate for transdermal administration.

The transdermal route of administration has been recognized as one of the potential route for the local and systemic delivery of drugs. The advantages of transdermal delivery, include therapeutic benefits such as sustained delivery of drugs to provide a steady plasma profile,

particularly for drugs with short half lives and hence reduced systemic side effects; reducing the typical dosing schedule to once daily or even once weekly hence generating the potential for improved patient compliance and avoidance of the first pass metabolism effect for drugs with poor bioavailability (4). However, the highly organized structure of stratum corneum forms an effective barrier to the permeation of drugs, which must be modified if poorly penetrating drugs are to be administered. The use of chemical penetration enhancers would significantly increase the number of drug molecules suitable for transdermal delivery (5). Terpenes present in naturally occurring volatile oils appear to be clinically acceptable enhancers (6). Moreover, a wide variety of terpenes have been shown to increase the percutaneous absorption of number of drugs (7). In this investigation, the penetration enhancers camphor, carvone, menthol, d-limonene, Transcutol and Labrasol at 5 % w/v concentration were used. Excised rat abdominal skin was used for *in vitro* permeation studies.

Previous studies, reported carvedilol transdermal therapeutic systems based on polymethacrylates (8) and membrane controlled matrix type patches using non ionic surfactants as penetration enhancers (9). The objective of present study was to investigate the effect of penetration enhancers on the permeation of carvedilol across rat abdominal skin and to select suitable penetration enhancer(s).

Materials and methods

Materials

Carvedilol was provided by Sun Pharmaceuticals, India. D-limonene, carvone menthol and poly ethylene glycol 400 (PEG 400) were purchased from Merck, India. Camphor was purchased from Sd fine chemicals India. Labrasol (PEG-8 caprylate/caprate), Transcutol (Diethyleneglycol monoethyl ether) were gifts

from Gattefosse (Cedex, France). All other chemicals and reagents used are of analytical grade.

Preparation of Rat Abdominal Skin

Albino rats weighing 150-200 gm were selected for permeation studies and the study was conducted with the approval of institutional ethical committee. The animals were sacrificed using anesthetic ether, hair of test animals was carefully trimmed short (<2 mm) with a pair of scissors and the full thickness skin was removed from the abdominal region. The epidermis was prepared surgically by heat separation technique (10), which involved soaking the entire abdominal skin in water at 60° C for 45 sec, followed by careful removal of the epidermis. The epidermis was washed with water and used for *ex vivo* permeability studies. The thickness of the skin was measured with digital micrometer (Mitotoyo, Japan).

In vitro permeability studies

Franz diffusion cell with a surface area of 3.56 cm² was used for *in vitro* permeation studies. Rat abdominal skin with a thickness of about 1.0 mm was mounted between the compartments of the diffusion cell with stratum corneum facing the donor compartment. The receiver phase is 12 ml of phosphate buffer saline (PBS) pH 7.4 containing 40 % v/v of PEG 400, stirred at 500 rpm on a magnetic stirrer; the whole assembly was kept at 37 ± 0.5°C. PBS (pH 7.4), containing 40 % v/v PEG 400 and 3 mg of carvedilol (3 mL) was placed in the donor compartment. Carvedilol is practically insoluble in water hence a buffer PEG 400 system was used for solubilizing carvedilol. All individual solutions in donor compartment were prepared separately with and without (5% w/v) penetration enhancers. Menthol, camphor, Transcutol, Labrasol, d-limonene and carvone as penetration enhancers and PBS pH 7.4 containing 40 % v/v PEG 400

as control were used in the study. The entire setup was placed over magnetic stirrer and temperature was maintained at about $37 \pm 0.5^\circ\text{C}$ by placing the diffusion cell in a water bath. The amount of drug permeated was determined by removing 1 mL of sample at appropriate time intervals up to 24 hr, the volume was replenished with an equal volume of PBS pH 7.4 containing 40 % v/v PEG 400. The drug content in the samples was determined by high performance liquid chromatography (HPLC) and the concentration was corrected for sampling effects according to the equation (11).

$$C_n^1 = C_n (V_T/V_T - V_S) (C_{n-1}^1 / C_{n-1})$$

Where C_n^1 is the corrected concentration of the n^{th} sample, C_n is the measured concentration of carvedilol in the n^{th} sample, C_{n-1} is the measured concentration of the carvedilol in the $(n-1)^{\text{th}}$ sample, V_T is the total volume of the receiver fluid and V_S is the volume of the sample drawn.

Estimation of drug content in the sample by HPLC method

The HPLC system (Shimadzu, Japan) consisted of a LC-10AT solvent module, and a model UV-Visible Spectrophotometric detector (SPD-10A) with LC 10 soft ware. Carvedilol was quantified according to a reported method (12). The column used was a Kromasil KR 100-5C8 (25 X 4.6 mm i.d, 5 μ). The mobile phase consisted of acetonitrile, 15 mM orthophosphoric acid (37:63), and 0.25 v/v % triethylamine mixture, and was adjusted to pH 2.5 with orthophosphoric acid. The elute was monitored at 238 nm with a flow rate of 1 mL/min. The sensitivity was set to 0.005 AUFS.

Data analysis

As described by Barry (13), the steady state flux (J_s), lag time (T_L), diffusion coefficient (D) and apparent permeation coefficient (P_{app}) are defined by

$$J_s = (dQ/dt)_{ss} / A \quad - (1)$$

$$D = \frac{h^2}{6T_L} \quad - (2)$$

$$P = \frac{dQ}{Dt} \frac{1}{A} \frac{1}{C} \quad - (3)$$

Where, A is the effective diffusion area; h, the thickness of skin; C_s , the concentration in the saturated solution and $(dQ/dt)_{ss}$ is the steady state slope.

Statistical Analysis

The Q_{24} (cumulative amount permeated in 24 hr) and flux values obtained from the various systems were tested for significant differences using a one-way analysis of variance (ANOVA) or unpaired t test. If the significant differences exist when ANOVA was used, the pair wise comparison of different systems was done to find out statistical significant difference in parameters using a Dunnet's test. When the normality test failed, Kruskal-Wallis one-way ANOVA was used to find out if the significant differences exist between different systems. The statistical analysis was conducted using SigmaStat software version 1.0 (Jandel Corp., California).

Results and Discussion

Effect of Penetration Enhancers

The effect of enhancers on permeation of a drug usually depends upon physicochemical characteristics of both permeant as well as enhancer molecule. Among enhancers, various terpenes have been widely used for transdermal delivery of compounds (13). The effects of various penetration enhancers on the percutaneous penetration profile of carvedilol was shown in Table 1, Figs. 1 and 2. The thickness of isolated skin was found to be in between from 844 to 1234 microns.

Solutions containing 5 % w/v camphor showed maximum permeation of 451.20 μg in 24 hr with

a flux of 5.23 $\mu\text{g/hr/cm}^2$, was significantly higher ($p < 0.05$) than the amount of carvedilol permeated by other permeation enhancers used in the study. Control sample showed lowest amount of permeation, 59.18 μg in 24 hr with a flux of 0.67 $\mu\text{g/hr/cm}^2$. Maximum flux (5.23 $\mu\text{g/hr/cm}^2$) obtained with camphor at 5 % w/v, was significantly higher ($p < 0.05$) than the flux obtained with other penetration enhancers, but was not significantly different ($p < 0.05$) from the flux obtained with Transcutol. Transcutol (4.87 $\mu\text{g/hr/cm}^2$) and d-limonene (4.37 $\mu\text{g/hr/cm}^2$) showed similar flux values with lag time of 0.30 hr and 0.40 hr respectively.

The comparison of carvedilol flux obtained from drug solutions containing 5 % w/v penetration enhancer through excised rat skin was shown in Fig 3. The effect of the various enhancers on the flux of carvedilol followed the order: Camphor > Transcutol > d-limonene > Carvone > Labrasol > Menthol > Control. The flux of carvedilol obtained from the solutions containing camphor, Transcutol, d-limonene, carvone, Labrasol and menthol (5 % w/v) were 7.81, 7.26, 6.52, 5.91, 4.21 and 2.28 times higher than that observed with control, respectively. The main findings of the study are the accelerants enhance diffusion or partition and thus permeation of drugs. The lipid partitioning theory was proposed by Barry to describe the mechanism of action of permeation enhancers (14), whether by (i) disruption of the highly ordered structure of SC lipids, (ii) interactions with intracellular proteins or (iii) improvement in partitioning of the drug, co enhancers or co solvent in to the stratum corneum.

In this study, we found that diffusion of carvedilol through the skin was increased by terpenes. It is reported that terpenes enhance diffusion of drugs by extracting lipids from stratum corneum (15, 16), it results in reorganization of lipid domain and barrier disruption (17, 18). The mechanism of barrier disruption may be due to the

competitive hydrogen bonding of oxygen-containing monoterpenes with ceramide head groups, thereby breaking the interlamellar hydrogen bonding network of lipid bilayer of stratum corneum and new polar pathways or channels are formed (19, 20). DSC proved the barrier disruptive action of terpenes, where there was a shift in endothermic transition temperature of stratum corneum lipids after treatment with terpenes (21). The other possible mechanism of action may be the lipid fluidizing activity of terpenes containing essential oils. Fourier transform infrared (FTIR) studies proved the lipid extractive action of terpenes from stratum corneum, where there was a decrease in heights and areas of both symmetric and asymmetric CH_2 stretching absorbance peaks of stratum corneum lipids (16, 22). Surfactants, Transcutol and Labrasol change lipid chain fluidity of the SC and improve drug partition (23).

Conclusion

The present study suggests that camphor, Transcutol and d-limonene at 5 % w/v concentration may be used as penetration enhancers, for the transdermal delivery of carvedilol. The data obtained in the present study using rat abdominal skin cannot be translated to *in vivo* delivery in humans as other factors such as cutaneous microvasculature, which prevents the accumulation of the drug in the skin and the cutaneous metabolism of the drug which significantly alter the permeation profile of the drug. The results obtained from this study will be helpful in the development of transdermal drug delivery systems. Further work is recommended to evaluate the optimum concentration of camphor, Transcutol and d limonene to meet the target flux.

Acknowledgements

The authors acknowledge the financial support received from AICTE, New Delhi, India. The

authors acknowledge M/s Sun Pharma, Baroda, India and M/s Gattefosse, France for providing gift samples of carvedilol and Transcutol and Labrasol, respectively.

References

1. Packer, M., Coats, A.J., Fowler, M.B., Kataus, H.A., Krum, H., Mohaosi, P., Rouleau, J.L., Tenaera, M., Castaigme, A., Roecker, E.B., Schultz, M.K. and De Mets, D.L. (2001) Effect of carvedilol on survival in severe chronic heart failure. *N. Engl. J. Med*, 344: 1651-1658.
2. Trefor, M. (1994) Clinical pharmacokinetics and pharmacodynamics of carvedilol. *Clin Pharmacokinet*, 26: 335-346.
3. Vamshi Vishnu, Y., Chandrasekhar, K., Ramesh, G. and Madhusudan Rao, Y. (2007) Development of mucoadhesive patches for buccal administration of carvedilol. *Current Drug Del*, 4: 27-39.
4. Guy, R.H. (1996) Current status and future prospects of transdermal drug delivery. *Pharm Res*, 13: 1765-1769.
5. Kanikannan, N., Andega, S., Burton, S., Babu, R.J. and Singh, M. (2004). *F, Drug Dev. Ind. Pharm*, 30: 205-212
6. Williams, A.C. and Barry, B.W. (1991). Species differences in percutaneous absorption of nicorandil, *Pharm. Res*, 8: 17-24
7. Moghimi, H., Williams, A.C. and Barry, B.W. (1997). A lamellar matrix model for stratum corneum intercellular lipids. V. Effects of terpene penetration enhancers on the structure and thermal behaviour of the matrix. *Int. J.Pharm*, 146: 41- 54
8. Udhumansha Ubaidulla, Molugu, V.S. Reddy., Kumaresan Ruckmani., Farhan, J. Ahmad. and Roop, K. Khar (2007) Transdermal therapeutic system of carvedilol: effect of hydrophilic and hydrophobic matrix on in vitro and in vivo characteristics, *AAPS PharmSciTech*, 8 (1) Article 2, E1-E8
9. Yuveraj Singh, T., Chetan Singh, C and Anshu Sharma (2007) Development and evaluation of carvedilol transdermal patches. *Acta Pharm*, 57: 151-159
10. Kaidi Zhao and Jagdish Singh (1999) In vitro percutaneous absorption enhancement of propranolol hydrochloride through porcine epidermis by terpenes/ethanol. *J. Control Rel*, 62: 359-366.
11. Hayton W.L. and Chen. T. (1982) Correction of perfusate concentration for sample removal. *J Pharm Sci*, 71: 820 - 821.
12. Ramesh Gannu, Vamshi Vishnu Yamsani, and Yamsani Madhusudan Rao. (2007). New RP-HPLC method with UV-detection for the determination of carvedilol in human serum. *J Liq. Chrom. Rel. Tech*, 30: 1677-1685
13. Barry B.W. (1983). Penetration enhancers In: *Dermatological formulations*. Marcel Dekker, New York: 160-172.
14. Barry B.W (1991) Lipid protein partitioning theory of skin penetration enhancement. *J. Control. Rel*, 15:237-248.
15. Ogiso, T. Lwaki, M, and Paky, T. (1995). Effect of various enhancers on transdermal penetration of indomethacin and urea, and relationship between penetration parameters and enhancement factors. *J. Pharm. Sci*, 84: 482-428
16. Kaidi Zhao. and Jagdish Singh. (2000). Mechanism(s) of in vitro percutaneous absorption enhancement of tamoxifen by enhancers. *J. Pharm. Sci*, 89: 771-780

17. Williams, A.C. and Barry, B.W. (1991). The enhancement index concept applied to terpene penetration enhancers for human skin and model lipophilic (oestrodiol) and hydrophilic (5-fluorouracil) drugs. *Int J Pharm*, 74: 157-168.
18. Williams, A.C., Barry, B.W. (1991). Terpenes and the lipid protein partitioning theory of skin permeation enhancement, *Pharm. Res*, 8: 17-24.
19. Cornwell, P.A., Barry, B.W. (1993). The routes of penetration of ions and 5-fluorouracil across human skin and the mechanisms of action of terpene skin penetration enhancers, *Int. J. Pharm*, 94: 189-194.
20. Thomas, N.S., Panchagnula, R. (2003). Transdermal delivery of zidovudine: effect of vehicles on permeation across rat skin and their mechanism of action, *Eur. J. Pharm. Sci*, 18: 71-79.
21. Vaddi, H.K., Ho, P.C., Chan, S.Y. (2002). Terpenes in propylene glycol as skin-penetration enhancers: Permeation and partition of haloperidol, fourier transform infrared spectroscopy, and differential scanning calorimetry, *J. Pharm. Sci*, 91: 1639-1651
22. Yamane, M.A., Williams, A.C., Barry, B.W. (1995). Terpene penetration enhancers in propylene glycol/water co-solvent systems: effectiveness and mechanism of action, *J. Pharm. Pharmacol*, 47: 978 -989
23. Takahashi, K., Sakano, H., Yoshida, M., Namata, N. and Mizuno, N. (2001). Characterization of the influence of polyol fatty acid esters on the permeation of diclofenac through rat skin, *J Control Rel*, 73: 351-358.

Table 1: Permeation parameters of Carvedilol through excised rat abdominal skin from PBS pH 7.4 containing 40 % v/v of PEG 400 and 5 % w/v of Penetration enhancer

Penetration enhancer	Q ₂₄ ^a Permeation	Js ^b (µg/cm ² /hr)	P _{app} ^c (cm/hr)	T _L ^d (hrs)	D ^e (cm ² /hr)
Control	59.18 ± 13.30	0.67 ± 0.095	0.22 ± 0.013	0.50 ± 0.042	0.13 ± 0.045
Menthol	135.06 ± 35.84	1.53 ± 0.125	0.51 ± 0.029	0.31 ± 0.029	0.08 ± 0.009
Camphor	451.20 ± 70.57	5.23 ± 0.331	1.87 ± 0.011	0.41 ± 0.034	0.11 ± 0.031
D-limonene	353.49 ± 12.52	4.37 ± 0.403	1.45 ± 0.014	0.30 ± 0.014	0.08 ± 0.002
Carvone	324.13 ± 27.32	3.96 ± 0.328	1.32 ± 0.021	0.35 ± 0.023	0.09 ± 0.006
Transcutol	384.18 ± 45.97	4.87 ± 0.571	1.62 ± 0.019	0.40 ± 0.032	0.10 ± 0.010
Labrasol	222.60 ± 45.21	2.82 ± 0.177	0.93 ± 0.059	0.34 ± 0.016	0.09 ± 0.003

^a Cumulative amount (µg) of drug permeated per cm², results are mean ± SD (n=3)

^b Js Transdermal flux, values represent mean ± SD (n=3).

^c P_{app} Permeability Coefficient, values represent mean ± SD (n=3).

^d T_L Lag Time, values represent mean ± SD (n=3).

^e D Diffusion Coefficient, values represent mean ± SD (n=3).

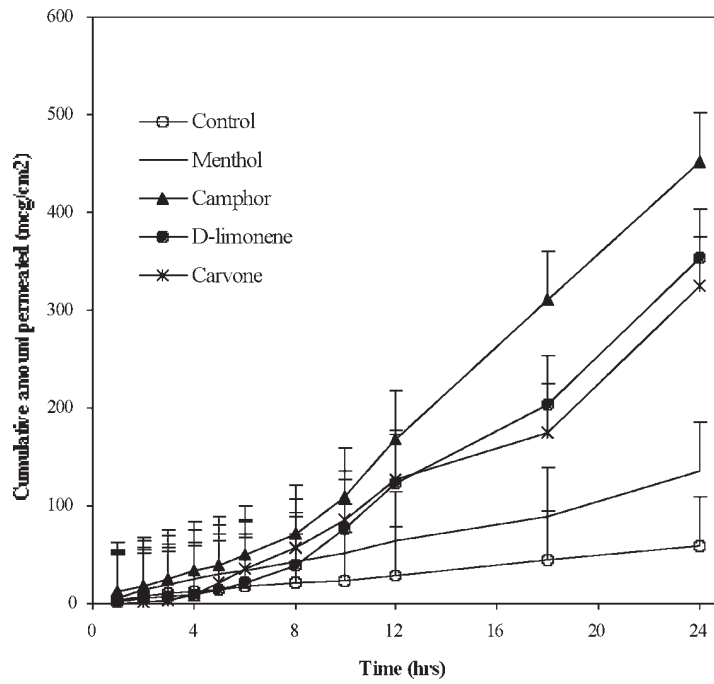


Fig 1: Effect of terpenes as penetration enhancers on *in vitro* permeation of carvedilol through rat abdominal skin, values represent mean \pm S.D (n=3)

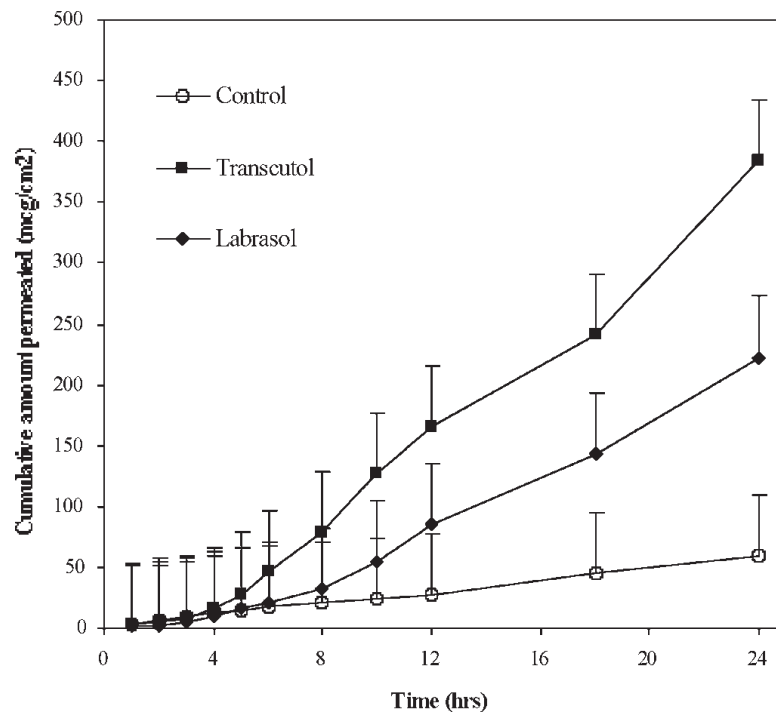


Fig 2: Effect of surfactants as penetration enhancers on *in vitro* permeation of carvedilol through rat abdominal skin, values represent mean \pm S.D (n=3)

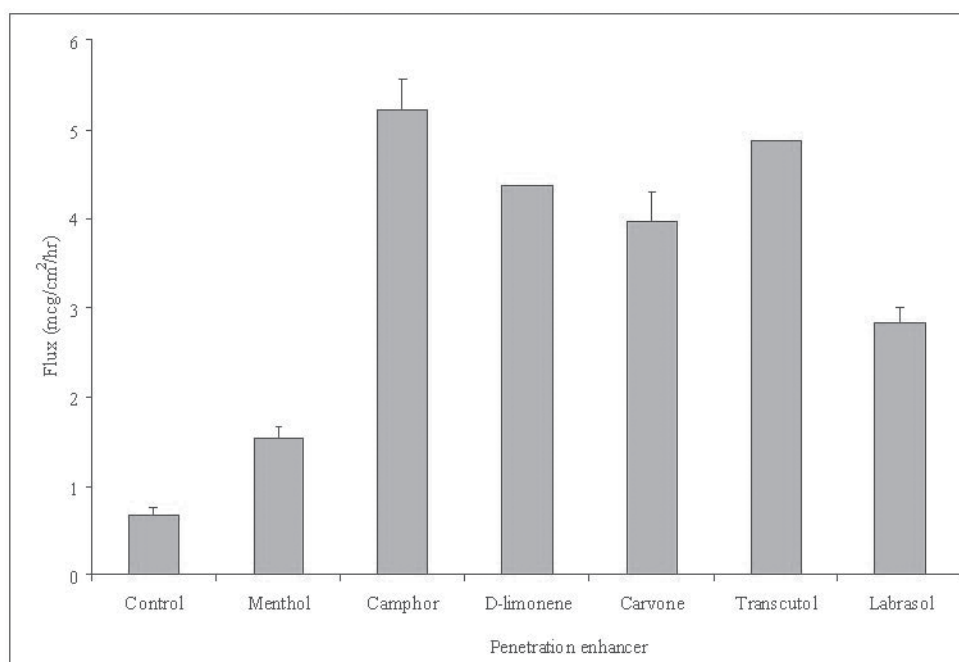


Fig 3: Comparison of carvedilol flux obtained from drug solutions containing 5 % w/v penetration enhancer through excised rat skin, values represent mean \pm S.D (n=3)

Characterization of Myostatin Gene and Identification of SNPs for Diversity Analysis

S. T. Bharani Kumar^{1,2}, Neeraj Dilbaghi², S P S Ahlawat³, Bina Mishra¹, M. S. Tantia^{1*} and R. K. Vijn²

¹National Bureau of Animal Genetic Resources, Karnal 132001, India.

²Guru Jambheshwar University of Science and Technology, Hisar

³Indian Veterinary Research Institute, Izatnagar.

* For correspondence-mstantia@yahoo.com

Abstract

In this present study we have sequenced the complete Myostatin gene with 3 exons, two introns, promoter region, 5' and 3' UTR region. We sequenced the entire gene by designing a set of 20 primers. Ten individuals from 5 breeds of Indigenous chicken were sequenced and the sequences obtained were aligned to develop a consensus sequence. We compared the sequences obtained among themselves, with Red Jungle Fowl and Chinese fowl. We estimated three genetic distances and constructed the phylogenetic tree using NJ method. The indigenous chicken joined together first followed by Red Jungle Fowl while the Chinese fowl was distinct. The indigenous gene sequence was similar among the various chicken breeds and might have been evolved from RJF following a separate course than the evolution of Chinese chicken.

Introduction

Myostatin (GDF-8) is an important candidate gene for growth and development of domestic animals and poultry. It is a member of TGF- β superfamily of secreted growth and differentiation factors. It is a negative regulator of skeletal muscle growth and is essential of proper regulation of skeletal muscle mass (1).

The gene has been studied widely in cattle (2, 3, 4), buffalo (5), mice (6) and chicken (7,8). This gene has been reported to provide genetic evidence of role of SNPs in *myostatin* gene in regulation of adipose growth and musculature in chicken (8). *Myostatin* SNPs have been reported to occur with different gene frequencies among chicken breeds⁷.

The comparative analysis of broiler, layer and silkie fowl genome with Red Jungle fowl (RJF) have revealed 3.2 million SNPs which are now available in public domain (Chicken VD Database, 9). The indigenous chicken are morphologically of two distinguished types, the game birds which have a very distinctive body conformation and well developed musculature compared to other normal layer type birds.

The present study was carried out to sequence the *myostatin* gene in five indigenous chicken populations and comparing the sequences among themselves to develop a consensus sequence of indigenous chicken. These included the normal birds as well as game birds. Aseel and Danki are the game birds and have well developed musculature with aggressive behaviour (10). These birds are found in junction of Andhra Pradesh, Jharkand and Orissa. Daothigir birds are found in the western Assam bordering West Bengal and are reared by Bodo tribals. Punjab

brown are normal birds of Punjab and Haryana of North India while Chittagong birds inhabit Meghalaya bordering Bangladesh. The five Indian chicken populations, RJF and Chinese chicken have been compared for identifying the variations. The purpose of the present study was to report variations among the chicken breeds of India and to reconstruct phylogeny with other chicken populations and RJF.

Material and Methods

Samples: Two samples each from the five populations of indigenous chicken were utilized. Genomic DNA was extracted from 0.5 ml of blood collected from wing vein in heparinised vacuutiners. The DNA was isolated using the standard laboratory protocols (11).

Sequencing of Myostatin gene: We designed twenty pairs of overlapping primers (Fig 1) for complete chicken *myostatin* gene sequences (Table 1) available in NCBI database (AF346599) using primer3 software. The PCR conditions were standardized for each oligonucleotide primer pair. Amplified PCR products were purified by treating with Exonuclease and Alkaline phosphatase (0.5 unit each) and incubating at 37°C for 2 hrs followed by inactivation at 85°C for 15 minutes. Purified PCR products were sequenced using Big Dye terminator chemistry on 3100-Avant (Applied Biosystems) automated DNA sequencer.

Sequence Analysis: *Myostatin* gene sequence from the five breeds of chicken were aligned using Seqscape version 3.0 software (Applied Biosystems, USA). The variations among the indigenous breeds were recorded. The consensus sequence was obtained for the indigenous breeds and was compared to Chinese native chicken (AF346599) and sequence of the gene of Red Jungle fowl (Ensembl release Ver 4.6 *Gallus gallus*) (12). The sequence of the indigenous breeds, Chinese fowl and RJF were subjected to

multiple alignment using ClustalW (13) and genetic distances based on nucleotide differences were obtained using Phylip software module DNADist (14). The output was utilised for the construction of Neighbor joining tree (15) and viewed using Treeview (16). We utilized the maximum composite method, Kimura-2 parameter model (using MEGA software, 17) and DNA dist (Phylip software) for estimating the distances.

Results and Discussion

The consensus sequence of these ten individuals was prepared covering the entire *myostatin* gene with promoter and 5' UTR region. The consensus sequence was submitted to NCBI database along with variations observed (DQ912835). The total nucleotide bases were 8175bp and consisted of promoter region (1-1433), 5'UTR (1434-1550), Exon1 (1434-1923), Exon2 (4015-4388) and Exon3 (6664-8175) with 3'UTR (7045-8175). The intervening sequences were for the two introns.

The comparison of the sequences obtained with the reference sequence AF346599 revealed several changes (Table 2). The variations observed included 17 deletions, 3 insertions of 2(CT), 3(ACC) and 11(TTAGTGTTTT) bases at 8527, 7561 and 4923 respectively. The total number of transitions and transversions compared to reference sequence were 15 and 17 respectively. At position 1784 there was a transition in Exon1 which was synonymous with no change in aminoacid. There was another change non synonymous in the Exon3 at position 7414 and 7415 (both transitions of pyrimidine) which lead to single aminoacid change from Proline to Serine. These changes were peculiar to indigenous chicken populations.

The comparison of GDF-8 gene sequence obtained in the present study with the gene sequence of Red Jungle fowl available in

Ensembl database revealed few variations (Table 3). The changes were T1280C in promoter region, C1468A and G1521A in 5'UTR region and G1610A and C1745G in Exon1. The variations among the indigenous chicken populations revealed 44 SNPs of which 31 were transitions and 9 transversions (Table 4). The SNP distribution is as follows- twenty three in promoter (Fig 2), five in exon 1 (Synonymous), seven in intron 1, eight in intron 2 and one in 3'UTR. Four deletions were observed in the promoter region.

The evolutionary history of the five indigenous chicken populations, Red Jungle fowl and Chinese fowl was inferred using the Neighbor-Joining method. The distance values obtained from maximum composite method are given in table 5. Among the fowl populations, the genetic distances were maximum for the Chinese fowl while the indigenous chicken genetic distance values were quite small followed by genetic distance from the Red Jungle Fowl. Thus the genetic distances reveal that the indigenous chicken populations have diverged separately from the Red jungle fowl and all the breeds have evolved by distance and isolation among themselves while Chinese fowl had taken a separate course and evolved differently than the indigenous chicken (Fig 3). The phylogenetic tree reconstructed was same for the DNAdist, Kimura-2-parameter model and maximum composite method.

Conclusion

The *Myostatin* gene sequences provide evidence that the Aseel and Dunki are game birds and close to one another in the phylogenetic tree. Daothigir join Aseel at the first node. Daothigir are normal layer birds but breed in close vicinity of the breeding tract of game birds which extend all along the coastal regions of India into Bangladesh. Chittagong and Punjab Brown birds are layers and have their breeding areas adjoining

to that of Red Jungle fowl which exists in wild all along the Himalayan belt from northern to north eastern India. Since the indigenous chicken are continuously distributed with no clear cut distinction between the areas inhabited by Red Jungle fowl, game birds and other layer birds and such a pattern is also revealed at the gene sequence level (*Myostatin* gene in the present case). Aseel and Danki come close to one another as both are selected for the game characteristics and are reared by the tribals.

References

1. McPherron, A. C. and Lee, S. J. (1997). Double muscling in cattle due to mutations in the myostatin gene. *Proc Natl Acad Sci USA*, 94: 12457-12461
2. Kambadur, R., Sharma, M., Smith, P.L.T. and Bass, J.J. (1997). Mutations in myostatin (GDF8) in Double-Muscled Belgian Blue and Piedmontese Cattle. *Genome Research*, 7(9): 910-916.
3. Grobet, L., Poncelet, D., Royo, L., Brouwers, B., Pirottin, D., Michaux, C., Menissier, F., Zanotti, M., Dunner, S. and Georges, M. (1998). Molecular definition of an allelic series of mutations disrupting the myostatin function and causing double-muscling in cattle. *Mammalian Genome*, 9:210-213.
4. Lee, S.J. and McPherron, A.C. (2001). Regulation of myostatin activity and muscle growth. *Proc. Natl. Acad. Sci. USA*, 98: 9306-9311.
5. Tantia, M. S., Vijn, R. K., Mishra, B. and Bharani Kumar, S. T. (2007). Sequence of GDF8 (Myostatin) in *Bubalus bubalis*. *Animal Biotechnology*, 18(3): 177-181.
6. Lin J., Arnold H.B., Della-Fera M.A., Azain M.J., Hartzell D.L. and Baile C.A. (2002). Myostatin Knockout in mice increases myogenesis and decreases

- adipogenesis. *Biochemical and biophysical research communications*, 291(3):701-706
7. Zhiliang, G.U., H.F. Zhang, D.H. Zhu and Li, H. (2002). Single nucleotide polymorphism analysis of the chicken Myostatin gene in different chicken lines. *Acta Genet. Sin*, 29: 599-632.
 8. Zhiliang, G.U., Dahai, Z.H.U., L.I. Ning, L.I. Hui, D.E.N.G. Xuemei and W.U. Changxin, 2004. The single nucleotide polymorphisms of the chicken myostatin gene are associated with skeletal muscle adipose growth. *Sci China*, 47: 26-31.
 9. Jing Wang., Ximiao He., Jue Ruan., Mingtao Dai., Jie Chen., Yong Zhang., Yafeng Hu., Chen Ye., Shengting Li., Lijuan Cong., Lin Fang., Bin Liu., Songgang Li., Jian Wang., David W. Burt., Gane Ka-Shu Wong., Jun Yu., Huanming Yang and Jun Wang. (2005). ChickVD: a sequence variation database for the chicken genome. *Nucleic acid research*, 33: 438-441.
 10. Vijh, P.K., Tania, M.S., Mishra, B., Bharani Kumar S.T. and Vijh, R.K. (2006). Characterization of Aseel, Dunki, Kalasthi and Ghagus breeds of Chicken. *Indian journal of Animal Science*, 76(11): 944-49.
 11. Sambrook, J., Fritsch, E.F. and Maniatis, T. (1989). *Molecular Cloning: A Laboratory Manual* 2nd Ed, Cold spring Harbour, Cold spring Laboratory Press, NY.
 12. Ensembl genome browser for chicken. http://www.ensembl.org/Gallus_gallus/index.html
 13. Thompson, J.D., Higgins, D.G. and Gibson, T.J. (1994) CLUSTAL W: improving the sensitivity of progressive multiple sequence alignment through sequence weighting, position specific gap penalties and weight matrix choice. *Nucleic Acids Research*.
 14. Felsenstein, J. 1993. Phylip: A software package <http://evolution.gs.washington.edu/phylip.html>
 15. Saitou, N. and Nei, M. (1987). The neighbor-joining method: A new method for reconstructing phylogenetic trees. *Molecular Biology and Evolution*, 4:406-425.
 16. Page, R. D. M. 1996. TREEVIEW: An application to display phylogenetic trees on personal computers. *Computer Applications in the Biosciences*, 12: 357-358. <http://taxonomy.zoology.gla.ac.uk/rod/treeview.html>
 17. Tamura, K., Dudley, J., Nei, M. and Kumar, S. (2007) MEGA4: Molecular Evolutionary Genetics Analysis (MEGA) software version 4.0. *Molecular Biology and Evolution*, 10.1093/molbev/msm092.

Table 1: List of primers, sequences and their product size used to amplify the complete myostatin gene

Primer Name	Forward Primer	Reverse primer	Size (bp)
GMST1	gCCAAATCCAAAgAACCAAC	CCAgggCACAggTATTgACT	526
GMST2	TggAAggACAATCAATTTCAA	TgCTTTCTgCATgAgATgCT	534
GMST3	AgCATgCCCAATgTCATCTA	CgTgCATTAAGCAGCTCAGA	591
GMST4	CAAAATgTTTATTCCTgCTCACC	CTAAACAgATCCgggACAgC	605
GMST5	TggCATATATAAggCACACCA	gggAgAgCCTgAgAAggAgT	607
GMST6	TAACAACCCTgCTgCTTTCg	CATTCTTCCTTggCACgACT	635
GMST7	AgCAATCAgCTCCAgtAgTCg	CTCCATgCCAggATAAAACAgt	648
GMST8	CTCCATgCCAgtATAAAACAgt	gAgCgATgTgTACAgtCAGA	694
GMST9	ggTgTgACAgtCAGATCCTT	gCCTgggTTCATgTCAAgtTT	638
GMST10	gTAAgACATCCTACATgATCTggAA	ACCTTCATCTgCCATTCTCg	569
GMST11	TggACgAgATCTTgCTgTCA	TgCATgCAGAAATAgggAgAA	480
GMST12	gAAgCAATTCAACTCTTCCTCTg	TTCACCTgCACTTCACTgCT	523
GMST13	CTgAAACAgtCTCAAACAACCA	AgTggATggAgAggAgCTgA	425
GMST14	gCTCTgCAGACCATgTgAgA	ggACTgCTgAgAgAgCCTTg	431
GMST15	ACACCgTCAGAAgtAAgCAT	TCATgAggATCCCTggTTTC	494
GMST16	TCTCTATAgAAgAACTCCCAAAAgg	TgggTTCTgAgAgAAgAggAA	442
GMST17	CCCAgAAgggAAgAAgTTCA	TTTATCgAAggggTCTCACg	564
GMST18	gCACACCCACCAAgATgTC	TCAgtATTTgTCCATTTACgTg	659
GMST19	gACAgAAgtAgCgggCTATT	TTgCATTggCTTATCATAgTgC	516
GMST20	AAAgtCAGCACgtAAgTCT	CCTgTggTTTACTCTgTTgCAC	340

Table 2: Variations observed in Indigenous domestic chicken compared to reference sequence

<i>S.No</i>	<i>Position</i>	<i>From</i>	<i>To</i>	<i>Region</i>	<i>S.No</i>	<i>Position</i>	<i>From</i>	<i>To</i>	<i>Region</i>
1.	517	T	C	Promoter	27.	5698	G	T	Intron 2
2.	606	G	Del		28.	5713	G	Del	
3.	703	A	Del		29.	5781	A	Del	
4.	704	A	Del		30.	6693	G	T	
5.	1160	A	G		31.	6978	A	Del	
6.	1161	A	C		32.	7017	A	T	
7.	1164	A	G		33.	7414	T	C	Exon 3
8.	1165	A	C		34.	7415	C	T	
9.	1166	G	Del		35.	7542-7545	TTTT	Del	3' UTR
10.	1468	A	Del		36.	7551	A	T	
11.	2018	A	G	5'UTR	37.	7559	C	T	
12.	2028	A	C		38.	7561	-	ACC (Ins)	
13.	2037	G	C		39.	7562	C	A	
14.	2046	A	T		40.	8118	A	Del	
15.	2047	A	C		41.	8527		CT (Ins)	
16.	2048	A	Del		42.	8548	A	G	
17.	2049	A	Del		43.	8549	A	G	
18.	2283	G	A	Exon 1	44.	8554	G	A	
19.	2672	T	Del	Intron 1	45.	8558	A	G	
20.	3605	C	T		46.	8562	G	T	
21.	3606	C	G		47.	8571	C	A	
22.	3716	G	Del		48.	8591	C	A	
23.	4026	G	Del		49.	8594	A	C	
24.	4923	-	TTAG TGTT TTT (Ins)	Intron 2	50.	8595	G	A	
25.	5379	C	Del		51.	8598	T	A	
26.	5778	G	Del		52.	8643	A	G	

Table 3: Variations observed between Indian indigenous Chicken and RJF sequences obtained from Ensembl gene Browser

<i>S.No</i>	<i>Position</i>	<i>From</i>	<i>To</i>	<i>Region</i>
1	1280	T	C	Promoter
2	1468	C	A	5' UTR
3	1521	G	A	
4	1610	G	A	Exon 1
5	1745	C	G	

Table 4: SNPs in myostatin gene among five different populations

<i>S.No</i>	<i>Position</i>	<i>From</i>	<i>To</i>	<i>Region</i>	<i>S.No</i>	<i>Position</i>	<i>From</i>	<i>To</i>	<i>Region</i>
1.	27	G	A	<i>Promoter</i>	24.	1601	G	A	<i>Exon 1</i>
2.	246	G	A		25.	1610	G	A	
3.	261	C	A		26.	1745	C	G	
4.	318	C	Del		27.	1784	G	A	
5.	319	A	G		28.	1874	C	T	
6.	360	T	Del		29.	2370	C	T	<i>Intron 1</i>
7.	424	T	Del		30.	2383	C	T	
8.	430	A	Del		31.	2975	T	C	
9.	450	A	G		32.	3407	A	C	
10.	721	A	G		33.	3529	G	A	
11.	741	A	G		34.	3858	G	A	
12.	782	T	C		35.	3903	A	C	
13.	840	G	A		36.	4529	C	G	<i>Intron 2</i>
14.	850	T	C		37.	4952	T	C	
15.	879	A	G		38.	5411	T	A	
16.	976	G	A		39.	5617	T	G	
17.	994	A	G		40.	5774	T	C	
18.	1017	C	T		41.	6001	C	T	
19.	1074	C	T		42.	6124	A	G	
20.	1166	A	G		43.	6153	C	T	
21.	1196	A	C		44.	7607	A	G	<i>3' UTR</i>
22.	1242	C	T						
23.	1253	G	T						

Table 5: DNA dist (above diagonal) and inter-population difference (below diagonal).

	Daothigir	Aseel	Chittagong	Danki	PBrown	RJF	Chinese fowl
Daothigir		0.0013	0.001	0.0006	0.0016	0.0018	0.0046
Aseel	0.00030		0.0011	0.0011	0.0017	0.0019	0.0053
Chittagong	0.00015	0.00015		0.0013	0.0012	0.0016	0.0048
Danki	0.00030	0.00030	0.00045		0.0017	0.0016	0.0047
PBrown	0.00015	0.00015	0.00000	0.00045		0.0024	0.0054
RJF	0.00090	0.00090	0.00075	0.00090	0.00075		0.0028
Chinese fowl	0.00254	0.00254	0.00239	0.00284	0.00239	0.00284	-

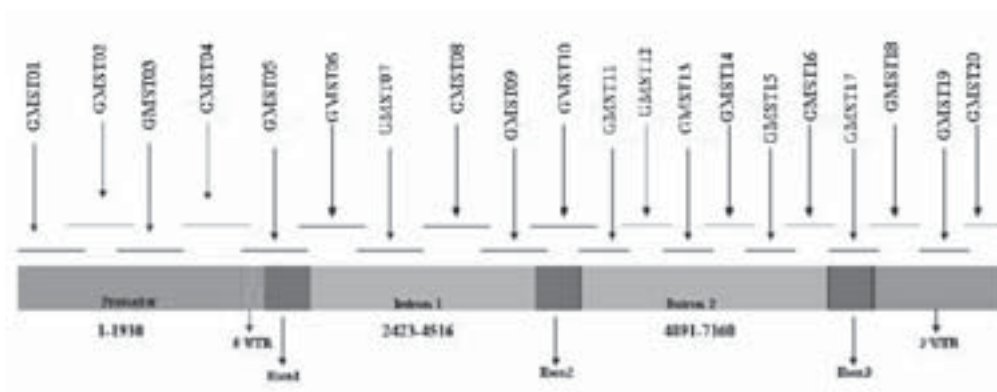


Fig 1: Overlapping primers designed for Myostatin (GDF-8) gene using primer3 software

Significant medium components for enhanced Jasmonic acid production by *Lasiodiplodia theobromae* using Plackett-Burman Design

P. C. Dhandhukia and V. R. Thakkar*

Lab#302B, BRD School of Biosciences, Sardar Patel Maidan, Vadatal Road, Satellite Campus, Post Box No. 39, Sardar Patel University, Vallabh Vidyanagar-388120, (Gujarat), India.

* For correspondence: vasuthakkar@gmail.com

Abstract

A Plackett-Burman design and statistical screening was employed to optimize medium components for jasmonic acid production by *Lasiodiplodia theobromae*. The seven medium components malt extract, sucrose, NaNO₃, yeast extract, FeSO₄ 7H₂O, MnSO₄ H₂O, and MgSO₄ 7H₂O were screened using a Plackett-Burman design to optimize medium component for jasmonic acid production using *L. theobromae*. When sucrose was used alone as a carbon source with these medium components, the jasmonic acid production was found to be 80 mg/l. Increase in jasmonic acid production (225.3 mg/l) was observed with augmentation of malt extract and changing other medium components concentration based on statistical screening. It was found that malt extract, sucrose, NaNO₃, MnSO₄ 7H₂O, and MgSO₄ 7H₂O were significant components influencing jasmonic acid production. Yeast extract and FeSO₄ 7H₂O also showed significantly negative effect on the jasmonic acid production. Therefore significantly positive factors could be increased and significantly negative factors could be decreased for higher jasmonic acid production.

Keywords

Jasmonic acid, *Lasiodiplodia theobromae*, Plackett-Burman design, Significant factors.

Introduction

Jasmonic acid (JA) (3-oxo-2-(2'-cis-pentenyl) cyclopentane-1-acetate) and methyl jasmonates are of importance in perfumery industries and being used world wide in various products like, toilet soaps, chewing gum, even in smoking preparations (1). JA and its derivatives are also very important secondary metabolites in the plant defense system (2, 3). JA was first isolated from the cultural filtrate of *Lasiodiplodia theobromae* (the synonym of *Botryodiplodia theobromae*) and its role was found as a plant growth regulator (4). In spite of high demand, very few fermentation studies were carried out for JA production using *L. theobromae* (5-7). This is the first report on screening of medium components for JA production using statistical experiment design.

The relevant literature and "prior art" serve only as starting point for the development of fermentation. By manipulating nutritional requirements, physical parameters and genetic makeup of the producing strain increase in productivity of microbial metabolite can be achieved. A fermentation improvement program may begin by measuring product yield as a response to factors like strength of medium components. Nutritional requirement can be manipulated either by the conventional or

statistical approach. Conventional methods involve changing one independent variable at a time (OVAT) while others are kept at fixed level. However statistical methods offer several advantages over conventional methods being rapid and reliable, shortlists significant nutrients, helps understanding the interaction among the nutrients at various concentrations and reduces total number of experiments tremendously resulting in saving time and cost of glassware, chemicals and manpower (8, 9). Screening is the first phase of an experimental study to eliminate non-significant factors so that efforts may be concentrated upon most significant ingredients selected for further optimization.

The selection of the medium components for this study was carried out based on the literature survey and our preliminary laboratory work. A systematic experiment was then carried out by setting the independent variables according to a Plackett-Burman design (10) at two levels and JA produced was measured in each batch, followed by statistical analysis in order to interpret the significant medium components. Such approach is a useful screening process employed to identify the contribution of each medium component to the response of the system and thus allows for a reduction in the number of variables that need to be considered (11).

The Plackett-Burman design is highly recommended when more than five factors have to be investigated. These designs are very useful for economically detecting large main effects, assuming all interactions are negligible when compared with the few important main effects. Two level factorial Plackett-Burman design, was selected because it screens up to v variable in just ' $v+1$ ' experimental run (10, 12). These experimental designs are available in multiple of four runs (13) and advantageous over multifactorial design as it is difficult and involves large number of variable to be screened in terms of number of experiments (2^v , where v is the total

number of variable). Higher-order linear full factorial and quadratic Box-Behnken designs would have required 66 and 52 experimental batches, respectively, which would have been prohibitively uneconomical (14). In this study, the aim was to screen the effects among seven independent variables (**Table 1**) in an economical manner (13). Due to orthogonal nature of the Plackett-Burman Design, it gives only pure effect of each variable not confounded with interaction among variables (15).

Materials and Methods

Microorganism

L. theobromae (MTCC 3068) strain was obtained from Microbial Type Culture Collection (MTCC) Institute of Microbial Technology, Chandigarh, India. This strain was maintained on potato dextrose agar (Hi-Media, Mumbai, India) slants. After inoculation, slants were incubated at 30°C for three to four days for obtaining growth and later stored at 4°C. Strain was sub-cultured every month.

Chemicals and solvents

(±) JA, a racemic mixture, was purchased from Sigma, Bangalore, India and used as a standard reference compound for quantification of JA. All dehydrated media components were purchased from Hi-media, Mumbai, India. All solvents (99.9%) were purchased from Qualigens, Mumbai, India. Ammonia (25% w/v) was used fresh.

Cultural technique

Sample of stock culture was transferred from working slants to potato dextrose agar plates and incubated for three days at 30°C. The basal medium contained (g/l) KH_2PO_4 , 2.0; KCl, 0.3; $\text{ZnSO}_4 \cdot 7\text{H}_2\text{O}$, 0.03; $\text{CuSO}_4 \cdot 7\text{H}_2\text{O}$, 0.003; and $\text{Na}_2\text{MoO}_4 \cdot 2\text{H}_2\text{O}$, 0.003. The pH was maintained 5.5 (6) through out the experiment and the

concentrations of other medium components malt extract, sucrose, NaNO₃, yeast extract, FeSO₄ 7H₂O; MnSO₄ 7H₂O and MgSO₄ 7H₂O were as per the combination given in **Table 1 and 2**. Agar plug (eight mm diameter) was cut with sterile cork borer and used for inoculation of 100 ml of the broth culture in 250 ml Erlenmeyer flask and incubated for eight days at 30°C in static condition.

Screening of important nutrient components

Total seven medium components (independent variables, $v=7$) were selected for the study with each variable represented at two levels, high (+) and low (-) concentrations also four dummy variables were kept at two concentrations. The input factor and their corresponding upper and lower level values are shown in **Table 1**. A two level design only minima and maxima of input variables were used to form a design space. The resulting twelve experimental cases for seven input parameters ($v+1+$ four dummy variables) are shown in **Table 2** with the number of positive signs and negative signs. Each column contained equal number of positive and negative signs. Thus each row represented a trial batch and each column represented an independent (assigned) or dummy (unassigned) variable. The effect of each variable was determined by the following equation:

$$E_{(xi)} = (JAi^+ - JAi^-) / N \quad - (1)$$

Where $E_{(xi)}$ is the concentration effect of the tested variable. JAi^+ and JAi^- are the jasmonic acid production from the trials where the variable (xi) measured was present at high and low concentrations, respectively; and N is the number of trial divided by two. Experimental error was determined by calculating the variance among the dummy variables as follows:

$$V_{eff} = (E_d)^2 / n \quad - (2)$$

Where V_{eff} is the variance of the concentration effect, E_d is the concentration effect for the dummy variable and n is the number of dummy variables. The standard error (SE) of the concentration effect was calculated by taking square root of the variance of an effect and the significance level (p -value) of each concentration effect was determined using student's t -test:

$$t_{(xi)} = E_{(xi)} / SE \quad - (3)$$

Where, $E_{(xi)}$ is the effect of variable xi (16).

Extraction and measurement of JA

Cultural filtrate of *L. theobromae* after acidification to pH 3 with 6 M HCl, was extracted with equal volume of ethyl acetate. Extract was concentrated to 100 times. JA measurement was carried out using high performance thin layer chromatography (HPTLC). Concentrated extract was loaded on silica gel 60 F₂₅₄ aluminum foils (Merck, Germany) along with standard JA using Linomate-5 spray on applicator (Camag, Switzerland) of HPTLC under the flow of N₂. Foils were run with iso-propanol: ammonia: water (10: 1: 1 (v/v)) (17). After running, foils were dried in air and scanned with Scanner-3 (Camag, Switzerland) and quantified with the help of winCATS software ver. 1.2.2 by measuring density of the JA band separated on the TLC foils (18).

Statistical analysis of data

Yields of JA obtained in experiments were calculated for determination of variable significance using Microsoft Excel regression coefficient and statistical t -values for equal unpaired samples. Ingredient with highest t -value was considered as best nutrient and thus selected for further optimization studies. A main effect with a positive sign indicates that the high concentration of this variable is near to optimum and a negative sign indicates that the low

concentration of this variable is nearer to optimum.

Results and Discussion

Selection of appropriate carbon source, nitrogen source and other nutrient is one of the most critical stages for the development of an efficient and economic fermentation process. In this study a Plackett-Burman design was employed to evaluate the main effect of the medium components for the JA production by *L. theobromae* at optimized physical parameters.

Table 1 represents the independent variables and the respective high and low concentrations of seven factors used in the optimization study. Malt extract was selected as it contains up to 3.4% of lipids in its dry matter with linoleic acid as their major constituent (50–60% of total lipids) (19). Sucrose was used previously in our study as well as elsewhere as main carbon source for same fungi and found significant, therefore included in the study (6). NaNO_3 was also selected based on our study for the screening of the carbon and nitrogen source for the JA production (data not shown). NaNO_3 was reported to be preferred nitrogen source either with glucose (1) or fructose (6) for JA production using *L. theobromae*. Manganese and iron salts were empirically used in media and they were also important as cofactors for one of the enzyme (lipoxygenase) in the pathway of JA production (20).

The twelve trial Plackett-Burman experimental design, with two levels of concentrations for each variable, was followed for the optimization of medium components for JA production is shown in **Table 2**. The variables X1-X7 represent the medium constituents and D1-D4 represent the dummy (unassigned) variables. Highest JA was produced in batch 2 of the design followed by batch 7, 5, and 1 (**Table 2**).

Table 3 represents the result of effect of each medium component on JA production as well as

the standard error, $t_{(xi)}$, p , confidence level and ranking of each component. The components were screened at the confidence level of 95% on the basis of their effects. That component, which showed significance at or above 95% confidence level and its effect was positive, was interpreted that it was required in higher concentration than the indicated high value (+). However if its effect was found negative, then it indicated that the component was effective in JA production but the amount required was lower than the indicated as low (-) concentration in Plackett-Burman design. All factors in this study have shown influence on the JA production with confidence level at or above 95% confidence limit and were considered to be significant for JA production by *L. theobromae* (**Table 3**). The main effects of the components in the medium for JA production are presented in the **Fig 1**. The malt extract showed the maximum positive effect on JA production, followed by $\text{MnSO}_4 \cdot 7\text{H}_2\text{O}$, $\text{MgSO}_4 \cdot 7\text{H}_2\text{O}$, Sucrose and NaNO_3 . The effect of $\text{FeSO}_4 \cdot 7\text{H}_2\text{O}$ and yeast extract were negative which suggested that these components are required in the medium for JA production but in lower concentration than the low level.

Malt extract was found better medium component than yeast extract. As shown in Table 2, in batches 6 and 10, where yeast extract was supplied in higher concentration but malt extract was not given, the yield of JA was reduced drastically and in batches 7, 8 and 9, high concentration of malt extract and low concentration of yeast extract resulted in higher production of JA. Low concentration of yeast extract may be required to meet requirement of vitamins for general metabolism as well as for some enzymes of JA pathway (for example, 12-oxo-phytodienoic acid reductase) (21). Supplementation of one or more vitamins of "B" group either as separate or in form of yeast extract improves the JA production (1). Yeast extract serve as dual-purpose nitrogen source as well as vitamin source but it is an expensive component

for designing an economical medium (15). From the results of the Plackett-Burman design it could be concluded that yeast extract is probably required for the growth but not for the JA production and should be supplied in low concentration.

Sucrose can not replace the malt extract, as the highest JA (225 mg/l) was produced in batch 2 does contain low level of malt extract and when only sucrose was used in previous experiment, it produced only 80 mg/l of JA (7). Moreover, malt extract is useful as it contain linoleic acid as its major constituent (which is the precursor of JA). (19).

The manganese showed positive effect and iron showed negative effect might be related with the metal ion required for the catalytic center of the lipoxygenase enzyme (20). $\text{MgSO}_4 \cdot 7\text{H}_2\text{O}$ is also very important medium component showing main effect same as sucrose. The requirement for Mg is evident as Mg is required as a catalyst for many intracellular enzymatic reactions. Mg salts have been found most useful in other metabolite and enzyme production as well (21, 22).

By selection of medium components using Plackett-Burman design in this study, about three-fold increase in the JA production was increased compared to earlier experiment where in BSB medium, which supported the maximum JA production as well as growth of *L. theobromae*, 80 mg/l of JA was produced (7).

Present study has short-listed the few significant nutrients useful in increasing the yield of JA and has also identified the nutrients, which should be used in less concentration.

Acknowledgement

Authors are thankful to University Grant Commission, India for financial support.

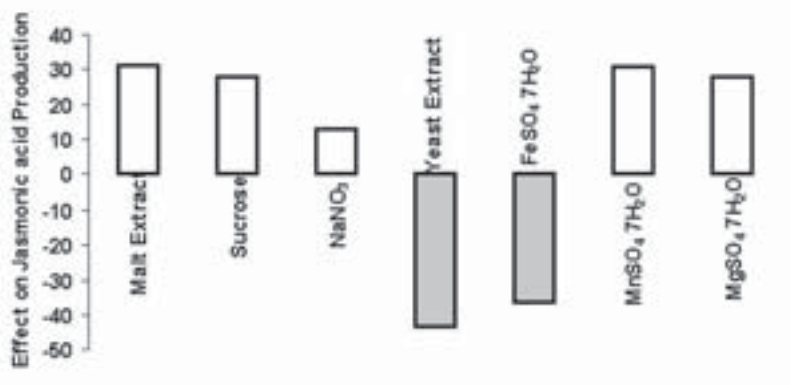
References

1. Farbood, M.I., Brlocker, R.W., McLean, L.B., Sprecker, M.A., McLean, M.P., Kossiakoff, N., Kim, A.Y., and Hagedron, M. (2002). United States Patent. No. 6, 458, 569.
2. Weber, H., Vick, B.A. and Farmer, E.E. (1997). Dinor-oxo-phytodienoic acid: A new hexadecanoid signal in the jasmonate family. *Proc Natl Acad Sci (USA)*, 94: 10473–10478.
3. Staswick, P.E. and Tiryaki, I. (2004). The Oxylinin Signal Jasmonic Acid Is Activated by an Enzyme That Conjugates It to Isoleucine in *Arabidopsis*. *The Plant Cell*, 16: 2117–2127.
4. Aldridge DC, Galt S, Giles D, Turner WB (1997) Metabolites of *Lasiodiplodia theobromae*. *Journal of Chemical Society (C)*, 1623-1629.
5. Günther. T., Miersch O., Wolfgang, F., Sembdner G (1990). Synthetic medium for manufacture of 7-iso-jasmonic acid with *Botryodiplodia theobromae*, Patent DD. WP 279688 A1 12 P7/40.
6. Eng, F., Gutierrez-Rojas, M. and Favela-Torres, E. (1998). Cultural conditions for jasmonic acid and biomass production by *Botryodiplodia theobromae* in submerged fermentation. *Process Biochemistry*, 33 (7): 715-720.
7. Dhandhukia, P.C. and Thakkar, V.R. (2007a). Standardization of growth and fermentation criteria of *Lasiodiplodia theobromae* for production of jasmonic acid. *African Journal of Biotechnology*, 6(6): 704-712.
8. Srinivas, M.R.S., Naginchand, K. and Lonsane, B.K. (1994). Use of Plackett–Burman design for rapid screening of several nitrogen sources, growth/product promoters, minerals and enzyme inducers

- for the production of alpha-galactosidase by *Aspergillus niger* MRSS 234 in solid state fermentation. *Bioprocess Engineering*, 10: 139–144.
9. El-sersy, N.A. and Abou-Elela (2006). Antagonistic effect of marine *Nocardia brasiliensis* against the fish pathogen *Vibrio damsela*: Application of Plackett-Burman experimental design to evaluate factors affecting the production of the antibacterial agent. *International Journal of Oceans and Oceanography*, 1(1): 141-150.
 10. Plackett, R.L., and Burman, J.P. (1946). The design of optimum multifactorial experiments. *Biometrika*, 33: 305–325.
 11. Liu, C., Liu, Y., Liao, W., Wen, Z. and Chen, S. (2003). Application of statistically-based experimental designs for the optimization of nisin production from whey. *Biotechnology Letters*, 25: 877–882.
 12. Bie, X., Lu, Z., Lu, F. and Zeng, X. (2005). Screening the main factors affecting extraction of the antimicrobial substance from *Bacillus* sp. fmbJ using the Plackett–Burman method. *World Journal of Microbiol Biotechnology*, 21: 925–928. DOI 10.1007/s11274-004-6722-z
 13. Naveena, B.J., Altaf, M., Bhadriah, K. and Reddy, G. (2005). Selection of medium components by Plackett-Burman design for the production of L (+) lactic acid by *Lactobacillus amylophilus* GV6 in SSF using wheat bran. *Bioresource Technology*, 96: 485-490.
 14. Stroble, R.J., and Sullivan, G.R. (1998). Ch 6. Experimental design for improvement of fermentations, In, Demain, A. L. and Davies, J. E, (Eds.) *A Manual of Industrial Microbiology and Biotechnology 2nd edition*, ASM Press, Washington DC, USA, pp. 80-93.
 15. Chauhan, K., Trivedi, U.B. and Patel, K.C. (2007). Statistical screening of medium components by Plackett–Burman design for lactic acid production by *Lactobacillus* sp. KCP01 using date juice. *Bioresource Technology*, 98: 98–103.
 16. Shi, F., and Zhu, Y. (2006). Application of statistically-based experimental designs in medium optimization for spore production of *Bacillus subtilis* from distillery effluent. *BioControl*, DOI 10.1007/s10526-006-9055-z
 17. Ueda, J. and Miyamoto, K. (1994). Separation of a new type of plant growth regulator, jasmonates, by chromatographic procedures. *Journal of Chromatography A*, 658, 29-142.
 18. Dhandhukia, P.C. and Thakkar, V.R. (2007b). Separation and quantification of jasmonic acid using HPTLC. *Journal of Chromatographic Science (In Press)*.
 19. Almeida, R.B., Garbe, L.A., Nagel, R., Wackerbauer, K. and Tressl, R. (2005). Regio- and Stereoselectivity of Malt Lipooxygenases LOX1 and LOX2. *The Journal of the Institute of Brewing and Distilling*, 111(3): 265–274.
 20. Su, C. and Oliw, E.H. (1998). Manganese Lipooxygenase purification and characterization. *The J Biol Chem*, 273 (21): 13072–13079.
 21. Vick, B.A. and Zimmerman, D.C. (1983). The biosynthesis of jasmonic acid: a physiological role for plant lipooxygenase. *Biochemical and Biophysical Research Communications*, 111: 470-477.
 22. Reddy, P.R.M., Reddy, G. and Seenayya, G. (1999). Production of thermostable α -amylase and pullulanase by *Clostridium thermosulfurogenes* SV2 in solid-state fermentation: Screening of nutrients using Plackett-Burman design. *Bioprocess Engineering*, 21: 175-179.

Table 3: *t*-value, probability, confidence level and ranking of variables for JA production

Component	Exi absolute value	Standard Error	$t_{(xi)}$	<i>p</i>	Confidence (%)	Ranking
Malt Extract	31.2250	4.4462	7.0228	0.0021	99.89	3
Sucrose	27.7716	4.4462	6.2461	0.0033	99.66	6
NaNO ₃	12.9316	4.4462	2.9084	0.0437	95.73	7
Yeast Extract	43.4650	4.4462	-9.7757	0.0006	99.94	1
FeSO ₄ 7H ₂ O	36.3083	4.4462	-8.1661	0.0012	99.88	2
MnSO ₄ H ₂ O	30.7816	4.4462	6.9231	0.0022	99.78	4
MgSO ₄ 7H ₂ O	27.9583	4.4462	6.2881	0.0032	99.68	5

**Figure. 1:** Effect of media components on JA production in batch culture

Characterization of Fusarium Wilt–Resistant and Susceptible Varieties of ginger (*Zingiber officinale*) through Random Amplified Polymorphic DNA Markers

R. Swetha Priya¹, A. Minaz Khimani², R. B. Subramanian¹ *

¹ Lab No: 103, B R D School of Biosciences, Sardar Patel University, Vadtal- Bakrol Road, V.V. Nagar Anand - 388 120, Gujarat, India. ² Department of Home science, Sardar Patel University, V.V.Nagar, Anand 388 100, Gujarat, India.

*For Correspondence: bagsubbs@yahoo.com

Abstract

Fusarium oxysporum f.sp *zingiberi* (FOZ) is one of the most important pathogens of ginger. Infection by FOZ is difficult to control since the fungus can grow saprophytically in the absence of the host. Conventional breeding methods for selection of disease resistant varieties are lengthy and cumbersome. Bioassays *in vitro* and *in vivo* were performed to assess different degrees of sensitivity of eight varieties of ginger. Random Amplified Polymorphic DNA (RAPD) analysis of genomes from the eight ginger varieties, using 15 different primers was performed to verify the DNA polymorphism. Five primers showed no polymorphic profiles, eight primers gave polymorphic bands and two primers produced highly specific polymorphic bands allowing us to obtain RAPD profiles typical of the most resistant or susceptible varieties. The RAPD pattern is correlated to the sensitivities of the ginger varieties to the pathogen as observed in the bioassays. Cloning and sequencing the most interesting polymorphic DNA fragment revealed 60% homology with putative reverse transcriptase in chickpea and Lotus plane tree, which was linked with resistance. This is the first report of a RAPD marker linked to resistance against fusarium yellows in ginger.

Key words

Fungal culture filtrate, *in vitro* and *in vivo* bioassays, molecular markers, reverse transcriptase, resistant varieties.

Introduction

Ginger is one of the economically important spices cultivated in India. Ginger is considered as the second most important spice exported from India, after black pepper. In recent years there is an increase in the cultivation of ginger (*Zingiber officinale*), leading to an increase in the incidence of diseases that attack this crop. Particularly, yellows and rhizome rot caused by *Fusarium oxysporum* f. sp. *zingiberi* are found to be the most severe diseases affecting this crop (1). Infection by *F. oxysporum* is difficult to control since the fungus can grow saprophytically in the absence of a host (2). The most effective method for the control of this pathogen is soil solarization, which is very expensive. Therefore the most preferred approach is the use of resistant varieties (2, 3). Field assessment for identification of resistant and susceptible varieties is time consuming and labor intensive. Marker Assisted Selection (MAS) using genetic markers is a very reliable approach for identification of resistant and susceptible varieties. Genetic markers provide useful

information at different levels such as population structure, level of gene and gene flow and phylogenetic relationship (4). RAPD, developed by Williams et al., (5) has been successfully used for identification of resistant varieties of Melons against Fusarium wilt (6). Similarly RAPD analysis was carried out in a number of economically important plant species. These include crop plants such as wheat (7), rice (8) and other economically important plants such as onion (9). Medicinal plants such as *Podophyllum hexandrum* (10) and *Andrographis paniculata* (11) were also subjected to RAPD analysis to elucidate the genetic relationship between different varieties. RAPD is a very easy, reliable and economic tool to study intraspecific polymorphisms in plants. In the present study, RAPD was used to study the genetic variation among the eight ginger varieties as well as to select markers linked to susceptibility and resistance for breeding and cultivation.

The present communication aims at identification of disease resistant and susceptible varieties from eight ginger varieties to FOZ using *in vitro* and *in vivo* methods and to identify potential molecular markers linked to disease resistance through RAPD analysis.

Materials and Methods

Plant material

Eight varieties of ginger (*Zingiber officinalis*) Varada, Mahima, Rajetha, Maran, Himachal and Suprabha were obtained from Indian Institute of Spices Research, Calicut, Kerala. The two local varieties, GL1 and GL2 were obtained from National Research Center- Medicinal and Aromatic Plants, Boriavi, Gujarat. Rhizome seedlings were maintained in the botanical garden of the department.

Resistance and susceptibility testing

In vitro bioassay

Tests for sensitivity of the ginger varieties against FOZ were carried out by *in vitro* bioassay. Callus

cultures were initiated by inoculating the meristematic portion of rhizome in half strength of Murashige and Skoog's media containing 3% sucrose and 1.5 mg/l 2,4D. A pure culture of FOZ was obtained from Microbial Type Culture Collection (MTCC Chandigarh). Fungal culture filtrate was prepared by inoculating 1mm² agar plug of the fungal mycelium on potato sucrose broth. After 10 days of incubation, the fungal culture was filtered through muslin cloth and was centrifuged at 3000g for 30 minutes and the supernatant was then filtered through whatman No.42 filter paper. The semi purified FCF was incorporated in different concentrations Viz. 20%, 40%, 60%, 80% and 100% in MS media. Control flasks contained 100 ml of half strength MS media with out culture filtrate along with sucrose and 0.6% agar at pH 5.8. Regenerated calli (0.5 gm) of each ginger variety was placed on the surface of the media and incubated in dark at 25°C for four weeks. Observations were made on healthy / dead calli as well as changes in callus colour and the results were recorded on a 1-5 scale of browning of calli (12).

In vivo bioassay

About 10 to 15 cm tall, healthy potted plants were selected for *in vivo* bioassay and 5 ml of freshly prepared 10-day-old mycelial homogenate was added to soil and the plants were observed daily for 30 days. The severity of the disease was recorded on a scale of 0-4 (13) with 0 indicating no symptoms (highly resistant), 1 indicating slight symptoms such as one wilted leaf at the stem base or a brown discoloration of the stem base surface (resistant), 2 indicating a well developed characteristic unilateral wilt or otherwise still healthy plants (moderately resistant), 3 indicating severe wilt (susceptible) and 4 indicating a wilt death (highly susceptible).

DNA isolation

Total nucleic acids was extracted from 1gm of fresh rhizome ground in liquid nitrogen in a pre-chilled mortar and was incubated with extraction

buffer 100 mM Tris-Cl (pH 8), 20 mM EDTA, 2 M NaCl, 4% CTAB, 0.3% β -Mercaptoethanol, 1% PVP (w/v) for 60 minutes at 60°C followed by Chloroform- Isoamyl alcohol treatment for 15 minutes. The supernatant was collected after centrifugation at 8410 g and 0.6 volume of ethanol was added and incubated for 2 hours at -20°C. The pellet was separated by centrifugation at 13,141 g for 10 minutes followed by phenol: chloroform: Isoamyl alcohol treatment as described by Syamkumar et al.,(14). DNA was diluted to 50 ng/ μ l final concentration in sterile deionised water. A total of 2 μ l of this solution was used in the amplification assay described below and stored in 1X TE buffer (10 mM Tris Cl pH 8, 1 mM EDTA pH 8) at -20°C.

RAPD Analysis

RAPD profiles were generated using 14 different 10-mers from Operon Technologies: C4, C7, C19, OPE 7, OPB 01, OPB 17, OPM 18, OPM 20 OPX 13, AG12, AM14, AD14, WM. In addition, one 11-mer sequence, AL16+ (15) (Bangalore Genei) was also used. The reaction mixture contained 0.3 μ M of primer, 200 μ M of dNTP's, 0.75 Units Taq DNA polymerase approximately diluted with 10X Taq DNA polymerase buffer with 15mM MgCl₂ and adjusted to a final volume of 12.5 μ l with sterile milli Q deionised water. RAPD reactions were performed twice for 2-4 replicates of each variety. A range of annealing temperatures (30°C- 40°C) was tested before establishing the optimum reaction conditions. RAPD - PCR reaction was performed in an Eppendorf 2000 Thermal cycler. The standard conditions used for 40 cycles were as follows: 94°C for 30 seconds, 32°C for 1 minute and 72°C for 1 minute with an initial denaturation temperature at 94°C for 1 minute and a final extension at 72°C for 5 minutes. Tubes containing all reaction components except DNA were used as negative control. Amplicons were analyzed by electrophoresis in a 1.5% agarose gel with 1X TAE buffer, visualized after ethidium bromide

staining under UV transilluminator and photographed.

Phylogenetic Analysis

Amplified bands were scored for presence or absence of bands in each variety for all the primers. Gels were scored thrice individually. Electrophoretic bands of low visual intensity that could not be readily distinguished as present or absent were considered ambiguous and were not scored. A similarity matrix was created using Jaccard's similarity coefficient and Clustering was done using UPGMA (16). Dendrogram was made using two-computer programmes free tree and tree explorer.

Cloning and sequencing of RAPD product

RAPD product linked to resistance was excised from agarose gels and was extracted using Clean Gene I kit (Bangalore Gene I). The DNA sequence was ligated to a PTZ5R/T vector Inst/A clone™ PCR product kit (Fermentas) in a vector: insert ratio of 1:3, competent *Escherichia coli* cells, strain JM109, were transformed and the clones were screened by blue/white colony selection. Plasmid DNA from the colony was isolated according to the alkali lysis method (17). Recombinant DNA was screened for the appropriate size of the insert digested with *Eco*RI restriction enzyme. The cloned RAPD product was sequenced following fluorescent dye terminator using ABI 377 PRISM™ sequencer (Applied Biosystem California) at Gene I using SP6, T7 promoter for primer annealing.

Results

The effect of culture filtrate of FOZ on the calli of all eight varieties was studied and the results are given in Table 1. The semi purified culture filtrate elicited morphological and physiological symptoms like browning and wilting. The percentage survival of the callus cultures on media containing CF at various concentrations decreased with the increase in CF concentration, reaching 100 % mortality. Conversely, in the

controls 100 % survival was recorded. Ginger varieties Himachal, GL2 and Rajetha showed less browning and callus growth occurred even at higher concentrations of CF such as 60%, 80% and 100%, whereas varieties Maran and GL1 showed maximum inhibition at 20% concentration of CF. Rajetha, Himachal and GL2 were found to be resistant, Maran and GL1 highly susceptible while other varieties such as Varada, Mahima, Suprabha were found to be moderately susceptible.

The disease symptoms were observed within 3 days of infection with mycelial homogenate. The symptoms were noted till 30 days. All the varieties exhibited variations in disease symptoms (Table 2). The *in vivo* bioassay results correlated with the *in vitro* bioassay results. Rajetha, Himachal and GL2 varieties were found to be highly resistant where as Maran and GL1 varieties were found to be highly susceptible as in *in vitro* bioassay.

RAPD analysis of the eight ginger varieties using 15 primers showed polymorphism among the varieties. Among the different primers employed, primer AD14 showed a very specific, unique band of 750bp, which was present only Rajetha and Himachal and absent in the highly susceptible varieties Maran and GL1 (Fig: 1). Primer WM showed a very specific, unique band of approximately 1.1kbp size in the most susceptible ginger varieties Maran and GL1, which was absent in resistant varieties Rajetha and Himachal. However, in Mahima and GL2, which are moderately resistant varieties, a faint band was observed (Fig: 2).

These bands of 0.75kb observed exclusively in Rajetha and 1.1kbp observed in GL1 were marked as specific polymorphic bands linked resistance to and susceptibility respectively. A phylogenetic tree was constructed using the data obtained from all the 15 random primers. The dendrogram shows that the highly resistant varieties like Rajetha and Himachal are found in

the same node whereas the susceptible varieties, Maran and GL1 share the same node. (Fig: 3). Sequencing of the 0.75kb RAPD marker yielded a readable sequence of 560 bp, translated to a stretch of 49 amino acids which was compared for homology (<http://ncbi.nlm.nih.gov/BLAST>) using the BLAST programme (GenBank accession number **DQ983234**). The highest homology of 60% was found with putative reverse transcriptase of chickpea and Lotus plane tree.

Discussion

A variety of tests to check for resistance against FOZ, based mainly on biological assays using varieties and species of various plants have been reported. Lax (18) and Soya bean (19). There is no report of biological assays on ginger till now against FOZ. Screening for resistance using the phytotoxic metabolites of FOZ on *in vitro* calli revealed different sensitivities. *In vitro* calli exhibited browning of the callus and of callus of highly susceptible varieties failed to grow further. A number of previous studies have shown that the toxin present in CF of pathogenic fungi was able to inhibit cell growth and that the cells of the host species were most sensitive to the toxin than those of non-host plants (20). Many attempts have been made since then to apply such selection schemes for crop improvement, including resistance to fusarium wilt (21).

In vivo plants exhibited symptoms after three days of inoculation. Since fusarium wilt is the most important disease caused by FOZ, wilt first appears as a vein clearing on the outer portion of younger leaves followed by epinasty of the older leaves (22). Wilting of young stem, defoliation and finally death of the entire plant follows. The present study suggests that the CF containing the toxin fusaric acid could be used for selection of resistant varieties of ginger. Screening varieties is most important to select resistant or susceptible varieties. The two bioassays established a strong correlation of

sensitivity in ginger plants against FOZ, which could be useful in screening programmes.

Primer AD 14 showed a specific band of 0.75kb in Rajetha and this band was found in Himachal and GL2, but the intensity was less than Rajetha. This may be because the sequence amplified is present as dominant homologous allele in the Rajetha and the same sequence may be present as heterologous allele in Himachal and GL2 varieties. The combined phylogenetic tree generated from the data obtained from all the primers, correlates with *in vitro* bioassay data.

RAPD markers linked to different sensitivities to FOZ resistance have been detected in *Pyrus* species (15) and *Gladiolus* (23). RAPD markers have also been reported to explain 85% of the total variance in disease resistance (24). To confirm the relationship between these results and FOZ resistance, cloning and sequencing of the most interesting RAPD fragments is necessary to verify DNA sequence homology with genes possibly involved in disease resistance or susceptibility. The RAPD marker linked to resistance showed homology with Putative reverse transcriptase, a retroelement. Retroelements are mobile genetic elements containing a reverse transcriptase gene. In addition, many transposable elements (including retrotransposons) can be activated by various stresses (25). Retrotransposons are mobile genetic elements that accomplish transposition via an RNA intermediate that is reverse transcribed before interation into a new location with in the host genome. They are ubiquitous in eukaryotic organisms and constitute a major portion of the nuclear genome in plants. These unique properties of retrotransposons have been exploited as genetic tools for plant genome analysis. Retro elements as molecular markers has been reported in plants like *Arabidopsis* (26), and relationship of activation of Tos 17 (LTR retro element) and rice adult plant resistance to bacterial blight was identified in rice (27). These unique properties of retrotransposons have been

exploited as genetic tools for plant genome analysis.

Conclusion

In recent times many DNA markers have been developed as powerful tools for reliable identification of varieties with desirable agronomic traits for plant breeding. In the present study a potential molecular marker linked to resistance in ginger against *Fusarium oxysporum* f.sp *zingiberi* (FOZ) has been successfully identified. This is the first report of a retroelement as a RAPD marker linked to resistance against fusarium yellows in ginger. This marker could be used in future to identify and select ginger varieties resistant to FOZ.

Acknowledgments: This work was supported by University grants Commission, Government of India. We are thankful to Dr B.R. Sasikumar (IISR Calicut) and Dr.V. Ramarao (NRC-MAP, Gujarat) for providing us the ginger varieties.

References

1. Strilings, A.M., (2004). The causes of poor establishment of ginger (*Zingiber officinale*) in Queensland, Australia. Australian Plant Pathology, Vol 33 (2): 203-210.
2. Agrios, (1988). Plant pathology, 3rd edition. Academic press, Inc: New York, 803pp.
3. Feral, J.P., (2002). How useful are the Genetic Marker to understand and manage marine biodiversity, Vol 268: 121-145.
4. Jones, J.P., Miller, W., (1982). Fusarium wilt on tomato, Department of Agriculture and Consumer Service, Division f Plant Pathology, Plant Pathology Circular No. 237.
5. Williams, J.G.K., Kubrlie, K.J., (1990). DNA polymorphism amplified by arbitrary primers are useful as genetic markers. Nucleic Acids Res, Vol 18: 6531-6535.

6. Zheng, X.Y., Wolff, D.W., (2000). Randomly Amplified polymorphic DNA Markers Linked to Fusarium Wilt Resistance in Diverse Melons. Hort. Sci, 35(4): 716-721.
7. Chawdhury, M.K.U., Vasil, V. and Vasil, I.K., (1994). Molecular analysis of plants regenerated from embryogenic callus of Wheat (*Triticum aestivum*) Theor. Appl. Genet, 87: 821-828.
8. Raghunathachari, P., Khanna, V.K., Singh, U.S. and Singh, N.K., (2000). RAPD analysis of genetic variability in Indian scented rice germplasm (*Oryza sativa* L.) Current Science, 79: 994-998.
9. Bardeen, J.M., Havey, M.J., (1995). Randomly amplified polymorphic DNA in blb onion and its uses to assess inbred integrity. Jour. of Americ. Society for Horticulture Sci, 120: 752-758.
10. Airi, S., Rawal, R.S., Dhar, U. and Purohit A.N., (1997). Population studies on *Podophyllum hexandrum* Royle – a dwindling medicinal plant of the Himalaya. Plant Genet. Resour. Newsl, 110: 29-34.
11. Padmesh, P., Sabu, K.K., Seeni, S. and Pushpangadan, P., (1999). The use of RAPD in assessing genetic variability in *Andrographis paniculata* Nees, a hepatoprotective drug. Current Science, Vol. 76 (6): 833-835.
12. Jin, H., Hartman, G.L., Nickel, C.D. and Widholm, J.M., (1996). Phytotoxicity of culture filtrate from *Fusarium solani*, the casual agent of sudden death syndrome of soyabean. Plant Disease, 80: 922-927.
13. Baayen, R.P., De Maat, A.L., (1987). Passive transport of microconidia of *Fusarium Oxysporum f.sp. diathii* in caranation after root inoculation. Neth. J. Plant pathology, 93:3-13.
14. Syamkumar, S., Lowarence, B., Sasikumar, B., (2003). Isolation and Amplification of DNA From Rhizomes of Turmeric and Ginger *Plant Molecular Biology Reporter*, 20: 305a–305f.
15. Schilirò, E., Predier, I.S., and Bertaccini, A., (2001). Use of random amplified polymorphic DNA analysis to detect genetic variation in *Pyrus* spp. Plant Mol Biol Rep, 19, 271 a-h.
16. Sneath, P.H.A., Sokal, R.R., (1973). Numerical taxonomy. San Francisco. Freeman.
17. Sambrook, J. and Russel, D.W., (2001). Plasmids and their usefulness in molecular cloning. In: *Molecular cloning, a laboratory manual*, 3rd edn, (Cold Spring Harbar Laboratory Press, NY, USA), 1.1-1.170.
18. Kroes, G.M.L.W., (1998). Two *in vitro* assays to evaluate resistance in *Linum usitatissimum* to *Fusarium* wilt disease. European Journal of Plant pathology, 104: 561-568.
19. Gray, L.E., Guan, Y.Q. and Widholm, J.M. (1986). Reaction of Soya been callus to culture filtrates of *Phialophora greeta* plant Sci, 47: 45-55.
20. Hartman, C.L., McCoy, T.J., Knous, T.R. (1984). Selection of alfalafa (*Medicago sativa*) cell lines and regeneration of plants resistant to the toxins produced by *Fusarium oxysporum* f.sp. *medicaginis*. Plant Sci Lett, 34: 183-194.
21. Behnke, R.P. (1980). General resistance to late blight of *Solanum tuberosam* plants regenerated from callus resistant culture filtrates of *Phytophthora infestance*. Theor Appl Genet, 56:151-152.
22. Smith, I.M., Dunez, J., Phillips, D.H., Lelliott, R.A. and Archer, S.A. eds. (1988)

- European handbook of plant diseases. Blackwell Scientific Publications: Oxford. 583pp.
23. Dallavalle, E., Aldo Zechini D., Aulerio, Verardi E, Bertaccini A, (2002) Detection of RAPD Polymorphisms in *Gladiolus* Varieties With Differing Sensitivities to *Fusarium oxysporum* f. sp. *gladioli*. *Plant Molecular Biology Reporter*, 20:305a-305f.
24. Jansen, R.C., (1996). A general Monte Carlo Method for mapping quantitative trait loci. *Genetics*, 142:305-311.
25. KejnovskΩ, E., (2000). (Institute of Biophysics, Academy of Sciences of the Czech Republic, Brno, Czech Republic): Retroelements. *Biologické listy*, 65 (2): 113-137.
26. Shunyuuan Xiao, Brent Emerson, Kumrop Ratanasut, Elaine Patrick, Carmel O’Neill, Ian Bancroft and John G. Turner (2004). Origin and Maintenance of a Broad-Spectrum Disease Resistance Locus in *Arabidopsis* *Mol. Biol. Evol*, 21(9): 1661-1672
27. Sha, A.H., Huang, J.B., Zhang, D.P. (2005). Relationship of activation of Tos17 and rice adult plant resistance to bacterial blight, *Yi Chuan*, Mar;27(2):181-4.

Table 1: Effect of different concentrations of CF on survival of calli of ginger varieties against FOZ

Varieties	CF(ml) ^b					
	Calli Brown Rating ^c					
	Control	20%	40%	60%	80%	100%
Varada	0	1	1	2	3	5
Mahima	0	1	1	2	4	5
Rajetha	0	1	1	1	1	2
Maran	0	1	2	3	4	5
Himachal	0	1	1	1	2	2
Suprabha	0	1	2	2	4	5
GL1	0	1	2	3	4	5
GL2	0	1	1	1	2	3

- a. Mean of the three experiments
- b. Culture filtrate added in 100ml (% V) callus culture media, control with out toxin.
- c. 0 = Control, 1 = no browning, 2 = callus surface slightly brown, 3= whole tissue brown, 4 = deep brown with restricted growth, 5 = deep brown with no growth.

Table 2: *In vivo* bioassay of 8 varieties of ginger plants for resistance and susceptibility against *Fusarium oxysporum*.f.sp *Zingiberi*.

Varieties	Plants ^a			Groups ^b		
	Inoculated	0	1	2	3	4
Varada	10	Nil	Nil	7	3	Nil
Mahima	10	Nil	Nil	6	4	Nil
Rajesh	10	5	5	Nil	Nil	Nil
Maran	10	Nil	Nil	Nil	4	6
Himachal	10	Nil	6	4	Nil	Nil
Suprabha	10	Nil	Nil	2	8	Nil
GL1	10	Nil	Nil	Nil	7	3
GL2	10	2	8	Nil	Nil	Nil

a Mean of the three experiments

b Described in Materials and methods

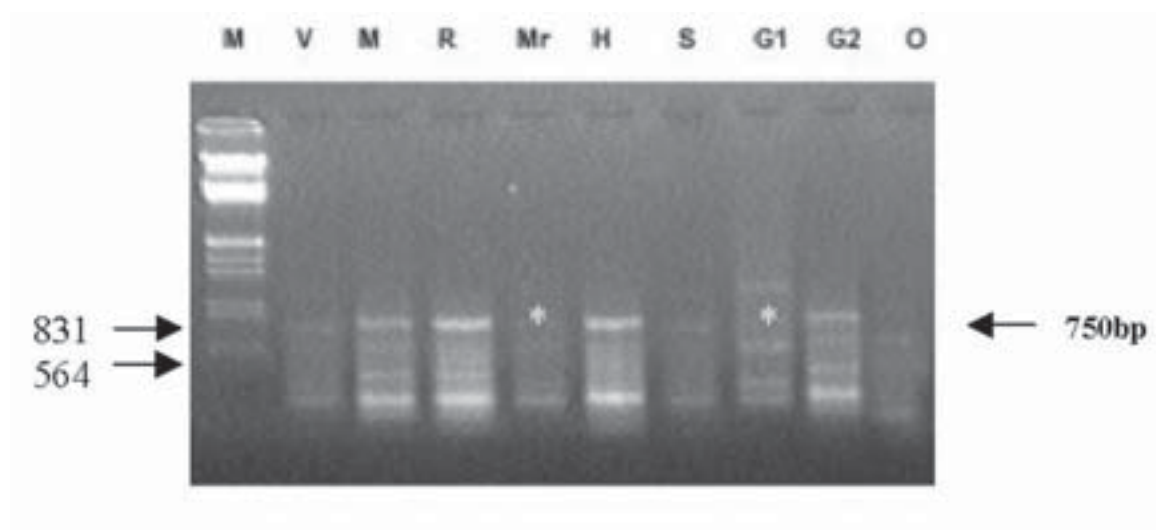


Fig 1: Polymorphic profile obtained from 8 ginger varieties after amplification with primer AD 14. The white asterisk indicates the absence of 750 bp polymorphic band in susceptible varieties like G1 and Mr and present as intense bands in R and H; abbreviations are in the text. Lane 1(M), Lambda DNA / EcoR I Hind III digest ladder. (Bangalore Gene I).

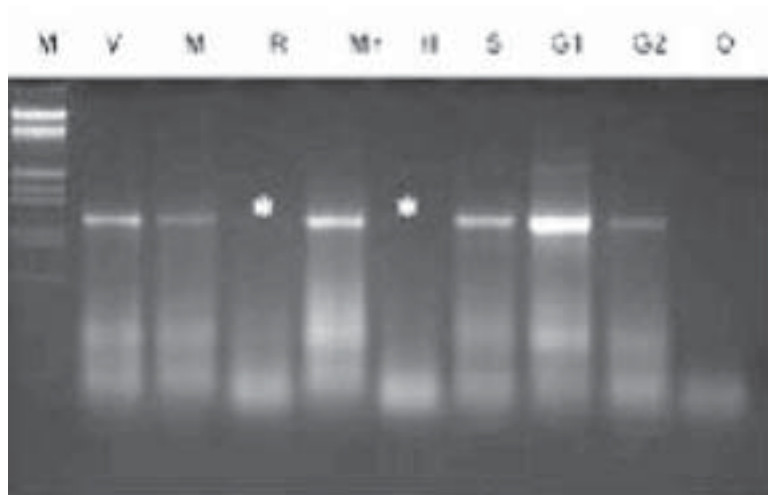


Fig 2 : Comparison of RAPD patterns obtained after amplification with primer WM. The white asterisk indicates the absence of 1.1kb polymorphic band in highly resistant varieties like R and H. Highly susceptible varieties like G1 and Mr shows thick band. Variety abbreviations are in the text. Lane 1(M), Lambda DNA / EcoR I Hind III digest ladder. (Banglore Gene I).

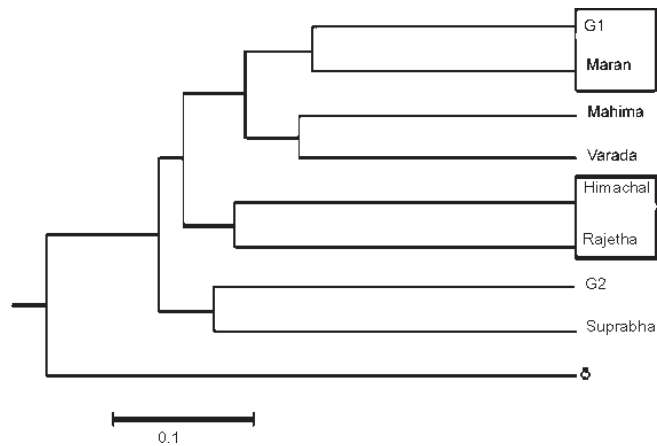


Fig 3 : Dendrogram resulting from analysis of RAPD s depicting the relationship between eight ginger varieties and the data obtained was from all the fifteen-primers. The bar represents the Jaccards coefficient.

Screening for siderophore producing PGPR from black cotton soils of North Maharashtra

P.D. Sarode, M.P. Rane, B.L. Chaudhari and S.B. Chincholkar*

School of Life Sciences, North Maharashtra University, P B 80, Jalgaon 425001

Phone: 91 257 22 58 417

* For Correspondence- chincholkar_sb@hotmail.com

Abstract

Study on indigenous micro-flora of local rhizosphere and identification of efficient plant growth promoters is important for development of good bioinoculants for re-strengthening of otherwise derailing IPM initiative. In this direction, we performed screening for efficient siderophoregenic PGPRs from rhizospheres of healthy and economically important crops in black cotton soils of North Maharashtra. *Pseudomonas putida* DFC31 isolated and identified in present study was able to improve overall vigor/ percent germination of groundnut seeds and also partially inhibit the growth of potent phyto-pathogens. Its sidero-analysis revealed that this siderophore molecule contains hydroxamate as well as catecholate iron chelating groups. Spectrometric study in various forms of siderophores confirmed that this siderophore belongs to pyoverdine type. In addition to siderophore production, IAA production and phosphate solubilization attributes were observed. Data presented herewith lays foundation for advanced studies on strain, in near future.

Key words

Pyoverdine, Siderophore, PGPR, Pseudomonas, Phytopathogen.

Introduction

Ability of rhizosphere-borne micro-organisms to improve growth and development of crops has

been scientifically accepted (1). Mechanisms involved in this phenomenon have been well-elucidated using biochemical and molecular biology tools (2, 3). However, these deliberations have failed to deliver user-friendly technology to farmers. PGPRs (Plant growth promoting rhizobacteria) and BCAs (Biocontrol agents) still form most important yet most fragile component of integrated pest management (IPM) leading to discouragement of IPM initiative throughout the world (4). This situation tempted us to screen for newer and region specific strain(s). Knowledge on the role of secondary metabolites viz. antibiotics, growth hormones and ISR (Induced systemic resistance) agents in plant growth promotion forms the basis of newer screening program. Similarly, the role of siderophores in plant growth promotion and biological control is well established (5). They have ability to mediate plant growth promotion directly as well as indirectly. Iron-siderophore complex is accepted by plants to quench iron thirst in calcareous soil, a direct mechanism (6), whereas chelation of soluble iron by microbial siderophores lead to shift of community structure in rhizospheres, an indirect mechanism (7). Few siderophores, e.g. salicylic acid and pyoverdine, are also involved in induction of systemic resistance. Audenaert et al., (8) have reported that chelated pyochelin and pyocyanin synergistically induce systemic resistance in tomato. Such unequivocal importance of siderophores in plant growth promotion encouraged us to screen new PGPR on the basis of this character.

Black cotton soil of North Maharashtra is known as high yielding soil. Long-standing cash crop like banana which completely covers top soil, maintain high moisture and enrich soil-microflora. Rotation of crops *viz.* cotton; gram, wheat and groundnut enrich and cherish the biological nature of soil further. Thus, this soil forms an un-explored treasure of PGPR.

Through this paper we present the data which lead to identification of siderophoregenic strain, *Pseudomonas putida* DF C31, as efficient plant growth promoter.

Materials and Methods

All media components were purchased from Hi-Media Laboratories Pvt. Ltd (India). Unless otherwise specified in the text, throughout the experimentation, analytical/ guaranteed reagent (AR/GR) grade chemicals from S. D. Fine chemicals. Pvt. Ltd (India) and ultra-pure (Millipore, USA) water was used. All glassware used were cleaned with 6N HCl to remove residual iron and rinsed with water and oven dried. All growth media and reagents were handled carefully to avoid iron contamination. Phytopathogens (*Colletotrichum capsicum*, *Fusarium oxysporum*, *Aspergillus niger*, *Aspergillus flavus*) were maintained on potato-dextrose agar (PDA) medium used for checking antifungal activities of strain. Isolates collected during this study were routinely cultivated on nutrient agar and preserved in 20% (vol/vol) glycerol at -70°C for long-term maintenance.

Field site and sampling

The sampling sites were located in Jalgaon district (Location: 21.05N; 75.40E, soil: black cotton type, annual rainfall 700 mm, annual temperature: above 27.5°C , commercial crops: banana, cotton and sugarcane) of North Maharashtra. Bacteria were preferably isolated from healthy looking plant in the vicinity of diseased plants. After removal of plant from soil, root portion was cut and packed in sterile plastic

bags. These bags were transported to laboratory under cold conditions for immediate processing.

Isolation of Rhizobacteria

Plants selected for isolation of organisms include banana, wheat, cotton, and gram. Adhering soil was carefully brushed off and the plants roots were washed with sterile buffered saline four to five times. These roots were then vigorously shaken with new batch of sterile buffered saline for 10 min. A hundred micro-liter aliquots of dilutions were then plated in triplicate on nutrient agar and King's B medium. Plates were incubated at 28°C for three days. Well-isolated colonies were selected, purified and maintained on nutrient agar. All cultures were stored at 4°C .

Screening for siderophore production

A loopful culture of each isolate from nutrient agar slant was separately inoculated in 100 ml of low strength nutrient medium and incubation was carried out for 18 h at 28°C on rotary shaker at 120 rpm. This culture was used as inoculum for studying siderophore production. Production of siderophores occurs only under iron deficient and highly aerobic conditions. Hence each isolate was inoculated in sterile succinate medium (SM) (9) and incubated on rotary shaker at 28°C , 120 rpm. Supernatants of 36 h incubated cultures were tested for siderophore production by using Universal Chemical Assay as per Schwyn and Neilands (10). Each siderophore positive isolate was separately inoculated in iron deficient succinate medium at the rate of one percent (v/v). Incubation was carried out at 28°C on rotary shaker at 120 rpm for 36 h. Fermented broth was centrifuged (10,000 rpm for 15 min) and supernatant was subjected to estimation of siderophore as per Payne (11). Briefly, 0.5 ml aliquot of culture filtrate was mixed with 0.5 ml of CAS reagent. It was read at 630 nm against un-inoculated succinate medium as a reference. Per cent decolorization was calculated by using following formula

$$\text{Percent decolorization} = \frac{Ar - As}{Ar} \times 10$$

Where,

Ar = Absorbance of reference

As = Absorbance of sample at 630 nm.

Seed bacterization

To test the effect of various rhizospheric strains on seed germination, seed bacterization was performed as per Ownley et al., (12). Briefly, groundnut seeds were surface sterilized with 0.1% HgCl₂ solution and after twice washing with sterile distilled water soaked for 1 h in siderophoregenic cultures having absorbance 0.6 at wavelength 600 nm (~10⁸ cfu ml⁻¹) containing 0.5% carboxy methyl cellulose as binder for bacterization. Aseptic conditions were maintained throughout the process. Seeds were dried on surface sterilized polyethylene sheet kept on clean bench. Bacterized seeds were aseptically introduced in sterile plates with water soaked blotting paper and incubated at room temperature in light and observed for seed germination every day. During the experiment, moisture in the plate was maintained by adding 1ml of sterile distilled water on blotting paper. Similarly, bacterized seeds were sown in pots with sieved soil (pH 7.3).

Identification of strain

The selected strain was subjected to biochemical identification testing as per Bergey's Manual of Systematic Bacteriology (13) and 16S rDNA gene sequencing with eubacteria specific primer set 16F27N (5'-CCAGAGTTTGATCMTGGCTCAG-3') and 16R1525XP (5'-TTCTGCAGTC TAGAAGGAGGTGWTCAGGC-3') (14).

Relevant properties of strain

In order to check the sensitivity of isolate towards different antibiotics, disc diffusion method was used. For this purpose culture was grown on Mueller Hinton Agar in presence of antibiotic impregnated sterile filter paper discs dispensable with octa-disc dispenser (Hi-Media, Mumbai). After 48-h incubation of plates at 28 °C development of zone of inhibition was observed. Results were interpreted as sensitivity (S) or resistivity (R). IAA was detected by a method described by Sharaf and Farrag (15). Briefly, bacteria were grown in nutrient media supplemented with 500 µg/ml of tryptophan for seven day at 28° C. A 2-ml aliquot of the supernatant was acidified with 2 drops of ortho-phosphoric acid and mixed with 4 ml of Salkowski's reagent (50 ml, 35% per-chloric acid + 1 ml 0.5% FeCl₃) and allowed to stand at room temperature for 20 min for development of pink color. Phosphate solubilization by strain was studied by growing the organism on Pikovskaya's agar (16). Plate was observed after 48 h incubation at 28°C for development of zone of clearance around colony. Antifungal activity against various phyto-pathogens was studied. Strain DF C31 was plated onto King's B agar plate and incubated at 28°C for 48 hours. Then the bottom of a Petri dish was placed (inverted) with the upper lid, which contained chloroform, and treated for 30 minutes to kill bacteria for further testing biocontrol ability in vitro. Various phytopathogens viz. *Colletotrichum capsicum*, *Fusarium oxysporum*, *Aspergillus niger*, *Aspergillus flavus* for testing were obtained from NCIM and cultivated individually on PDA plates for 2 to 6 days until mycelia reached the edge of plates. An 8-mm diameter agar, plugged with actively growing mycelia mats of tested phytopathogens was placed in the center of a prepared Petri dish and incubated at 28°C to determine antifungal activities of the secondary metabolites produced by strain. Un-inoculated King's B agar plates treated in the same manner

were inoculated with the above-referred phytopathogens as controls.

Sideroanalysis

For determining functional groups involved in iron chelation, Csaky (17) and Arnow's (18) tests were performed. In order to determine the threshold level of iron at which pyoverdine biosynthesis is completely repressed, culture was grown in iron supplemented (1-50 μ M of iron as FeCl_3) SM. To determine the effect of various carbon sources on production of pyoverdine, organism was grown in media containing various carbon sources. Although visual appearance of yellow-green fluorescence indicated presence of pyoverdine type of siderophores in supernatants (19), for confirmation, concentrated supernatants were subjected to XAD column purification with a small modification of method described by Budzikiewicz (20). Briefly, cell free supernatant was acidified to pH-6 with 12 M HCl and passed through Amberlite XAD-4 column at the rate 1-2 bed volumes per hour (40 x 6 cm). This was followed by washing consecutively with water, 50% methanol, 75 % methanol (@ 4-8 bed volumes per hour). For recovery of siderophores, column was eluted with 100% methanol (@ 1 bed volume per hour). Fractions showing same spectrometric properties were pooled together and lyophilized to obtain yellow-brown colored powder. Small fraction of this purified material was dissolved in 0.05 M sodium phosphate buffer at pH 5.5 on UV-visible spectrophotometer (Model 1601, Shimadzu, Japan) (21).

Results and Discussion

The main aim of present investigation was to screen for efficient siderophoregenic PGPR strains. Considering this fact, while performing isolation, only healthy plants in the vicinity of stunted plants were selected. During isolation of bacteria from these plants, loosely associated microflora was discarded as PGPR strains are known to colonize root surface more intimately (22). Moreover, fields having record of consistent

high yield of cash crops were selected as probability of isolating better PGPR from such fields is high. As shown in Table 1, altogether 35 isolates were obtained from wheat, banana, gram and cotton. On King's B agar, conducive for production of pyoverdine, 15 isolates showed production of fluorescein (viewed under UV light) however, 5 isolates either failed to grow on succinate medium or did not show siderophore production within 36 h. Moreover, supernatants of 12 isolates grown in succinate medium produced siderophores which was evident from instant decolorization of CAS reagent to golden yellow color when 0.5 ml supernatant was mixed with 0.5 ml of CAS reagent (10). Most isolates from banana rhizosphere produced pigment on King's B agar and were CAS positive. Twenty-three isolates were rejected on the basis of inability to produce siderophores in iron deficient succinate medium. PGPR activity of rest twelve isolates was assessed by direct as well as indirect methods. In direct method, ability to promote seed germination was assessed whereas in indirect method, quantification of siderophores, in terms of de-colorization of CAS reagent, was done. It was observed that cotton rhizosphere isolate designated DFC31 produced maximum amount of siderophores in the succinate medium (Figure 1) as well plate experiment showed that DFC31 strain treated seeds of groundnut germinated more vigorously resulting in increased overall length of seedling and well-ramified roots. Improvement in seed germination was observed in almost all strains except B4 and C35. DFC 31 and SCW1 caused significant improvement in seed germination, 42.85% and 36% respectively (Table 2). Pot study (Figure 2) revealed that out of 12 isolates studied, B4, which impaired seed germination (in plate assay), also caused significant reduction in shoot and root biomass compared to control. Strains B5, B6, C31 and SCW1 showed improved biomass in shoot as well as roots. After three repetitions of these experiments with same outcome, strain DFC31 was selected for further studies.

Isolate DFC31 was identified as a member of the fluorescent pseudomonad group as per Bergey's Manual of Systematic Bacteriology (see Table 3). Finally it was confirmed by using 16S rDNA gene sequencing method as *Pseudomonas putida*. Other PGPR strains B5 and B6 obtained during present study were also identified as *Pseudomonas aeruginosa* where as SCW1 as *Acinetobacter calcoaceticus*. Antibiotic sensitivity/resistance assay of DFC31 revealed that this strain is sensitive to amikacin, ceftazidime, ciprofloxacin, colistin, gentamycin, netillin, norfloxacin, and tobramycin whereas resistant to ampicillin, augmentin, cephoxitin, chloramphenicol and piperacillin.

After 2 to 6 days of exposure to the metabolites of strain DFC31 excreted in King's B agar plates, the growth of tested phytopathogens-including *Colletotrichum capsicum*, *Fusarium oxysporum*, *Aspergillus niger*, *Aspergillus flavus* - was partially suppressed, whereas these phytopathogens on the blank King's agar plates, showed normal growth. These results indicate that metabolites of strain DFC31 suppress the growth of phyto-pathogens.

P putida DFC31 produced yellow-green fluorescent pigment that possessed the properties typical of pyoverdine type of siderophore having capacity to strongly chelate iron. Further the Csaky's and Arnow's assays were performed. Csaky's test gave a strong positive reaction, indicating the presence of the hydroxamate type of functional group. Where as Arnow's assay gave yellow color after addition of sodium-molybdate reagent indicating presence of catecholate type of group but did not turn red after addition of sodium hydroxide which is characteristic of pyoverdines. Amendment of iron in iron deficient media (Figure 3) resulted in decrease in siderophoregenesis. A 30iM of iron completely inhibited siderophore synthesis.

In addition to iron, carbon sources also determined extent of siderophoregenesis. Among

various sources tested maltose, sucrose, arabinose, xylose, mannose, malate, propionate did not supported growth. Among others (Figure 4), lactate, fumarate and pyroglutamate supported pyoverdin synthesis. Among, glucose, succinate and lactate, highest growth and siderophore synthesis was supported by lactate. When growth and siderophore synthesis was studied together (Figure 5), it was observed that organism attains stationary phase earlier in lactate compared to succinate. The absorption spectrum of the unpurified *P. putida* DFC31 supernatant (pH around 8) showed a peak at about 404-405nm which shifted to shorter wavelength with a decrease in pH (23). Pyoverdine was isolated and purified in desferric form using Amberlite™ XAD-4. One liter of supernatant yielded 78 mg of XAD-4 purified pyoverdin which showed the absorption maxima at 382 nm in 0.05-sodium phosphate buffer at pH 5.5 (Figure 6). Our results are in agreement with Abdallah (24).

Pseudomonas putida DFC31 isolated and identified in present study was established as plant growth promoting rhizobacterium. In addition to pyoverdine type siderophore organism may help plant growth by IAA production and phosphate solubilization. In a separate study, we have observed that seed bacterization by this strain leads to improvement in iron content of wheat grain by almost eighteen per cent (unpublished results). Positive results of Csaky's and Arnow's test confirm that this siderophore molecule contains hydroxamate as well as catecholate group which is characteristic of pyoverdines (19). UV spectrum of cell-free supernatant in desferri- and ferric- form as well as XAD purified siderophore at pH 5.5 further support characterization of this siderophore as pyoverdin. To our knowledge this is first report on isolation of pyoverdin producing *Pseudomonas putida* from black cotton soils of North Maharashtra. As PGPR activity of DFC31 is established herewith; the strain stands as

excellent representative for further investigation in the context of formulation, field trial and molecular mechanisms to realize its potential.

Acknowledgements

For this work financial support was received from University Grants Commission of India through (Special Assistance Program – Departmental Research Scheme) SAP-DRS program.

Authors are indebted to Prof. R. S. Mali, Vice-Chancellor, NMU, India for stimulating discussions.

References

- 1 Persello-Cartieaux, F., Nussaume, L., Robaglia, C. (2003). Tales from the underground, molecular plant-rhizobacteria interactions. *Plant Cell Environ*, 26: 189-199.
- 2 Montesinos, E., Bonaterra, A., Badosa, E., Frances, J., Alemany, J., Llorente, I., Moragrega, C. (2002). Plant-microbe interactions and the new biotechnological methods of plant disease control. *Int. Microbiol*, 5:169–175.
- 3 Whipps, J.M.(2001). Microbial interactions and biocontrol in the rhizosphere. *J. Expt. Bot*, 52: 487-511.
- 4 Fravel, D. R. (2005). Commercialization and implementation of biocontrol. *Annu. Rev. Phytopathol*, 43: 337-359.
- 5 Hass, D. and Defago, G. (2005). Biological control of soil borne pathogens by fluorescent pseudomonads. *Nat. rev. Microbiol*, 3: 307-319.
- 6 Sharma, A. and Johri, B. N. (2003). Combat of iron-deprivation through a plant growth promoting fluorescent *Pseudomonas* strain GRP3A in mumb bean, (*Vigna radiata* L. Wilzeck). *Microbial. Res*, 158: 77-81.
- 7 Bano, N., Musarrat, J. (2003). Characterization of a new *Pseudomonas aeruginosa* Strain NJ-15 as a potential biocontrol agent. *Current Microbiol*, 46: 324-328.
- 8 Audenaert, K., Pattery, T., Cornelis, P., Höfte, M. (2002). Induction of systemic resistance to *Botrytis cinerea* in tomato by *Pseudomonas aeruginosa* 7NSK2, role of salicylic acid, pyochelin, and pyocyanin. *Mol. Plant-Microbe Interact*, 15:1147-1156.
- 9 Meyer, J. M. and Abdallah, M. A. (1978). The fluorescent pigment of *Pseudomonas fluorescence*, biosynthesis, purification and physico-chemical properties. *J. Gen. Microbiol*, 107: 319-328.
- 10 Schwyn, B. and Neilands, J. B. (1987). Universal chemical assay for the detection and determination of siderophores. *Anal. Biochem*, 160: 47-56.
- 11 Payne, S.M. (1994). Detection, isolation and characterization of siderophores. In, *Methods in Enzymology*, 235: 329-344.
- 12 Ownley, B. H., Duffy, B. K., Weller, D. M. (2003). Identification and manipulation of soil properties to improve the biological control performance of phenazine producing *Pseudomonas fluorescens*. *Appl. Environ. Microbiol*, 69: 3333-3343.
- 13 Palleroni, N.J. (1984). Pseudomonadaceae In: *Bergey's Manual of systematic Bacteriology*. (Ed. Krieg, N. R.) Vol. Williams Wilkins Baltimore, I. MD. pp. 141- 199.
- 14 Pidiyar, V. J., Jangid, K., Patole, M. S., Shouche, Y. S. (2004). Studies on cultured and uncultured microbiota of wild *Culex quinquefasciatus* mosquito midgut based on 16S ribosomal RNA gene analysis. *Am. J. Trop. Med. Hyg*, 70: 597-603.

- 15 Sharaf, E. F. and Farrag, A. A. (2004). Induced resistance in tomato plants by IAA against *Fusarium oxysporum lycopersici*. *Pol. J. Microbiol*, 53: 111-116.
- 16 Pikovskaya, R. I. (1948). Mobilization of phosphorus in soil, in some microbial species. *Mikrobiologia*, 17: 363-370.
- 17 Csaky, T. (1948). On estimation of bound hydroxylamine in biological materials. *Acta Chemica Scandinavica*, 2: 450-454.
- 18 Arnow, L. E. (1937). Colorimetric determination of the components of 3, 4-dihydroxyphenylalanine-tyrosine mixtures. *J. Biol. Chem*, 118: 531-537.
- 19 Manwar, A.V. (2001). Application of microbial iron chelators (siderophores) for improving yield of groundnut. PhD Thesis, North Maharashtra University Jalgaon.
- 20 Budzikiewicz, H. (1993). Secondary metabolites from fluorescent pseudomonads. *FEMS Microbiol, Rev.* 204: 209-228.
- 21 Khalil-Rizvi, S., Stephen, I. T., van der Helm, D., Vidavsky, I., Gross, M. L. (1997). Structures and characteristics of novel siderophores from plant deleterious *Pseudomonas fluorescens* A225 and *Pseudomonas putida* ATCC 39167. *Biochem*, 36: 4163-4171.
- 22 Glandorf, D. C. M., van der Sluis, I., Anderson, A. J., Bakker, P. A. H. M., Schippers, B. (1994). Agglutination, adherence and root colonization by fluorescent pseudomonads. *Appl. Environ. Microbiol*, 60: 1726-1733.
- 23 Elliot, R.P. (1958). Some properties of pyoverdin, the water soluble fluorescent pigment of *Pseudomonas*. *Appl. Microbiol*, 6 (4): 241-246
- 24 Abdallah, M. A. (1991). in *Handbook of Iron Chelates*. (Winkelmann G, Ed) Florida, CRC press, pp. 139-154.

Table 1: Isolation of rhizobacteria from black cotton soil

Host plant	Isolate designation	Pigmentation on King's B agar	CAS test
Plant: Banana Variety: Shrimanti	B1	+	+
	B2	+	+
	B3	+	+
	B4	+	+
	B5(SBC5)	+	+
	B6	+	+
	B7	-	-
Plant: Cotton Variety: Dyana	C22	+	-
	C23	-	-
	C24	-	-
	C25	-	-
	C26	+	-
	C27	-	ND
	C28	-	-
	C29	-	ND
	C30	-	-
	DFC31	+	+
	C32	-	-
	C33(PP)	+	+
	C34	+	-
	C35(PA)	+	+
Plant: Gram Variety: Vijaya	G1	-	+
	G2	+	+
	G3	-	-
	G4	-	ND
Plant: Wheat Variety: Lokvan	SCW1	-	+
	SCW2	-	-
	SCW3	-	-
	SCW4	-	-
	SCW5	+	ND
	SCW6	-	-
	SCW7	+	ND
	SCW8	-	-
	SCW9	-	-
	SCW10	-	-
ND : Not Determined due to poor growth in medium			

Table 2 : Plate assay after six days

Isolates	Percent Germination (%)	Average root length(cm)	Average number of root lets(cm)
B1	62.50	2.44 (0.87)	4.71 (1.99)
B2	66.67	2.52 (0.85)	4.75 (2.75)
B3	62.50	2.39 (0.95)	4.89 (2.14)
B4	54.17	2.24 (0.92)	4.65 (2.52)
B5	62.50	3.11 (0.71)	5.01 (2.10)
B6	75.00	3.35 (0.76)	5.59 (1.98)
DFC31	83.33	3.89 (0.81)	6.78 (2.77)
C33	62.50	2.40 (0.96)	4.60 (2.40)
C35	54.17	2.37 (0.95)	4.57 (2.50)
G1	75.00	2.41 (0.64)	4.63 (1.80)
G2	66.67	2.39 (0.94)	4.61 (2.10)
SCW1	79.17	3.81 (0.93)	6.0 (1.94)
Control	58.33	2.36 (0.57)	4.56 (2.83)

Note: Values in parenthesis indicate standard deviation

Table 3: Biochemical properties of DFC31

Biochemical test	Result
Gram Character	Gram negative
Shape	Short rods
Motility	Motile
Enzyme production	
Catalase	} Positive
Oxidase	
Urease	} Negative
Phenylalanine deaminase	
Pigment production	
King's B medium	Green fluorescence
King's A medium	No pigmentation
Nitrate reduction	Positive
H ₂ S production	} Negative
Blood hemolysis	
DNase	
Sugar utilization	
Glucose	} Positive
Citrate	
Adonitol	} Negative
Lactose	
Arabinose	
Sorbitol	
Mannitol	
Other PGPR Properties	
IAA production	Positive
Phosphate solubilization	Positive

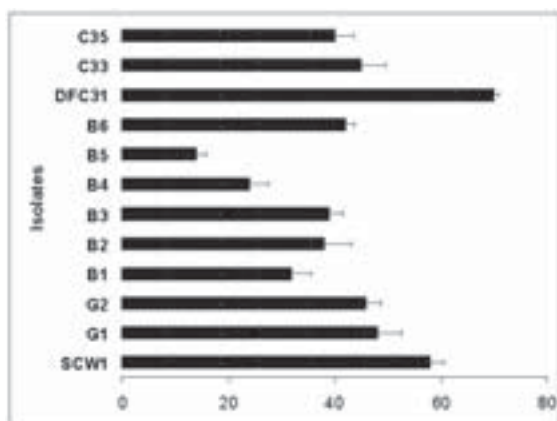


Fig 1: Per cent decolourization of CAS reagent by siderophore containing cell-free supernatant of various isolates

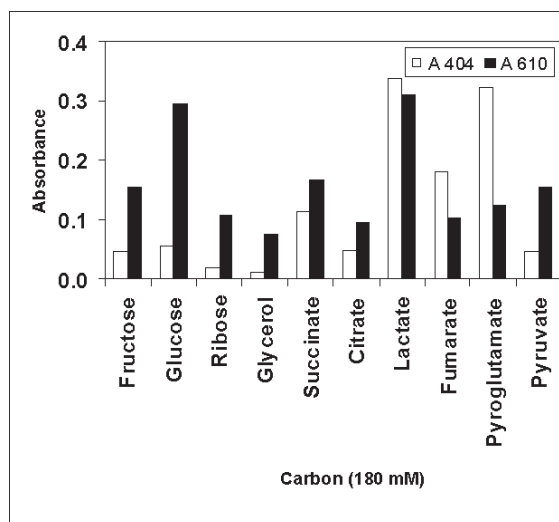


Fig 4: Effect of carbon source on production of siderophore by DFC31

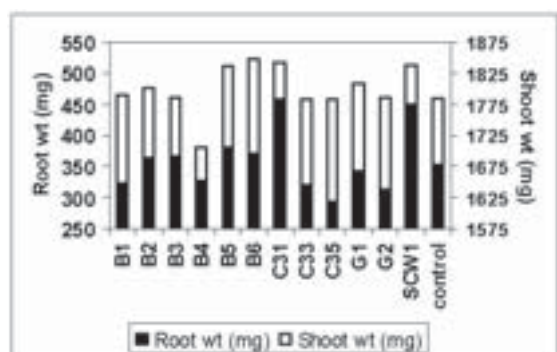


Fig 2: Pot assay of groundnut seed bacterization

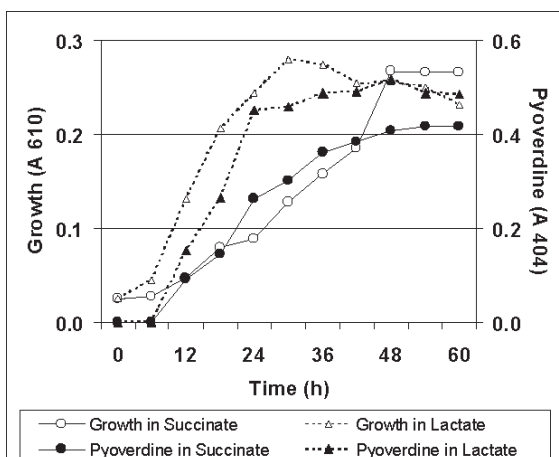


Fig. 5: Growth phase dependence of siderophoregenesis.

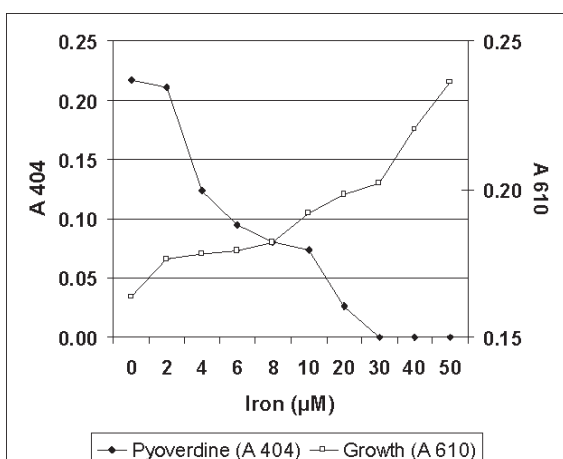


Fig 3. Effect of exogenous iron on production of siderophore by DFC31

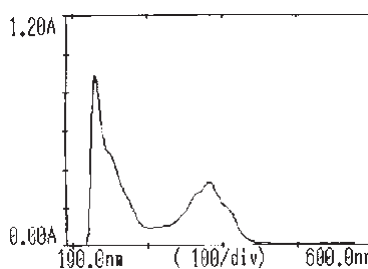


Fig. 6: Absorption maxima of the purified *P putida* DFC31 siderophore

Desiccation tolerance and Starvation resistance exhibit opposite altitudinal cline in Indian populations of *Drosophila immigrans*

Manvender Singh*, Pankaj K.Tyagi and Shruti

Molecular Genetics Research Laboratory, Department of Biotechnology,
N. C. College of Engineering , Israna, Panipat-132107

* For correspondence - pktgenetics@gmail.com

Abstract

Altitudinal variations in desiccation tolerance and starvation resistance in *D.immigra*ns populations are organized into adaptive clines. *D.immigra*ns populations are characterized by increase in desiccation while starvation decreases and such opposite clines match climatic conditions. Regression analysis helps in explaining such adaptations. Upto now, there is no detailed data on altitudinal clines in *Drosophila* species and populations. Present data on genetic differentiation in *D.immigra*ns populations evidence that such geographical clines are adaptive and maintained due to environmental gradients along the altitude.

Key words

Starvation resistance, desiccation tolerance, clinal patterns, altitudinal populations and *D.immigra*ns.

Introduction

Geographical variations in morphological traits have been observed in some taxa along latitude but data on longitudinal and altitudinal populations are limited (9, 4,8). *D.immigra*ns, a cosmopolitan and cold adapted species, is most suitable for analysing altitudinal genetic divergence. Investigations on this cosmopolitan spe-

cies include allozymic variations in some Indian populations (12) and Korean populations (11) while there is no information on population genetic differentiation along altitude and longitude. Along the altitudinal transect which comprises elevational sites, varying from 253 to 2050 m over a linear distance of about 350 km, the thermal stress conditions differ significantly all around the year. Thus, it is expected that *D.immigra*ns populations have adapted to various abiotic conditions and are genetically differentiated. Present investigations demonstrate that for climatic stresses, Indian populations of *D.immigra*ns demonstrate opposite clines i.e. starvation tolerance decreases with altitude, desiccation tolerance increases, and such clinal variations suggest that the two traits are independently adapted to altitudinal climatic conditions.

Material and Methods

*D.immigra*ns were collected from five altitudinal sites (Manali, Shimla, Solan, Kalka and Rohtak). Desiccation and starvation tolerance was analysed in five altitudinal populations of *D.immigra*ns. Mass cultures were established and were analysed for starvation and desiccation tolerance. Adults were grown at 25°C in highly nutrient killed yeast axenic food medium. After emergence, adults were lightly etherized and distributed into groups of ten, put in food vials having corn meal sugar food seeded with

live yeast and aged for three days. On emergence, ten adult males were aged for two days on *Drosophila* food medium and were then subjected to desiccation and starvation experiments as explained by (6). The females were reared for the next generation so that the F2 males could be tested for desiccation and starvation tolerance. Studying two successive generations for each population assessed repeatability of the measurements.

For starvation tolerance, water was provided in each vials i.e. the vials were provided with a piece of foam sponge impregnated with 2 ml of water + 0.2ml sodium methyl parabenzoate (0.1%), which was used to prevent any bacterial infection. Thus, under these conditions, the relative humidity (RH) was close to 100%. All starvation experiments were done in the incubator set at a particular temperature. Vials were observed daily at 6 a.m. & 5 p.m. As the number of dead approached 5, vials were observed even at 3 hours intervals. For measuring desiccation tolerance, adult was introduced in dry, plastic vials closed with a plastic cap. Desiccation was mediated by 2 gm of silica gel/calcium chloride at the bottom of each vial. Flies were prevented from direct contact with silica gel/calcium chloride by a disc of plastic foam piece. Since the vials were airtight it was assumed that the relative humidity (RH) under these conditions was to 0%. All desiccation experiments were done in the incubator set at a particular temperature in accordance with the method of *Da Lage* (3). Vials were observed every hours and the number of dead flies (completely immobile) was recorded. When the number of dead approached 5, vials were observed every 30 min.

Results and Discussion

Basic data on starvation and desiccation tolerance in five altitudinal populations are given in Table 1. Genetic basis of these traits is evident from genetic repeatability in two generations (G_1

and G_2) i.e. mean values for all the populations are almost identical. It may be noted that within population variability for these traits (as evidenced by C.V.) for all the populations is significantly lower (0.95 to 4.51) for starvation while C.V. for desiccation tolerance is significantly higher (2.55 to 10.61). Altitudinal populations demonstrate decrease in starvation and increase in desiccation tolerance i.e. the two traits depict opposite clines and seem to be genetically independent. Desiccation increases with a slope of 7 hrs per 1000 m and starvation decreases by 2 hrs per 100 m (Table 3). Desiccation as well as starvation tolerance are significantly correlated with altitude but in opposite directions i.e. $r = 0.96$ for desiccation and $r = -0.95$ for starvation (Fig. 1). For desiccation and starvation tolerance, genetic divergences in five altitudinal populations are given in Fig. 3. The basic data was subjected to ANOVA for testing the effect of population, generation and their interaction (Table 2). The variations in desiccation/starvation tolerance are largely due to diverse altitudinal populations while effect due to generations is non-significant.

Occurrence of regular increase of desiccation and decrease of starvation tolerance along the altitude reflect adaptations of *D. immigrans* populations to climatic conditions. The climatic data (drawn from Climatological Tables published by Indian meteorological department, New Delhi) of five altitudinal sites were analyzed on the basis of annual average temperature (12 to 28°C) resulting in significant negative correlation ($r = -0.99$) with altitude; and with thermal amplitude (C.V. of temperature) varies from 27 to 36%, which indicated significant positive correlation ($r = 0.88$). The average temperature at Kalka is 30°C and average minimum relative humidity (RH) is 60 to 65% while in Manali the corresponding values are 12°C and 40 to 45% RH. Such climatic diversity provides special opportunities for local adaptations to geographic genetic variations. Thus, species individuals cope

with colder temperature and lesser RH in high altitudinal sites, which are responsible for desiccation stress. The survival period with respect to starvation is always much longer than that for desiccation. *Drosophila* populations from warm and humid environment survive longer and are characterized by a smaller body weight and higher dispersal ability (10). In *Drosophila immigrans*, foothill population have a smaller body size compared with Top hill and show a positive correlation of body weight with increase altitude. The wind velocity at the foothill sites during winter is very high (6-7 kmh⁻¹) compared with Top hill (3.5 kmh⁻¹). Thus, both smaller body size and higher wind speed may favor greater dispersal under more humid conditions in the Foothill populations and contribute to starvation stress. On the contrary, prolonged unfavorable colder climatic conditions are known to favor starvation in higher mountainous populations. Thus, the causes and starvation tolerance seem quite different under diverse climatic conditions.

For desiccation and starvation tolerance, there are significant values of regression coefficients for all the thermal parameters as well as relative humidity (Table 3). Seasonal thermal amplitude (T_{cv}) is positively correlated with altitude and can explain 78% and 91% of total variability for desiccation and starvation tolerance. Thus, altitudinal effect is largely due to environmental gradient of thermal and humidity variables. Selecting for increased desiccation tolerance (5,7,1,2) found a correlated increase in starvation tolerance i.e. laboratory selection led to a decreased locomotor activity and a reduced rate of reserve utilization due to lower metabolic rate which are able to modify the two different physiological phenotypes. Under laboratory conditions, correlated selection response for desiccation and starvation could be due to their common association with longevity. Thus, laboratory selection may not reflect what happens under natural conditions. We observed opposite latitudinal clines in natural populations i.e. an overall

negative correlation between the two traits and interpretation is that the two traits are genetically independent and submitted to opposite directional selections related to climatic conditions.

Acknowledgements

The authors are thankful to the Dr. Ravi Parkash Professor & Head Department of Biochemistry and Genetics, M.D. University Rohtak for providing laboratory facilities and his valuable suggestions.

References

1. Blow, M.W. and Hoffmann, A.A. (1993) The genetics of central and marginal populations of *Drosophila serrata*. I. Genetic variation for stress resistance and species borders. *Evolution*, 47: 1255-1270.
2. Chippindale, A.K., Terence, J.F.C. and Rose, M.R. (1996). Complex trade-offs and the evolution of starvation resistance in *Drosophila melanogaster*. *Evolution*, 50: 753-766.
3. Da Lage, J.L., Capy P. and David, J.R. (1990) Starvation and Desiccation tolerance in *D. melanogaster*: differences between European, North African and Afrotropical populations. *Genetics Selection and Evolution*, 22:381-391.
4. Endler, J.A. (1986). *Natural Selection in the wild*. Princeton University Press, Princeton.
5. Hoffmann, A.A. and Parsons, P.A. (1989) Selection for increased desiccation resistance in *Drosophila melanogaster*: adaptive genetic control and correlated responses for other stresses. *Genetics*, 122, 837-845.
6. Hoffmann, A.A. (1991) *Evolutionary genetics and environmental stress*. Oxford University Press, Oxford.

7. Hoffmann, A.A. (1993) Selection for adult desiccation resistance in *Drosophila melanogaster*: fitness components, larval resistance and stress correlations. *Biological Journal of the Linnean Society*, 48: 43-54.
8. Lemeunier, F., David, J.R., Tsacas, L. and Ashburner, M. (1986) The *melanogaster* species group. In: Ashburner, M.; Carson, H.L.; Thompson, J.N. Jr. (eds), *Genetics and Biology of Drosophila*, Vol. 3e, London: Academic Press, pp. 147-256,
9. Parsons, P.A. (1983) *The Evolutionary Biology of Colonising Species*. Cambridge University Press, Cambridge, London.
10. Parkash, R., Tyagi, P.K., Sharma, I. and Rajpurohit, S. (2005). Adaptations to environmental stress in altitudinal populations of two *Drosophila species*. *Physiological Entomology*, 30:353-361
10. Steiner, W.W.M., Sung, K.C. and Paik, Y.K. (1976). Electrophoretic variability in populations of *D.simulans* and *D.immigrans*. *Biochem. Genet*, 14:495-506.
11. Yadav, J.P. and Parkash, R. (1991). Allozyme variation in ten Indian natural populations of *D.immigrans*. *Korean J. Genetics*, 13 (4): 233-246.

Table 1: Duration of life (hrs) under desiccating conditions (desiccation tolerance) or provided with water (starvation tolerance) at 25°C in five altitudinal populations of *D.immigrans*.

Population	Starvation		m ± s.e.	Desiccation C.V.
	m ± s.e.	C.V.		
Rohtak (alt: 253)	G ₁ = 117.80 ± 0.64 G ₂ = 115.80 ± 0.76 M = 116.80	0.95 1.13	7.00 ± 0.30 6.60 ± 0.40 6.80	7.42 10.61
Kalka (alt: 600)	G ₁ = 110.00 ± 1.15 G ₂ = 113.00 ± 1.15 M = 111.50	1.82 1.77	9.00 ± 0.29 10.67 ± 0.33 9.84	5.56 5.41
Solan (alt: 1250)	G ₁ = 104.33 ± 1.20 G ₂ = 105.67 ± 0.88 M = 105.00	2.00 1.45	14.50 ± 0.87 15.17 ± 0.73 14.84	10.34 8.30
Shimla (alt: 1950)	G ₁ = 90.33 ± 2.03 G ₂ = 92.00 ± 1.15 M = 91.17	3.89 2.17	18.17 ± 0.44 17.67 ± 0.60 17.92	4.20 5.89
Manali (alt: 2050)	G ₁ = 80.33 ± 1.45 G ₂ = 80.00 ± 2.08 M = 80.17	3.13 4.51	21.17 ± 0.60 22.67 ± 0.33 21.92	4.92 2.55

G₁ = generation first, G₂ = generation second, M = mean of both generations m ± s.e. ± mean = standard error C.V. = Coefficient of Variation

Table 2: Results of two way ANOVA applied on each character for testing the effects of population and generation on desiccation and starvation tolerance in five altitudinal populations of *D. immigrans*.

Traits	Source	df	MS	F
Desiccation	Population 1	4	156.01	26.93**
	Generation 2	1	4.17	2.83
	1 x 2	4	1.47	2.28
Starvation	Population 1	4	1183.26	148.68**
	Generation 2	1	12.04	4.27
	1 x 2	4	2.82	0.61

** Significant at < 0.001

Table 3: Regression analysis of climatic variables (T_{max} , T_{min} , $T_{average}$, T_{CV} , RH) with starvation-desiccation tolerance in Indian populations of *D. immigrans*. Altitudinal correlation and slope values are also given for all the traits

Temperature variables	Desiccation		Starvation	
	b (p-level)	R ²	b (p-level)	R ²
T_{max}	-0.99* (.0004)	0.96	0.98* (.002)	0.96
T_{min}	-0.97* (.008)	0.91	0.99* (.00001)	0.99
T_{aver}	-0.98* (.003)	0.95	0.99* (.0008)	0.98
T_{CV}	0.92* (.029)	0.78	-.97* (.008)	0.91
RH	-0.98* (.003)	0.95	0.96* (.009)	0.90
Altitude	(r)	0.96*		-0.95*
Slope		0.007		-0.02

b = partial regression coefficient

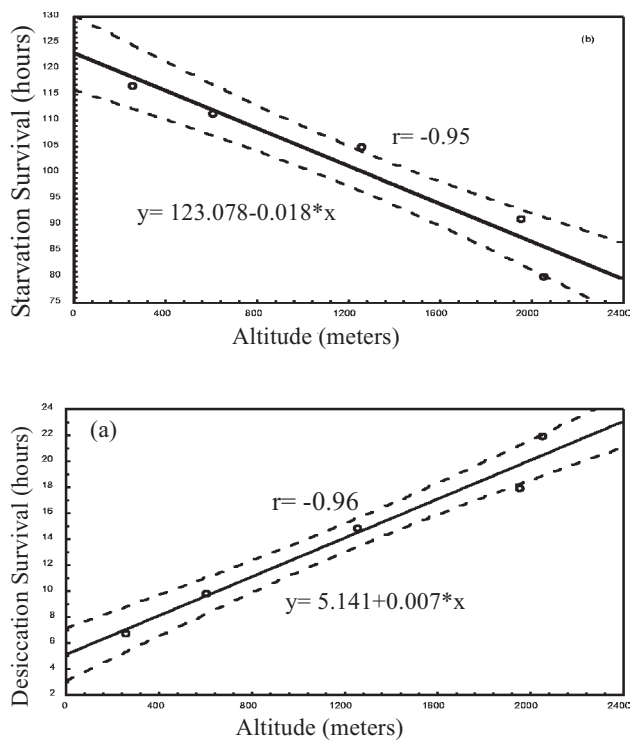
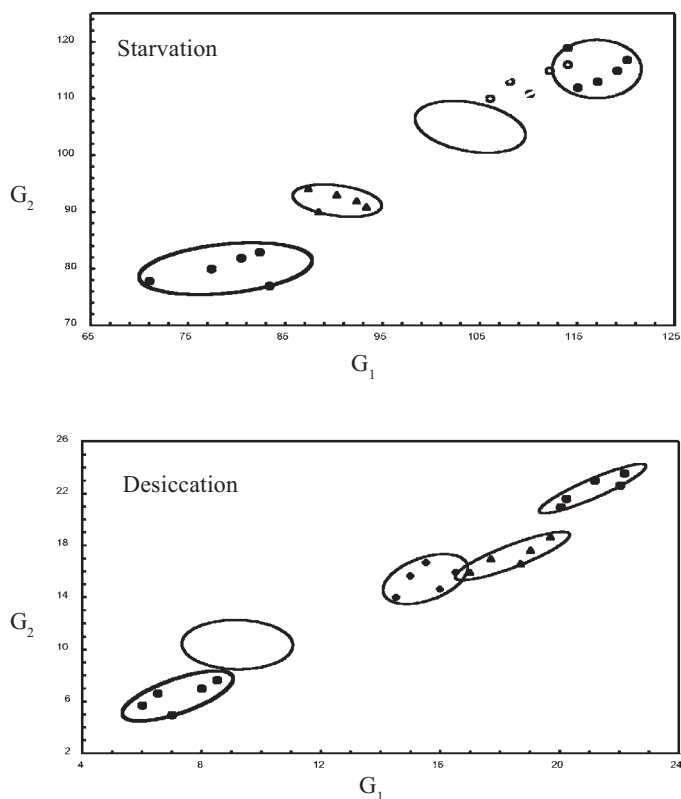


Fig. 1. Relation between desiccation and starvation survival hours with the origin of altitude infive populations of *D.immigrans*.

Fig. 2. Relationship between two generations (G_1 and G_2) for starvation and desiccation survival hours in five altitudinal populations of *D.immigrans*.



Anticonvulsant Potential of Essential oil of *Artemisia abrotanum*

S.P.Dhanabal*, N.Paramakrishnan, S.Manimaran, B.Suresh

Department of Phytopharmacy & Phytomedicine, JSS College of Pharmacy
Post box No.20, Rocklands, Ootacamund, Tamilnadu, India

* For correspondence - dhanskanaksahil@rediffmail.com

Abstract

Epilepsy is a neurological disorder characterized by excessive electrical discharge in brain, which causes seizures. Epilepsy is the second most common neurological disorder in India. It is a very common disorder, characterized by seizures, which take various forms and result from episodic neuronal discharges, the form of the seizure depending on the part of the brain affected. The anti-convulsant properties of the essential oil obtained from the aerial parts of *Artemisia dracunculus* has been reported. The present study was aimed to evaluate the anticonvulsant potential of essential oil of *Artemisia abrotanum* which is available abundantly in Nilgiri Hills. The fresh leaves and flowering tops of *A. abrotanum* were subjected to extraction of essential oil by hydro distillation method using Clevenger apparatus. Experimental convulsion, in Swiss albino mice was induced by intra peritoneal administration of Pentylentetrazole (PTZ) at 100 mg/kg in sterile distilled water after 1h administration of the test drug (100, 400 and 800 mg/kg). Then onset and latency of seizures and mortality were estimated and compared with the solvent control group. Diazepam (1 mg/kg), which was used as a positive control showed significant ($P < 0.01$) delay in the onset of myoclonic seizures (140.3 ± 19.78) and significant increase in time to death latency (1800 ± 0.0) when compared to control. All the animals of the Diazepam group survived against the Pentylentetrazole challenge. The tested essential oil at 100 mg/kg showed significant ($P < 0.05$)

delay in the onset of myoclonic seizures (49.0 ± 1.95). However, at doses of 400 and 800mg/kg did not produce any significant changes in the convulsive parameters, when compared to control.

Introduction

Epilepsy is a neurological disorder characterized by excessive electrical discharge in brain, which causes seizures. Epilepsy is the second most common neurological disorder in India (1,2). Epilepsy affects an estimated 7 million people in India, and 50 million worldwide, approximately 40% of them are women. The prevalence of epilepsy is 0.7% in India, which is comparable to the United States and other developed nations.

Epilepsy is a very common disorder, characterized by seizures, which take various forms and result from episodic neuronal discharges, the form of the seizure depending on the part of the brain affected. Often there is no recognizable cause, although it may develop after brain damage, such as trauma, infection or tumour growth, or other kinds of neurological disease, including various inherited neurological syndromes. Epilepsy is treated mainly with drugs, though brain surgery may be used for severe cases. Current antiepileptic drugs are effective in controlling seizures in about 70% of patients, but their use is often limited by side-effects (3).

Significant advances are being made in recent years to treat epilepsy using second-generation drugs. Polypharmacy is often advocated to 30%

of all epileptic patients for refractory partial or generalized tonic clonic seizures. However, none of the new drugs fulfills the ultimate goal of drug treatment of epilepsy, namely complete control of seizures (4).

A number of medicinal herbs containing Essential oils are reported to have Antiepileptic potential (5-10). The anti-convulsant properties of the essential oil obtained from the aerial parts of *Artemisia dracunculus* has been reported (11). Hence, the present study was aimed to evaluate the anticonvulsant potential of essential oil of *Artemisia abrotanum* which is available in Nilgiri Hills.

Materials and Methods

Aerial parts of *Artemisia abrotanum* was collected in the month of September 2005 from Medicinal Plants Development Area (MPDA), Doddabetta, The Nilgiris, identified and confirmed its authentication by comparing with voucher specimen by Dr.Suresh baburaj, Botanist, Survey of Medicinal Plants and collection Unit, Ooty.

Extraction

The fresh leaves and flowering tops were cleaned, cut into small pieces and subjected for extraction of essential oil by hydro distillation method using Clevenger apparatus. The distilled oil was collected and the residual water was removed by adding anhydrous sodium sulfite and stored in refrigerator.

Animals

Swiss albino mice (18-22 g) of female sex and male sex were used for acute toxicity and anticonvulsant studies, respectively. The animals were obtained from the Animal house, JSS College of Pharmacy, Ooty, maintained in suitable nutritional and environmental condition throughout the experiment period. The experimental protocol was approved by Institutional Animal Ethical Committee (IAEC)

and CPCSEA to carryout pharmacological screening in animals (mice).

Acute toxicity studies

Toxicity study was conducted as per internationally accepted protocol drawn under OECD guidelines 423 in Albino mice (Swiss strain) at a starting dose level of 2000 mg/kg.

Female mice (18-22g) were fasted for overnight and maintained with water *ad libitum*. The mice were separated into four groups of 5 in each. The essential oil was administered at a dose level of 2000 mg/ kg, orally as a solution in sesame oil and animals were observed individually and continuously for 30 min, 1, 4, 6, 12, 48 and 72hrs to detect changes in the behavioral responses like vocalization on touch, locomotor activity and palpebral reflex, and also autonomic responses like tremors, convulsion, salivation, diarrhea, sleep and coma and then monitored for any mortality for the following 14 days.

Screening of essential oils for anticonvulsant activity

Experimental convulsion, in Swiss albino mice was induced by intra peritoneal administration of Pentylentetrazole (PTZ) at 100 mg/kg in sterile distilled water after 1h administration of the test drug. Then onset and latency of seizures and mortality were estimated and compared with the solvent control group. The standard drug, Diazepam (1 mg/kg) dissolved in sterile distilled water was used as positive control.

The male Swiss albino mice (18-22 g) were divided in to groups of 5 mice each. Group I received Sesame oil (1 ml/kg), served as solvent control. Group II received Diazepam (1mg/kg), served as Positive control. Group III, IV and V received essential oil of *A. abrotanum* at 100, 400 and 800 mg/kg respectively.

Statistical Analysis

The values are expressed as Mean \pm SE. The data were subjected to the One way Analysis of

Variance (ANOVA) followed by Dunnett's multiple comparison test. The treatment groups were compared with the control group and $P < 0.05$ was considered to be significant. Data analysis was carried out by using GraphPad Prism V.4

Results

GC analysis of the essential oil of *Artemisia abrotanum* have shown the presence of 19 compounds, which accounted for total 100% of oil. The presence of three compounds namely 1, 8-cineole, Davanone and Nerolidol at the retention time of 1.750, 14.717 and 10.883 min respectively have been confirmed by GC-MS analysis.

Diazepam (1 mg/kg), which was used as a positive control showed significant ($P < 0.01$) delay in the onset of myoclonic seizures (140.3 ± 19.78) and significant increase in time to death latency (1800 ± 0.0) when compared to control. All the animals of the Diazepam group survived against the Pentylene-tetrazole challenge.

The tested essential oil at 100 mg/kg showed significant ($P < 0.05$) delay in the onset of myoclonic seizures (49.0 ± 1.95). However, at doses of 400 and 800mg/kg did not produce any significant changes in the convulsive parameters, when compared to control.

Discussion

The most popular and widely used animal seizure models are the traditional MES and PTZ tests. Prevention of seizures induced by PTZ in laboratory animals is the most commonly used preliminary screening test for characterizing potential anticonvulsant drugs. The MES test is considered to be a predictor of likely therapeutic efficacy against generalized tonic-clonic seizures. By contrast, the PTZ test represents a valid model for human generalized myoclonic and also absence seizures. Other chemoconvulsant models for primary generalized seizures include bicuculline (α -amino butyric acid_A, (GABA_A)-receptor antagonized), strychnine (glycine

receptor antagonist) and aminophylline (adenosine-receptor antagonist. The PTZ (Metrazol) assay has been used primarily to evaluate antiepileptic drugs. However, it has been shown that, most anxiolytic agents are also able to prevent or antagonize Metrazol-induced convulsions. Generally, compounds with anticonvulsant activity in the petitmal epilepsy are effective in PTZ induced seizure model (12).

Lactones are common components in essential oils (specialty aromatic) bearing plants are extensively used in traditional medical systems in various parts of the world. Accordingly, essential oils have been revealing usual compounds as well as unexpected pharmacological activity (13). From the chemical and by/or ethno pharmacological point of view, the study of essential oils is further complicated by its rather complex mixture of compounds, the volatile nature of several commonly present constituents, the presence of photo reactive substances and the wide variability of the chemical profile obtained with different samples.

G.P.Coelho de Souza (1997) (14) reported the presence of lactones viz., E- α -farnesene, α -decan-2-lactone, linalyl acetate and linalool in the essential oil of *Acollanthus suaveolens* (used as an anticonvulsant in the Brazilian Amazon, has sedative properties). Our present study revealed the presence of linalool and α -farnesene in the essential oil of *Artemisia* species.

Some researchers have reported anticonvulsant activity of monoterpenes, SL-1, a synthetic monoterpene homologue of GABA, demonstrated anticonvulsant activity in PTZ induced seizures. Monoterpenes have protective effects against PTZ, picrotoxin and NMDA induced convulsions (15). The anticonvulsant activity of essential oil of *Lippia alba* (Verbenaceae) is also reported (16). Therefore it seems that antiseizure profile of *A.abrotanum* may be related in part to terpenoids present in the plant.

Mohammed Sayyah *et al.*, (2004) (17) reported the anticonvulsant and chemical composition of essential oil of *Artemisia dracunculus* L. The GC-MS analysis showed that 68% of the essential oil was composed of monoterpenoids. Modulation of glutamatergic and GABAergic transmission mechanisms are indicated for anticonvulsant activity of the monoterpenes, *trans*-anethole, α and β -pinene and methyl eugenol (18, 19).

Hence, the monoterpenoids especially *trans*-anethole, pinene and methyl eugenol present in the essential oil of *A. dracunculus*, seems to mediate anticonvulsant activity. This is in agreement with the study of Sayyath *et al.*, (2002) (20) where monoterpenes methyleugenol, eugenol and pinene present in the essential oil of *Laurus nobilis* (Lauraceae) protected mice against tonic convulsions induced by MES and PTZ.

GABA is the major inhibitory neurotransmitter in the brain and the inhibition of its neurotransmission has thought to be an underlying factor in epilepsy (21). The standard antiepileptic drugs, phenobarbitone and diazepam are thought to produce their antiepileptic effects by enhancing GABA neurotransmission (22).

Acknowledgements

Authors wish to thank the management JSS Mahavidyapeetha, Mysore, Karnataka, India for providing necessary facilities and encouragement to complete the work.

References

1. Bharucha, N.E. (2003). Epidemiology of epilepsy in India. *Epilepsia*, 44: 9-11.
2. Gouriedevi, M., Gururaj, G., Satishchandra, P. and Subbakrishna, D.K. (2004). Prevalence of neurological disorders in Bangalore, India: A community-based study with a comparison between urban and rural areas. *Neuroepidemiology*, 23: 261-268.
3. Rang, H.P., Dale, M.M., Ritter, J.M. and Moore, P.K. (1998). *Pharmacology*, 5th edi, pp.550-559.
4. Loscher, W. (1998). New vision in the pharmacology of anti convulsion. *European Journal of Pharmacology*, 342: 1-13.
5. Pourgholami, M.H., Kamalinejad, M., Javadi, M., Majoob, S. and Sayyah, M. (1999a). Evaluation of the Anticonvulsant activity of the essential oil of *Eugenia caryophyllata* in male mice. *Journal of Ethnopharmacology*, 64 (2): 167-171.
6. Santos Fa Rao, V.S. and Silveria, E.R. (1997). The leaf essential oil of *Psidium guyanensis* offers protection against pentylenetetrazole induced seizures. *Planta Medica*, 63 (2): 133-135.
7. Yamada, K., Mimaki, Y. and Sashida, Y. (1994). Anticonvulsant effects of inhaling lavender oil vapour. *Biology and Pharmaceutical Bulletin*, 17 (2): 359-360.
8. Nwaiwu, J.I. and Akah, P.A. (1986). Anticonvulsant activity of the volatile oil from the fruit of *Tetrapleura tetraptera*. *Journal of Ethnopharmacology*, 18 (20): 103-107.
9. Sugaya, E., Ishige, A. and Sekiguchi, K. (1988). Inhibitory effect of a mixture herbal drugs on pentylenetetrazole-induced convulsions in El mice. *Epilepsy Research*, 2: 337-339.
10. Amabeoku, G.J., Leng, M.J. and Syce, J.A. (1998). Antimicrobial and anticonvulsant activities of *Viscum capense*. *Journal of Ethnopharmacology*, 61: 237-241.
11. Mohammad Sayyah., Leila Nadjafna. and Mohammad Kamalinejad (2004). Anticonvulsant activity and chemical composition of *Artemisia dracunculus* L.essential oil. *Journal of Ethnopharmacology*, 94: 283-287.

12. Loscher, W. and Schmidt, D. (1988). Which animal models should be used in the search for new antiepileptic drugs? A proposal based on experimental and clinical considerations. *Epilepsy Research*, 2: 145-181.
13. Gobel, H., Schmidt, G., Dworschak, M., Stolze, H. and Heuss, D. (1995). Essential oils and head mechanisms. *Phytomedicine*, 2: 93-102.
14. Coelho de Souza, G.P., Elisabetsky, E., Nunes, D.S., Rabelo, S.K.L. and Nascimento da Silva. (1997). Anticonvulsant properties of gamma-decanolactone in mice. *Journal of Ethnopharmacology*, 58 (3): 175-181.
15. Librowski, T., Czarnecki, R., Mendyk, A. and Jastrzebska, M. (2000). Influence of new monoterpene homologues of GABA on the central nervous system activity in mice. *Poland Journal of Pharmacology*, 52: 317-321
16. Viana, G.S., Do Vale, T.G., Silva, C.M., Matos, F.J. (2000). Anticonvulsant activity of essential oils and active principles from chemotypes of *Lippia alba* (Mill) N.E.Brown. *Biology and Pharmaceutical Bulletin*, 23 (11): 1314-1317.
17. Pourgholami, M.H., Majzoob, S., Javadi, M., Kamalinejad, M., Fanaee, G.H.R. and Sayyah, M. (1999b). The fruit essential oil of *Pimpinella anisum* exerts anticonvulsant effects in mice. *Journal of Ethnopharmacology*, 66 (2): 211-215.
18. Brum, L.F., Elisabetsky, E. and Souza, D. (2001). Effects of linalool on [(3) H] MK 801 and [(3) H] muscimol binding in mouse cortical membranes. *Phytotherapy Research*, 15: 422-425.
19. Sayyah, M., Valizadch, J. and Kamalinejad, M. (2002). Anticonvulsant activity of the leaf essential oil of *Laurus nobilis* against pentylenetetrazole - and maximal electroshock - induced seizures. *Phytomedicine*, 9 (3): 212-216.
20. Gale, K. (1992). GABA and Epilepsy: basic concepts from preclinical research. *Epilepsia*, 33 (5): 12-14.
21. Olsen, R.W.J. (1981). GABA-benzodiazepine-barbiturate receptor interactions. *Journal of Neurochemistry*, 37: 1-3.

Table No:1 Anti convulsant activity of essential oil of *Artemisia abrotanum*

Groups	Dose (mg/kg)	Monitoring of Seizures (in Sec)			
		Onset of myoclonic seizure	Duration of clonic seizure	Latency to death	No. of animal survived
Control	10	39.75± 3.17	95.50± 24.60	427.4± 64.97	0/6
Diazepam	1	140.3± 19.78**	21.50± 4.48	1800.0± 0.0**	6/6
EOAA	100	49.0± 1.95*	42.0± 3.92	569.5± 75.87	3/6
„	400	59.67± 5.60	50.0± 12.8	477.7± 63.78	1/6
„	800	56.0± 5.74	119.5± 29.77	882.3± 308.5	1/6

EOAA : Essential oil of *A. abrotanum* Superscripts ** and * statistical significance over control group at P< 0.01, P< 0.05.